# The structure and history of populations in a geographic mosaic of predator-prey coevolution

Michael Thomas Jonathan Hague
Bradford, New Hampshire

Bachelor of Arts, Whitman College, 2009
Master of Science, San Francisco State University, 2013

A Dissertation presented to the Graduate Faculty
of the University of Virginia in Candidacy for the Degree of
Doctor of Philosophy

Department of Biology

University of Virginia
December, 2018

## ABSTRACT

Antagonistic coevolution occurs across a heterogeneous landscape of reciprocal selection, in which species interactions and their fitness consequences vary from one location to the next. While reciprocal selection drives local adaptation, broader landscape patterns of coevolution arise in the often-overlooked context of geographically structured populations, connected by gene flow and ancestry. I investigated how the genetic structure of populations, and their evolutionary histories, contribute to the geographic mosaic of arms race coevolution between common garter snakes (*Thamnophis sirtalis*) and their toxic prey, rough-skinned newts (*Taricha granulosa*). Garter snakes in western North America evolved resistance to the deadly tetrodotoxin (TTX) in newts as a result of mutations to the skeletal muscle sodium channel ($Na_V1.4$) that disrupt toxin-binding. To characterize the evolutionary history of predator populations, I phylogenetically reconstructed the historical order of mutations to $Na_V1.4$ in two geographically-distinct hotspots of coevolution. Both lineages of *Th. sirtalis* convergently evolved resistance by passing through a repeated first-step mutation to the channel pore, suggesting the initial change had permissive effects on the subsequent evolution of resistance. I investigated how constraints might bias the evolution of $Na_V1.4$ towards repeatable outcomes, and I found that negative trade-offs arise once TTX-resistant mutations have accumulated, disrupting channel excitability and muscle performance. The evolutionary trajectory of $Na_V1.4$ strikes a balance between TTX resistance and the maintenance of channel function, and these pleiotropic effects seem to underlie variation in resistance across the landscape. Finally, I tested how geographic population structure also contributes to phenotypic divergence in the coevolutionary mosaic. I first showed that allopatric

populations of *Ta. granulosa* have low, but unexpectedly variable levels of TTX, indicating that factors other than selection imposed by *Th. sirtalis* contribute to toxicity. In sympatry, phenotypic divergence in TTX toxicity is tightly correlated with population genetic structure, implying that neutral processes like drift and gene flow—not reciprocal selection—determine variation in toxicity. In contrast, TTX resistance of *Th. sirtalis* deviates from neutral expectations and tracks prey toxicity, such that mosaic variation in resistance and toxicity are both predicted by the population structure of *Ta. granulosa*. This research highlights how two coevolving species are unlikely to undergo a symmetrical response to reciprocal selection. Asymmetries arise at the level of populations, for example, due to drift or contingency. I demonstrate that unique population-level processes occur in both predator and prey, and their combinatory effects explain mosaic variation in species interactions across the landscape, limiting the fixation of species-level traits.

# ACKNOWLEDGMENTS

This dissertation was made possible through the extraordinary mentorship of my advisor, Butch Brodie III. Foremost, Butch taught me to err boldly as a scientist. I learned the value in challenging myself—by asking big questions, writing clearly, and never selling my data short. Butch always puts his students first and I am deeply thankful for his enthusiastic commitment to my intellectual and professional development. I am also grateful for his taste in music. I will carry lessons I learned in the Brodie lab with me for the rest of my career.

My research relied on the expertise and hard work of a network of TTX collaborators. At the center of the TTX network is Butch Brodie Jr., an amazing source for natural history and lore surrounding the arms race between garter snakes and newts. He provided key pieces to my dissertation by measuring the TTX resistance of all garter snakes in this research. Chris Feldman was indispensable in the field. He connected me with landowners, helped me identify new field sites, and provided me with tissue samples. Amber Stokes worked overtime to finish assaying TTX in over 300 of my newt samples. Joel McGlothlin provided valuable feedback on my work, especially Chapters 1 and 4. Charles Hanifin and Shana Geffeney added new perspective to my research, helping me to interpret my results in Chapter 3 in the context of muscle electrophysiology and protein function.

My committee members, past and present, provided me with guidance and advice throughout my dissertation. Bob Cox, Dave Carr, Doug Taylor, Alan Bergland, and Ben Blackman all challenged me to think critically about my data. I am especially thankful for my first reader, Bob, who provided feedback on most of the writing in this dissertation. I

benefitted from the tight link between the Brodie and Cox labs, and Bob served as a model for success as an early-career faculty member.

I am grateful for the entire EEBio group at UVA. The community contributed to my overall wellbeing, in addition to helping me with statistics, lab work, and feedback on talks and manuscripts: graduate students Corlett Wood, Brian Sanderson, Malcolm Augat, Gaby Toledo, Robin Costello, Liza Mitchem, Phoebe Cook, Aaron Reedy, Ariel Kahrl, Amanda Hanninen, Rachana Bhave, Tyler Wittman, Chris Robinson, and Cory Weller; undergraduates Lauren Miller and Josh Eiland; lab managers Christine Alencar and Eileen Butterfield; and post-docs Christian Cox and Heidi Seears. Special thanks to Gaby, who helped me incorporate her electrophysiology data into Chapter 3. Her work dramatically improved the manuscript, but also helped me think about my own data in a more integrative way. In my first few years at UVA, the critical eyes of Corlett, Brian, and Malcolm were invaluable as I developed my dissertation proposal. Thanks to Cory for being a great roommate (despite his weight-lifting-related eccentricities).

My fieldwork would not have been possible without a number of field stations and their excellent managers: Jeff Wilcox at Sonoma Mountain Ranch, Cathy Koehler at McLaughlin Reserve, Hannah Bird at Hopland Research and Extension Center, Peter Steel at Angelo Coast Range, and Christy Wyckoff at Santa Lucia Preserve. Tanner St. Pierre volunteered to fly across the country to help with fieldwork in Washington state. Although he only caught one snake, I was extremely thankful for his company.

Finally, I thank my family for their unyielding love and support. I am grateful for Kim Stanek sticking with me through thick and thin. Fortunately for me, she was never too off-put by the idea of me living out of my car every summer and catching snakes.

Most importantly, I thank my parents, Betty and Mike, and my brother Christopher. Growing up in New Hampshire, my family taught me to work hard, play hard, and love the outdoors. I could not ask for a more supportive family, and this dissertation is a testament to the formative role they play in my life.

This work was supported by the Society for the Study of Evolution, the Society for Integrative and Comparative Biology, the American Museum of Natural History, and a Doctoral Dissertation Improvement Grant from the National Science Foundation. I am also thankful to the Jefferson Scholars Foundation for a Dissertation Year Fellowship.

# TABLE OF CONTENTS

# INTRODUCTION

Antagonistic coevolution is considered a major driver of evolutionary diversity (Dawkins and Krebs 1979; Vermeij 1987; Zaman et al. 2014). Reciprocal selection between natural enemies, like predator and prey or host and parasite, generates adaptation at the phenotypic interface of coevolution, the set of traits in each species that mediate their interactions (Brodie and Brodie 1999; Brodie and Ridenhour 2003). Diversity arises at the level of populations, because the fitness consequences of antagonistic interactions vary across the geographic range of a coevolutionary relationship (Thompson 2005). Spatial heterogeneity in reciprocal selection is expected to produce a geographic mosaic of local adaptation, in which both species have roughly matched abilities at the phenotypic interface of coevolution (Thompson 1999, 2005; Brodie and Ridenhour 2003). However, local adaptation at the phenotypic interface occurs within the broader evolutionary context of each species. Interacting species are each comprised of many diverging populations scattered across the landscape—connected contemporarily by gene flow and historically by ancestry. This context is certain to shape phenotypic variation across the landscape, but its importance remains largely unexplored in coevolutionary mosaics. In this dissertation, I examine how the geographic structure and history of populations contribute to mosaic patterns of adaptation at the phenotypic interface of coevolution.

## *Geographic mosaic theory of coevolution*

The Geographic Mosaic Theory of Coevolution (GMTC) predicts that variation in species interactions, in combination with population structure, should generate a

geographic mosaic of coevolutionary dynamics (Thompson 1999, 2005). This prediction stems from the observation that ecological interactions between species are usually highly variable across the sympatric range (e.g., trematodes and snails, Dybdahl and Lively 1996; crossbills and lodgepole pine, Benkman 1999; moths and host plants, Thompson 1999). A coevolutionary mosaic is defined by three key properties: (1) spatial variation in the coevolutionary phenotypes of each species, (2) phenotypic mismatches between species in some locations, and (3) few coevolved traits that are fixed at the species level. These mosaic patterns arise due to three spatial processes that are predicted to contribute to variation: (1) hotspots and coldspots, (2) selection mosaics, and (3) trait remixing. Hotspots represent regions of reciprocal selection at the phenotypic interface of coevolution, whereas coldspots lack reciprocity. The selection mosaic refers to geographic variation in the fitness function that describes reciprocal selection. Lastly, trait remixing encompasses processes associated with population structure, included genetic drift, gene flow, and metapopulation dynamics, which are primarily thought to drive maladaptation and phenotypic mismatch in the mosaic.

*Contemporary population dynamics in a geographic mosaic*

Under the framework of the GMTC, coevolution occurs at the level of local populations. In each species, populations are distributed across the landscape and experience some degree of isolation, for example, due to geographic distance or barriers to dispersal. As a result, subdivided populations will evolve independently in the presence of divergent selection or genetic drift (Wright 1931, 1949; Holsinger and Weir 2009). In contrast, populations may also be connected by gene flow, which is expected to

homogenize genetic variation across the landscape and constrain local adaptation (Haldane 1930; Wright 1931; Slatkin 1987; Lenormand 2002; Garant et al. 2007).

In the GMTC, the effects of population genetic structure and connectivity are considered part of the process of trait remixing. Under strong reciprocal selection, interacting species are expected to have well-matched abilities at the phenotypic interface of coevolution (Brodie and Ridenhour 2003). Trait remixing, which includes drift and gene flow, is primarily thought to drive maladaptation and mismatch at the phenotypic interface (Thompson et al. 2002; Thompson 2005; Hanifin et al. 2008). The effects of trait remixing ultimately depend on their relative geographic scale compared to that of the selection mosaic (Gomulkiewicz et al. 2007). For example, gene flow may be particularly influential when dispersal occurs among populations with different coevolutionary fitness optima, because locally adaptive alleles are exported to a different region of the mosaic where the foreign phenotype is poorly matched to coevolutionary dynamics.

Simulated models of coevolution and experimental microcosms both generally support the predictions of trait remixing in a geographic mosaic. Finite population sizes and genetic drift permit populations to diverge, which can lead to asynchrony in coevolutionary dynamics across the mosaic (Gandon 2002; Gandon and Nuismer 2009). Most work, however, focuses on the effects of gene flow on adaptation in a heterogeneous landscape of reciprocal selection. Low-to-moderate gene flow tends to help maintain within-population polymorphism and promote adaptation to temporal changes in coevolutionary dynamics (Gandon et al. 1996, 1998; Gandon 2002; Gandon and Michalakis 2002; Nuismer 2006). Eventually, increasing levels of gene flow homogenize variation across the landscape and the population with the strongest

reciprocal effects on fitness tends to dictate global patterns of coevolution (Gandon et al. 1996; Lively 1999; Nuismer et al. 1999, 2000; Gomulkiewicz et al. 2000; Gandon 2002; Gandon and Michalakis 2002; Forde et al. 2004; Morgan et al. 2005). The spatial configuration of populations can also modulate the effects of gene flow. For example, migration out from a hotspot may alter dynamics in a coldspot (Gomulkiewicz et al. 2000; Gandon and Nuismer 2009; Gibert et al. 2013).

*Historical processes shape contemporary variation*

Contemporary patterns of population divergence described in the GMTC result from the unique evolutionary history of each species. Simulated models or experimental microcosms cannot account for historical processes, like vicariance and contingency, that inevitably shape contemporary patterns of genetic variation across the geographic mosaic. The unique evolutionary history of each organism is thought to play a major role in evolutionary outcomes (Gould 1990; Gould and Woodruff 1990). Historical events, like glacial cycles or tectonic uplift, can reshape the geographic distribution of populations through evolutionary time (e.g., Swenson et al. 2005; Shafer et al. 2010). Contemporary patterns of phenotypic and genetic variation contain the signature of ancestry, including population bottlenecks, range expansions, and adaptation to earlier conditions. As a result, historical processes can influence contemporary responses to selection (Huey et al. 2000; Taylor and McPhail 2000; Langerhans and DeWitt 2004). For example, the geographic distribution of ecologically-relevant variation (e.g., loci under reciprocal selection) may be the result of historical biogeography (Thorpe et al. 1995; Alexander et al. 2006; Weese et al. 2012). Ancestral genetic variants could also

have sudden beneficial effects should coevolutionary dynamics change, especially if alleles have been pre-tested by selection at a previous point in time (Orr and Betancourt 2001; Hermisson and Pennings 2005; Barrett and Schluter 2008).

The order of historical events through time can also influence the trajectory of adaptation at the phenotypic interface of coevolution. At a molecular level, proteins consist of a complex relationship among amino acid residues, such that a single mutation can affect multiple aspects of protein structure and function (Wang et al. 2002; DePristo et al. 2005; Weinreich et al. 2006; Harms and Thornton 2013; Storz 2016). Experimental resurrection of inferred ancestral proteins suggests the combinatorial effects of each successive mutation in a series can give rise to non-additive epistatic properties, in which the trajectory of evolution is contingent on prior events (Weinreich et al. 2005, 2006; Bloom et al. 2010; Gong et al. 2013; Natarajan et al. 2016). For example, certain function-altering mutations are contingent on a specific genetic background where prerequisite (or "permissive") mutations have already occurred (Ortlund et al. 2007; Blount et al. 2008; Bridgham et al. 2009; Harms and Thornton 2013). In such instances, an identical mutation can have opposite phenotypic effects on different genetic backgrounds—a phenomenon known as sign epistasis (Weinreich et al. 2005; Storz 2016). Thus, divergent lineages in the geographic mosaic may evolve along different adaptive trajectories due to contingency of prior events.

Population structure and history clearly have the potential to contribute variation to the geographic mosaic, but their relative importance in the coevolutionary process still remains unclear. For example, some simulations suggest that trait remixing and gene flow

are not influential relative to the selection mosaic (Nuismer 2006; Gandon and Nuismer 2009) or if coevolving traits are polygenic (Ridenhour and Nuismer 2007).

Empirical tests in the wild are understandably rare due to the difficulties of quantifying phenotypic and genetic variation in many populations across a heterogeneous landscape of species interactions. If, for example, coevolutionary phenotypes or genotypes covary with neutral population genetic markers, then population structure and historical biogeography—not reciprocal selection—may be the most parsimonious explanation for spatial patterns in the geographic mosaic (Langerhans and DeWitt 2004; Gomulkiewicz et al. 2007). Ecologically relevant loci must also be known in order to assess the role of historical contingency at the phenotypic interface of coevolution. Only then can phylogenetic analyses be used to reconstruct the historical trajectory of coevolving populations, including the temporal sequence of changes at important loci (e.g., Colosimo et al. 2005; Harms and Thornton 2013; McGlothlin et al. 2016).

In one study, population divergence and local co-adaptation between the ant *Myrmica rubra* and its social parasite, the Alcon blue butterfly (*Maculina alcon*), was attributed to geographic population structure and limited gene flow, but the authors only assessed divergence at three microsatellite loci (Nash et al. 2008). In another example, spatial patterns of gene flow among weevil populations predicted levels of escalation in an arms race with its host plant, the Japanese camellia, indicating that dispersal of the seed-predator could determine the overall pace of coevolution (Toju et al. 2011). While studies like these estimate contemporary patterns of population divergence in coevolving species, they still do not account for historical processes—especially contingency at

ecologically relevant loci—that have likely shaped variation across the geographic mosaic.

*The role of populations in a geographic mosaic of predator-prey coevolution*

My dissertation investigates how contemporary genetic structure and the evolutionary history of populations determine adaptation in predator and prey across a geographic mosaic of coevolution. In western North America, common garter snakes (*Thamnophis sirtalis*) evolved resistance to the neurotoxin tetrodotoxin (TTX) as the result of an apparent coevolutionary arms with toxic prey, Pacific newts of the genus *Taricha* (Brodie and Brodie 1990; Brodie et al. 2002). Throughout their range, garter snakes prey on sympatric newts and other amphibians. Individual differences in snake resistance and newt toxicity predict whether a specific interaction between predator and prey goes to completion, resulting in the consumption of prey and/or incapacitation of predator (Williams et al. 2003, 2010). Population patterns of predator resistance and prey toxicity tend to covary across the geographic mosaic of coevolution, such that both species have roughly matched abilities at the interface of toxin-binding (Brodie et al. 2002; Hanifin et al. 2008).

The deadly effects of TTX occur because the compound binds to the outer pore of voltage-gated sodium channels ($Na_V$) and prevents the propagation of action potentials (Fozzard and Lipkind 2010; Tikhonov and Zhorov 2012). Phenotypic TTX resistance in *Th. sirtalis* is largely the result of specific amino acid substitutions in the fourth domain pore-loop (DIV p-loop) of the skeletal muscle sodium channel ($Na_V1.4$), which disrupt toxin-binding and confer resistance (Geffeney et al. 2002, 2005). Channel-level TTX

resistance conferred by each allele in the DIV p-loop is tightly correlated with muscle and whole-animal levels of phenotypic resistance in *Th. sirtalis* (Geffeney et al. 2002, 2005; Feldman et al. 2010). Although a considerable body of work has described the genetic basis of TTX resistance in *Th. sirtalis*, similar information regarding the genetic basis of toxicity of *Taricha* is currently unavailable. Some research suggests that external factors, like environmentally derived precursors, may affect the ability of *Taricha* to synthesize or sequester TTX (Yasumoto et al. 1986; Yotsu et al. 1990; Yasumoto and Yotsu-Yamashita 1996). Others hypothesize that TTX is an inducible response to sustained stressful conditions, like predation (Bucciarelli et al. 2016, 2017).

My dissertation explores how population processes shape contemporary patterns of TTX resistance in *Th. sirtalis* and TTX toxicity in *Ta. granulosa*. Levels of phenotypic divergence are roughly matched in predator and prey populations across the geographic mosaic, which is largely thought to result from spatial heterogeneity in reciprocal selection (Brodie et al. 2002; Hanifin et al. 2008). However, this perspective neglects landscape processes that arise due to population structure in each species. The relative contribution of forces like gene flow and historical biogeography to trait divergence in the mosaic remains almost entirely untested. Because the genetic basis of TTX resistance is well-characterized in *Th. sirtalis* (Geffeney et al. 2002, 2005; Feldman et al. 2010), it is also possible to evaluate how contemporary patterns of phenotypic variation are contingent on the evolutionary history of the $Na_V1.4$ channel.

In Chapter 1, I characterized the historical order of TTX-resistant mutations that arose in the $Na_V1.4$ channel of *Th. sirtalis* during the arms race (Hague et al. 2017). I found clear evidence that TTX resistance evolved repeatedly in $Na_V1.4$ in two separate

coevolutionary hotspots, California and the Pacific Northwest. In each independent lineage, TTX-resistant changes began with the same isoleucine-valine mutation (I1561V) within the channel pore that disrupts toxin-binding. Other point mutations, shown to confer much greater resistance, accumulate later in the evolutionary progression and always occur together with the initial I1561V change. Convergence in the evolutionary trajectory of $Na_V1.4$ is likely the result of constraint—only a few mutational routes can confer TTX resistance while also maintaining the conserved function of voltage-gated sodium channels in muscle tissue.

In Chapter 2, I tested whether TTX-resistant mutations to $Na_V1.4$ generate pleiotropic consequences in *Th. sirtalis* (Hague et al. 2018). Trade-offs are expected to arise in the process adaptation if beneficial mutations have antagonistic effects on other aspects of protein function. I found that snakes that were homozygous for an allele known to confer large increases in toxin resistance ($Na_V1.4^{LVNV}$) had significantly reduced crawl speed compared to individuals with the ancestral TTX-sensitive channel. Heterologous expression of native snake $Na_V1.4$ proteins demonstrated that the same $Na_V1.4^{LVNV}$ allele confers a dramatic increase in TTX resistance and a correlated decrease in overall channel excitability. These results suggest that reductions in channel function and organismal performance occur as a consequence of accumulating mutations in the arms race that beneficially interfere with toxin-binding and confer resistance. In the context of Chapter 1, my findings suggest the evolutionary trajectory of $Na_V1.4$ strikes a balance between TTX resistance and the maintenance of conserved channel function. The pleiotropic effects of mutations in $Na_V1.4$ likely contribute to observation variation in TTX resistance across the geographic mosaic of coevolution.

In Chapter 3, I examined variation in toxicity and population structure of *Ta. granulosa* in Alaska and British Columbia, outside the geographic range of *Th. sirtalis* (Hague et al. 2016). In sympatry, population levels of newt toxicity and snake resistance are closely correlated, presumably due to reciprocal selection in the arms race. Outside the geographic range of resistant predators, I expected to find uniformly low levels of newt toxicity due to the absence of reciprocal selection. While overall levels of TTX are low in allopatry, I found unexpected variation in toxicity despite a lack of neutral population divergence, suggesting that factors other than reciprocal selection with *Th. sirtalis* contribute to geographic patterns of toxicity in *Ta. granulosa*.

In Chapter 4, I tested how contemporary population structure and historical biogeography contribute to geographic mosaic patterns of newt toxicity and snake resistance in the Pacific Northwest. I found that escalation in TTX toxicity and resistance are tightly correlated across the geographic landscape, as expected in the predator-prey arms race. However, contrary to conventional wisdom, variation in toxicity of *Ta. granulosa* is best explained by neutral population divergence, not selection from resistant predators. In contrast, variation in TTX resistance of *Th. sirtalis* appeared to be the clear result of selection from toxic prey. Mosaic patterns of toxicity and resistance are both correlated with population structure of *Ta. granulosa*, indicating that neutral processes, absent of an adaptive signature in one species, seem to underlie landscape variation in predator-prey dynamics in the Pacific Northwest.

My dissertation underscores how local adaptation in the geographic mosaic of coevolution is bounded within the unique evolutionary context of each species. The evolution of TTX resistance in *Th. sirtalis* is contingent on specific mutations to the

$Na_V1.4$ channel, whereas variation in TTX toxicity in *Ta. granulosa* appears to be driven mostly by neutral processes like drift and gene flow. These results establish that evolutionary responses on each side of an antagonistic interaction are likely to differ due to the distinct properties of populations in each species. Natural enemies are almost certain to experience reciprocal selection in a different evolutionary context, whether it be due to contingency or drift, and these asymmetries may explain broader patterns of trait variation across the geographic mosaic. The asymmetry I found in the Pacific Northwest seems to dictate mosaic variation in coevolutionary traits—both predator resistance and prey toxicity are predicted by neutral population divergence in *Ta. granulosa*. While reciprocal selection may drive adaptation in specific populations, my dissertation suggests that broader patterns of variation across the coevolutionary mosaic result from the combinatory effects of each species' unique evolutionary circumstances.

**Literature Cited**

Alexander, H. J., J. S. Taylor, S. S.-T. Wu, and F. Breden. 2006. Parallel evolution and vicariance in the guppy (*Poecilia reticulata*) over multiple spatial and temporal scales. Evolution 60:2352–2369.

Barrett, R. D. H., and D. Schluter. 2008. Adaptation from standing genetic variation. Trends Ecol. Evol. 23:38–44.

Benkman, C. W. 1999. The selection mosaic and diversifying coevolution between crossbills and lodgepole pine. Am. Nat. 153:S75–S91.

Bloom, J. D., L. I. Gong, and D. Baltimore. 2010. Permissive secondary mutations enable the evolution of influenza oseltamivir resistance. Science 328:1272–1275.

Blount, Z. D., C. Z. Borland, and R. E. Lenski. 2008. Historical contingency and the evolution of a key innovation in an experimental population of *Escherichia coli*. Proc. Natl. Acad. Sci. 105:7899–7906.

Bridgham, J. T., E. A. Ortlund, and J. W. Thornton. 2009. An epistatic ratchet constrains the direction of glucocorticoid receptor evolution. Nature 461:515–519.

Brodie III, E. D., and E. D. Brodie, Jr. 1999. Predator-prey arms races. BioScience 49:557–568.

Brodie III, E. D., and E. D. Brodie, Jr. 1990. Tetrodotoxin resistance in garter snakes: an evolutionary response of predators to dangerous prey. Evolution 44:651–659.

Brodie III, E. D., and B. J. Ridenhour. 2003. Reciprocal selection at the phenotypic interface of coevolution. Integr. Comp. Biol. 43:408–418.

Brodie, Jr., E. D., B. J. Ridenhour, and E. D. Brodie III. 2002. The evolutionary response of predators to dangerous prey: hotspots and coldspots in the geographic mosaic of coevolution between garter snakes and newts. Evolution 56:2067–2082.

Bucciarelli, G. M., D. B. Green, H. B. Shaffer, and L. B. Kats. 2016. Individual fluctuations in toxin levels affect breeding site fidelity in a chemically defended amphibian. Proc. R. Soc. B Biol. Sci. 283.

Bucciarelli, G. M., H. B. Shaffer, D. B. Green, and L. B. Kats. 2017. An amphibian chemical defense phenotype is inducible across life history stages. Sci. Rep. 7.

Colosimo, P. F., K. E. Hosemann, S. Balabhadra, G. Villarreal Jr, M. Dickson, J. Grimwood, J. Schmutz, R. M. Myers, D. Schluter, and D. M. Kingsley. 2005. Widespread parallel evolution in sticklebacks by repeated fixation of ectodysplasin alleles. Science 307:1928–1933.

Dawkins, R., and J. R. Krebs. 1979. Arms races between and within species. Proc. R. Soc. Lond. B Biol. Sci. 205:489–511.

DePristo, M. A., D. M. Weinreich, and D. L. Hartl. 2005. Missense meanderings in sequence space: a biophysical view of protein evolution. Nat. Rev. Genet. 6:678–687.

Dybdahl, M. F., and C. M. Lively. 1996. The geography of coevolution: comparative population structures for a snail and its trematode parasite. Evolution 50:2264–2275.

Feldman, C. R., E. D. Brodie, Jr., E. D. Brodie III, and M. E. Pfrender. 2010. Genetic architecture of a feeding adaptation: garter snake (*Thamnophis*) resistance to tetrodotoxin bearing prey. Proc. R. Soc. B Biol. Sci. 277:3317–3325.

Forde, S. E., J. N. Thompson, and B. J. M. Bohannan. 2004. Adaptation varies through space and time in a coevolving host-parasitoid interaction. Nature 431:841–844.

Fozzard, H. A., and G. M. Lipkind. 2010. The tetrodotoxin binding site is within the outer vestibule of the sodium channel. Mar. Drugs 8:219–234.

Gandon, S. 2002. Local adaptation and the geometry of host–parasite coevolution. Ecol. Lett. 5:246–256.

Gandon, S., Y. Capowiez, Y. Dubois, Y. Michalakis, and I. Olivieri. 1996. Local adaptation and gene-for-gene coevolution in a metapopulation model. Proc. R. Soc. Lond. B Biol. Sci. 263:1003–1009.

Gandon, S., D. Ebert, I. Olivieri, and Y. Michalakis. 1998. Differential adaptation in spatially heterogeneous environments and host-parasite coevolution. Pp. 325–342 *in* S. Mopper and S. Y. Strauss, eds. Genetic Structure and Local Adaptation in Natural Insect Populations. Springer US.

Gandon, S., and Y. Michalakis. 2002. Local adaptation, evolutionary potential and host–parasite coevolution: interactions between migration, mutation, population size and generation time. J. Evol. Biol. 15:451–462.

Gandon, S., and S. L. Nuismer. 2009. Interactions between genetic drift, gene flow, and selection mosaics drive parasite local adaptation. Am. Nat. 173:212–224.

Garant, D., S. E. Forde, and A. P. Hendry. 2007. The multifarious effects of dispersal and gene flow on contemporary adaptation. Funct. Ecol. 21:434–443.

Geffeney, S., E. D. Brodie, Jr., P. C. Ruben, and E. D. Brodie III. 2002. Mechanisms of adaptation in a predator-prey arms race: TTX-resistant sodium channels. Science 297:1336–1339.

Geffeney, S. L., E. Fujimoto, E. D. Brodie III, E. D. Brodie, Jr., and P. C. Ruben. 2005. Evolutionary diversification of TTX-resistant sodium channels in a predator-prey interaction. Nature 434:759–763.

Gibert, J. P., M. M. Pires, J. N. Thompson, and P. R. G. Jr. 2013. The spatial structure of antagonistic species affects coevolution in predictable ways. Am. Nat. 182:578–591.

Gomulkiewicz, R., D. M. Drown, M. F. Dybdahl, W. Godsoe, S. L. Nuismer, K. M. Pepin, B. J. Ridenhour, C. I. Smith, and J. B. Yoder. 2007. Dos and don'ts of testing the geographic mosaic theory of coevolution. Heredity 98:249–258.

Gomulkiewicz, R., J. N. Thompson, R. D. Holt, Nuismer Scott L., and M. E. Hochberg. 2000. Hot spots, cold spots, and the geographic mosaic theory of coevolution. Am. Nat. 156:156–174.

Gong, L. I., M. A. Suchard, and J. D. Bloom. 2013. Stability-mediated epistasis constrains the evolution of an influenza protein. eLife 2:e00631.

Gould, S. J. 1990. Wonderful life: the Burgess Shale and the nature of history. WW Norton & Company.

Gould, S. J., and D. S. Woodruff. 1990. History as a cause of area effects: an illustration from Cerion on Great Inagua, Bahamas. Biol. J. Linn. Soc. 40:67–98.

Hague, M. T. J., L. A. Avila, C. T. Hanifin, W. A. Snedden, A. N. Stokes, E. D. Brodie, and E. D. Brodie. 2016. Toxicity and population structure of the Rough-Skinned Newt (*Taricha granulosa*) outside the range of an arms race with resistant predators. Ecol. Evol. 6:2714–2724.

Hague, M. T. J., C. R. Feldman, E. D. Brodie, Jr., and E. D. Brodie III. 2017. Convergent adaptation to dangerous prey proceeds through the same first-step mutation in the garter snake *Thamnophis sirtalis*. Evolution 71:1504–1518.

Hague, M. T. J., G. Toledo, S. L. Geffeney, C. T. Hanifin, E. D. Brodie, and E. D. Brodie. 2018. Large-effect mutations generate trade-off between predatory and locomotor ability during arms race coevolution with deadly prey. Evol. Lett. 2:406–416.

Haldane, J. B. S. 1930. A mathematical theory of natural and artificial selection. (Part VI, Isolation.). Math. Proc. Camb. Philos. Soc. 26:220–230.

Hanifin, C. T., E. D. Brodie, Jr., and E. D. Brodie III. 2008. Phenotypic mismatches reveal escape from arms-race coevolution. PLoS Biol 6:e60.

Harms, M. J., and J. W. Thornton. 2013. Evolutionary biochemistry: revealing the historical and physical causes of protein properties. Nat. Rev. Genet. 14:559–571.

Hermisson, J., and P. S. Pennings. 2005. Soft sweeps: molecular population genetics of adaptation from standing genetic variation. Genetics 169:2335–2352.

Holsinger, K. E., and B. S. Weir. 2009. Genetics in geographically structured populations: defining, estimating and interpreting FST. Nat. Rev. Genet. 10:639.

Huey, R. B., G. W. Gilchrist, M. L. Carlson, D. Berrigan, and L. Serra. 2000. Rapid evolution of a geographic cline in size in an introduced fly. Science 287:308–309.

Langerhans, R. B., and T. J. DeWitt. 2004. Shared and unique features of evolutionary diversification. Am. Nat. 164:335–349.

Lenormand, T. 2002. Gene flow and the limits to natural selection. Trends Ecol. Evol. 17:183–189.

Lively, C. M. 1999. Migration, virulence, and the geographic mosaic of adaptation by parasites. Am. Nat. 153:S34–S47.

McGlothlin, J. W., M. E. Kobiela, C. R. Feldman, T. A. Castoe, S. L. Geffeney, C. T. Hanifin, G. Toledo, F. J. Vonk, M. K. Richardson, E. D. Brodie, Jr., M. E. Pfrender, and E. D. Brodie III. 2016. Historical contingency in a multigene family facilitates adaptive evolution of toxin resistance. Curr. Biol. 26:1616–1621.

Morgan, A. D., S. Gandon, and A. Buckling. 2005. The effect of migration on local adaptation in a coevolving host–parasite system. Nature 437:253–256.

Nash, D. R., T. D. Als, R. Maile, G. R. Jones, and J. J. Boomsma. 2008. A mosaic of chemical coevolution in a large blue butterfly. Science 319:88–90.

Natarajan, C., F. G. Hoffmann, R. E. Weber, A. Fago, C. C. Witt, and J. F. Storz. 2016. Predictable convergence in hemoglobin function has unpredictable molecular underpinnings. Science 354:336–339.

Nuismer, S. L. 2006. Parasite local adaptation in a geographic mosaic. Evolution 60:24–30.

Nuismer, S. L., J. N. Thompson, and R. Gomulkiewicz. 2000. Coevolutionary clines across selection mosaics. Evolution 54:1102–1115.

Nuismer, S. L., J. N. Thompson, and R. Gomulkiewicz. 1999. Gene flow and geographically structured coevolution. Proc. R. Soc. Lond. B Biol. Sci. 266:605–609.

Orr, H. A., and A. J. Betancourt. 2001. Haldane's sieve and adaptation from the standing genetic variation. Genetics 157:875–884.

Ortlund, E. A., J. T. Bridgham, M. R. Redinbo, and J. W. Thornton. 2007. Crystal structure of an ancient protein: evolution by conformational epistasis. Science 317:1544–1548.

Ridenhour, B. J., and S. L. Nuismer. 2007. Polygenic Traits and Parasite Local Adaptation. Evolution 61:368–376.

Shafer, A. B. A., C. I. Cullingham, S. D. Côté, and D. W. Coltman. 2010. Of glaciers and refugia: a decade of study sheds new light on the phylogeography of northwestern North America. Mol. Ecol. 19:4589–4621.

Slatkin, M. 1987. Gene flow and the geographic structure of natural populations. Science 236:787–792.

Storz, J. F. 2016. Causes of molecular convergence and parallelism in protein evolution. Nat. Rev. Genet. 17:239–250.

Swenson, N. G., D. J. Howard, A. E. M. E. Hellberg, and E. J. B. Losos. 2005. Clustering of contact zones, hybrid zones, and phylogeographic breaks in North America. Am. Nat. 166:581–591.

Taylor, E. B., and J. D. McPhail. 2000. Historical contingency and ecological determinism interact to prime speciation in sticklebacks, Gasterosteus. Proc. R. Soc. Lond. B Biol. Sci. 267:2375–2384.

Thompson, J. N. 1999. Specific hypotheses on the geographic mosaic of coevolution. Am. Nat. 153:S1–S14.

Thompson, J. N. 2005. The Geographic Mosaic of Coevolution. University of Chicago Press, Chicago.

Thompson, J. N., S. L. Nuismer, and R. Gomulkiewicz. 2002. Coevolution and maladaptation. Integr. Comp. Biol. 42:381–387.

Thorpe, R., A. Malhotra, H. Black, J. Daltry, and W. Wüster. 1995. Relating geographic pattern to phylogenetic process. Phil Trans R Soc Lond B 349:61–68.

Tikhonov, D. B., and B. S. Zhorov. 2012. Architecture and pore block of Eukaryotic voltage-gated sodium channels in view of NavAb bacterial sodium channel structure. Mol. Pharmacol. 82:97–104.

Toju, H., S. Ueno, F. Taniguchi, and T. Sota. 2011. Metapopulation structure of a seed-predator weevil and its host plant in arms race coevolution. Evolution 65:1707–1722.

Vermeij, G. J. 1987. Evolution and Escalation: An Ecological History of Life. Princeton University Press.

Wang, X., G. Minasov, and B. K. Shoichet. 2002. Evolution of an antibiotic resistance enzyme constrained by stability and activity trade-offs. J. Mol. Biol. 320:85–95.

Weese, D. J., M. M. Ferguson, and B. W. Robinson. 2012. Contemporary and historical evolutionary processes interact to shape patterns of within-lake phenotypic divergences in polyphenic pumpkinseed sunfish, *Lepomis gibbosus*. Ecol. Evol. 2:574–592.

Weinreich, D. M., N. F. Delaney, M. A. DePristo, and D. L. Hartl. 2006. Darwinian evolution can follow only very few mutational paths to fitter proteins. Science 312:111–114.

Weinreich, D. M., R. A. Watson, and L. Chao. 2005. Perspective: Sign epistasis and genetic constraint on evolutionary trajectories. Evolution 59:1165–1174.

Williams, B. L., E. D. Brodie, Jr., and E. D. Brodie III. 2003. Coevolution of deadly toxins and predator resistance: self-assessment of resistance by garter snakes leads to behavioral rejection of toxic newt prey. Herpetologica 59:155–163.

Williams, B. L., C. T. Hanifin, E. D. Brodie, Jr., and E. D. Brodie III. 2010. Tetrodotoxin affects survival probability of rough-skinned newts (*Taricha granulosa*) faced with TTX-resistant garter snake predators (*Thamnophis sirtalis*). Chemoecology 20:285–290.

Wright, S. 1931. Evolution in Mendelian populations. Genetics 16:97–159.

Wright, S. 1949. The genetical structure of populations. Ann. Eugen. 15:323–354.

Yasumoto, T., H. Nagai, D. Yasumura, T. Michishita, A. Endo, M. Yotsu, and Y. Kotaki. 1986. Interspecies distribution and possible origin of tetrodotoxin. Ann. N. Y. Acad. Sci. 479:44–51.

Yasumoto, T., and M. Yotsu-Yamashita. 1996. Chemical and etiological studies on tetrodotoxin and its analogs. Toxin Rev. 15:81–90.

Yotsu, M., M. Iorizzi, and T. Yasumoto. 1990. Distribution of tetrodotoxin, 6-epitetrodotoxin, and 11-deoxytetrodotoxin in newts. Toxicon 28:238–241.

Zaman, L., J. R. Meyer, S. Devangam, D. M. Bryson, R. E. Lenski, and C. Ofria. 2014. Coevolution drives the emergence of complex traits and promotes evolvability. PLoS Biol 12:e1002023–9.

# CHAPTER ONE:

## Convergent adaptation to dangerous prey proceeds through the same first-step mutation in the garter snake *Thamnophis sirtalis*[1]

[1] As published: Hague, MTJ, CR Feldman, ED Brodie, Jr., ED Brodie III. 2017. Convergent adaptation to dangerous prey proceeds through the same first-step mutation in the garter snake *Thamnophis sirtalis*. *Evolution*, 71: 1504-1518.

**Abstract**

Convergent phenotypes often result from similar underlying genetics, but recent work suggests convergence may also occur in the historical order of substitutions en route to an adaptive outcome. We characterized convergence in the mutational steps to two independent outcomes of tetrodotoxin (TTX) resistance in separate geographic lineages of the common garter snake (*Thamnophis sirtalis*) that coevolved with toxic newts. Resistance is largely conferred by amino acid changes in the skeletal muscle sodium channel ($Na_V1.4$) that interfere with TTX-binding. We sampled variation in $Na_V1.4$ throughout western North America and found clear evidence that TTX-resistant changes in both lineages began with the same isoleucine-valine mutation (I1561V) within the outer pore of $Na_V1.4$. Other point mutations in the pore, shown to confer much greater resistance, accumulate later in the evolutionary progression and always occur together with the initial I1561V change. A gene tree of $Na_V1.4$ suggests the I1561V mutations in each lineage are not identical-by-decent, but rather they arose independently. Convergence in the evolution of channel resistance is likely the result of shared biases in the two lineages of *Th. sirtalis* – only a few mutational routes can confer TTX resistance while maintaining the conserved function of voltage-gated sodium channels.

## Introduction

When faced with a similar evolutionary challenge, unrelated lineages often arrive at convergent phenotypic solutions. Accumulating evidence now illustrates that many examples of phenotypic convergence can be attributed to underlying genetic convergence (Gompel and Prud'homme 2009; Christin et al. 2010; Storz 2016). Convergent phenotypes can evolve in unrelated taxa through repeated genetic changes to the same gene family, gene, and even amino acid position (Woods et al. 2006; Castoe et al. 2009; Li et al. 2010; McGlothlin et al. 2014). Highly specific amino acid changes reoccur in protein evolution associated with traits like insecticide resistance in insects (Dong 2007), high-altitude adapted hemoglobin in birds (Natarajan et al. 2015), and color vision pigments in vertebrates (Yokoyama and Radlwimmer 2001; Shi and Yokoyama 2003). The prevalence of genetic convergence raises fundamental questions about the repeatability (or "predictability") of molecular evolution (Weinreich et al. 2006; Stern and Orgogozo 2009). If many conceivable solutions exist to an evolutionary problem, when and why does adaptation proceed through a repeated or predictable route?

Repeated outcomes of molecular evolution are attributed to a number of non-exclusive biases in the substitution process of amino acids, for example, biases towards the few changes that can produce a highly specific phenotypic outcome (Gompel and Prud'homme 2009; Christin et al. 2010) or fixation biases associated with negative pleiotropy (DePristo et al. 2005; Miller et al. 2006; Weinreich et al. 2006; Tokuriki and Tawfik 2009; Storz 2016). However, it is unclear if convergent outcomes arise through a repeated order of mutational changes. The combinatorial effects of each successive mutation in a series can give rise to non-additive epistatic properties, in which only a

subset of trajectories can achieve a specific outcome (Weinreich et al. 2005, 2006; Bloom et al. 2010; Gong et al. 2013; Natarajan et al. 2016). In extreme examples, certain function-altering mutations are contingent on a specific genetic background where prerequisite (or "permissive") mutations have already occurred (Ortlund et al. 2007; Blount et al. 2008; Bridgham et al. 2009; Harms and Thornton 2013).

We characterized convergence in the historical order of accumulation of mutations that gave rise to a convergent molecular outcome: tetrodotoxin (TTX) resistance in the skeletal muscle sodium channel ($Na_V1.4$) of the common garter snake (*Thamnophis sirtalis*). In western North American, *Th. sirtalis* has evolved resistance to the neurotoxin TTX found in its prey, the Pacific newt (*Taricha* spp.). Arms race coevolution between predator and prey has driven convergent escalation of phenotypic TTX resistance in two separate geographic "hotspots", central California and the Pacific Northwest (see Figure 2A; Brodie et al. 2002). Phenotypic convergence in the two hotspots appears to be the result of convergent genetic changes to the $Na_V1.4$ sodium channel (Geffeney et al. 2005; Brodie and Brodie 2015; Toledo et al. 2016).

Tetrodotoxin binds to the outer pore of voltage-gated sodium ($Na_V$) channels (Fozzard and Lipkind 2010; Tikhonov and Zhorov 2012), preventing the propagation of action potentials in muscle and nerve tissue. $Na_V$ channels are comprised of four homologous domains (DI-DIV), each containing a pore-loop ("p-loop") that together combine to form the extracellular pore of the channel where TTX binds (Terlau et al. 1991; Fozzard and Lipkind 2010; Payandeh et al. 2011; Tikhonov and Zhorov 2012; Toledo et al. 2016). Geffeney et al. (2005) conducted an initial screen of amino acid variation in the $Na_V1.4$ pore in TTX-resistant populations of *Th. sirtalis*. Domains I, II,

and III were found to be invariant, but the DIV p-loop sequence contained three unique, derived alleles (one in California and two in the Pacific Northwest; Figure 1). Functional expression of these three DIV sequences confirmed they confer varying levels of TTX resistance to the channel by disrupting TTX-binding at the pore (Geffeney et al. 2005). Channel-level TTX resistance conferred by each DIV allele was also tightly correlated with population differences in muscle and whole-animal levels of resistance (Geffeney et al. 2002, 2005).

To infer the historical order of mutations in the DIV p-loop at each geographic hotspot, we first evaluated variation in $Na_V1.4$ sequence across populations of *Th. sirtalis* throughout western North America. Although the three DIV alleles observed by Geffeney et al. (2005) imply genetic convergence in the two hotspots, these sequences came from an extremely limited sample of only three wild individuals. In this study, we initially assessed population variation in the full $Na_V1.4$ coding sequence, then conducted an expanded geographic survey of variation within the DIV p-loop – the only pore region of the channel found to vary among populations. We sought to enumerate all contemporary p-loop variants, including other intermediate or unique combinations of the five identified point mutations (Figure 1) or other previously unidentified mutations.

Our survey found unique TTX-resistant alleles localized within each geographic hotspot, confirming convergence within the DIV p-loop of the $Na_V1.4$ channel pore. In both instances, however, TTX-resistant changes to protein structure clearly began with the same Ile-Val change in the DIV p-loop (I1561V; Figure 1). Next, we generated a gene tree to evaluate if the genealogical history of $Na_V1.4$ was concordant or discordant with geographic patterns of divergence between the California and Pacific Northwest

hotspots. Specifically, we used ancestral sequence reconstruction to test the hypothesis that the I1561V change, which confers a low-to-moderate increase in TTX resistance, evolved independently in each hotspot as an intermediate mutational step towards greater resistance. Sequence reconstruction, combined with contemporary patterns of DIV variation, permitted a comprehensive test of convergence in the historical order of changes in the DIV p-loop at each hotspot.

## Methods

*Sampling scheme and estimates of phenotypic TTX resistance*

To assess patterns of $Na_V1.4$ variation in populations of *Th. sirtalis* throughout western North America, and relate genetic variation to phenotypic variation, we utilized tissue samples from previous work on phenotypic variation in TTX resistance (Brodie et al. 2002; Ridenhour 2004; Feldman et al. 2010). These data were supplemented with additional collections to increase sample size and the geographic scope of our analysis. Our final dataset included 368 individuals sampled from 27 different locations in western North America (Table 1; Figure 2). We included three sites where *Taricha* do not co-occur with *Th. sirtalis* (Feather Lake, Lofton Lake, and Bear Lake), in order to assess $Na_V1.4$ variation in the absence of selection from toxic newts.

The following analyses relied predominately on previous population estimates of phenotypic TTX resistance in *Th. sirtalis* (Brodie et al. 2002; Ridenhour 2004; Feldman et al. 2010). We scored three additional populations (Carmel Valley, n=26; Feather Lake, n=24; Howard Lake, n=4) for resistance with the same well-established bioassay of whole animal performance used in previous studies (see Supplemental Information S1,

S2; Brodie and Brodie 1990; Brodie et al. 2002; Ridenhour et al. 2004). Briefly, each individual was assayed on a 4m racetrack to characterize its "baseline" crawl speed, then injected intraperitoneally with a known dose of TTX and assayed for "post-injection" speed. Resistance was estimated as relative performance after injection. Population estimates of TTX resistance are reported on a scale of mass-adjusted mouse units (MAMUs) to adjust for population differences in body size (Brodie et al. 2002). The 50% MAMU dose represents the dose of TTX that reduces the performance of the average snake in a population to 50% of baseline speed. The original data were collected in a manner that precludes estimation of individual-level physiological resistance, so we were able to evaluate population patterns of TTX resistance only (see Brodie et al. 2002).

*Preliminary survey of whole-locus variation in $Na_V1.4$*

The $Na_V1.4$ protein is encoded by *SCN4A*, a 5,625bp gene that consists of 26 exons. Although amino acid variation in the DIV p-loop strongly contributes to phenotypic variation in TTX resistance in western *Th. sirtalis* (Geffeney et al. 2005; Feldman et al. 2010), previous studies have not focused on intra-specific variation in other regions of $Na_V1.4$. Amino acid changes to the p-loops of the other three domains (DI-III) have been associated with TTX resistance in other taxa (Brodie and Brodie 2015), including additional species of *Thamnophis* and other snakes (Feldman et al. 2009, 2012), and TTX-bearing species of newts (Hanifin and Gilly 2015) and pufferfish (Jost et al. 2008). Therefore, we chose an initial sample of 20 individuals and sequenced the full protein-coding sequence of *SCN4A*. We sampled two geographically distinct sites, the

Bay Area in California (n=10) and Benton, OR (n=10), each located within the hotspots with elevated phenotypic TTX resistance (Brodie et al. 2002).

We extracted genomic DNA using the DNeasy Blood & Tissue kit (Qiagen, Inc.). We used custom primers to amplify all 26 exons of *SCN4A* (Supplemental Information S3), and sequenced fragments in both directions on an Applied Biosystems 3730*xl* DNA Genetic Analyzer at the DNA Analysis Facility at Yale University. We used Geneious 4.8.5 (Biomatters) to align, edit, and translate protein-coding regions, and then we examined functional variation in the four p-loops (DI-DIV). All sequences were deposited in GenBank (KY744954 - KY745723).

We also used a number of metrics to assess genetic variation across the full *SCN4A* coding sequence. We estimated levels of nucleotide diversity at synonymous and non-synonymous sites using Nei's θ ($\pi$; Watterson 1975; Tajima 1983) and Watterson's θ ($\theta$; Watterson 1975) in DnaSP 5.10.1 (Librado and Rozas 2009). We used the same program to test for departures from neutral expectations using Tajima's D (Tajima 1989). We then used pairwise $F_{ST}$ estimates to characterize among-population variation between the California and Oregon sites. We calculated estimates of $F_{ST}$ using the 'diveRsity' package in R (Keenan et al. 2013; R Core Team 2016) and estimated 95% confidence intervals with 1000 bootstrap iterations.

*Expanded survey of variation in the DIV p-loop*

The initial survey of 20 individuals indicated that the majority of $Na_V1.4$ coding sequence, including the p-loops in Domains I-III, is invariant among populations (see Results). Therefore, we focused our expanded population survey on the variable DIV p-

loop region in our full dataset of 368 individuals from 27 different locations. The DIV p-loop is located approximately in the center of exon 26 of *SCN4A* (McGlothlin et al. 2014). For each individual, we sequenced a 666bp fragment of exon 26 that included the DIV p-loop region. We identified heterozygous sites by visual inspection in Geneious and confirmed heterozygosity in both directions with sequencing. We inferred gametic phase computationally with the program PHASE (Stephens et al. 2001) and recovered gametic phase above a 90% confidence threshold for all but two individuals.

To assess functional variation in the DIV p-loop in relation to TTX resistance, we translated the exon 26 coding sequence and scored unique alleles based on amino acid sequence of the DIV p-loop where TTX binds (e.g. those shown in Figure 1). For each sampling location, we calculated the number of unique alleles ($N_A$), observed heterozygosity ($H_O$), and expected heterozygosity ($H_E$) in Arlequin 3.5 (Excoffier and Lischer 2010). We estimated inbreeding coefficients ($F_{IS}$) and tested for deviations from Hardy-Weinberg equilibrium (HWE) using exact tests in GenePop v4 (Raymond and Rousset 1995; Rousset 2008). We estimated p-values with the Markov chain method, running 100 batches and 2000 iterations per batch, then adjusted p-values with a sequential Bonferroni correction (Holm 1979). As a preliminary estimate of the evolutionary relationship among DIV alleles, we used the 666bp of coding sequence to generate a TCS parsimony haplotype network (Templeton et al. 1992; Clement et al. 2002) implemented in the program PopART (Leigh and Bryant 2015).

If amino acid variation in the DIV p-loop explains phenotypic variation in TTX resistance, then we expect populations with a high frequency of TTX-resistant DIV alleles to also have high estimates of phenotypic TTX resistance. We used a non-

parametric Spearman's rank correlation test ($r_S$) to test for a relationship between population patterns of DIV variation and phenotypic TTX resistance. Specifically, we tested for a correlation between a population's cumulative frequency of all TTX-resistant DIV alleles and its estimate of phenotypic TTX resistance. We used ArcMap 10.3 (ESRI) to visualize population patterns of allele variation and phenotypic TTX resistance.

*Historical analysis of the DIV p-loop*

We generated a *SCN4A* gene tree to characterize the evolutionary history of the $Na_V1.4$ channel in western *Th. sirtalis*. We selected a subset of 40 individuals from our collection that represent (1) a broad geographic sample of western North America and (2) a representative sample of all unique DIV alleles identified in the preceding analysis. We did our best to include a thorough distribution of localities and DIV alleles throughout the range of western *Th. sirtalis* to avoid biasing a particular geographic region or DIV sequence in our analysis. We then included four individuals from central and eastern North America and used two sister taxa, the western ribbon snake (*Th. proximus*) and eastern ribbon snake (*Th. sauritus*), as outgroups.

We used *SCN4A* sequence data in our phylogenetic analysis of $Na_V1.4$ (rather than unlinked neutral markers) in order to limit potential issues with hemiplasy – the incorrect inference of genetic convergence due to incomplete lineage sorting and gene tree-species tree discordance (see Storz 2016). We used the 666bp from the previous analysis, combined with another primer pair, to sequence the majority of exon 26 (1144bp), the final exon at the 3' end of *SCN4A* protein-coding sequence that includes the DIV p-loop (McGlothlin et al. 2014). Because most of the *SCN4A* coding sequence

lacked sufficient variation for a phylogenetic analysis, we used walking primers to sequence a 3,606bp fragment of non-coding sequence to the immediate 3' flank of exon 26 (Supplemental Information S3). We focused our analysis on this 3' non-coding region because it is tightly linked to the DIV p-loop in exon 26. Assuming recombination has not occurred, sequence variation in the 3' flank should reflect the genealogical history of the DIV p-loop. Phylogenetic analyses assume no recombination, and recombinants can confound inference when they contain merged haplotypes from different evolutionary histories. Given the tight proximity of the DIV p-loop and the 3' flanking fragment, we did not anticipate recombination problems in our dataset. As a precaution, we implemented a suite of recombination tests in the program PhiPack (Jakobsen and Easteal 1996; Smith and Smith 2002; Bruen et al. 2006).

In our sample of western *Th. sirtalis*, we avoided heterozygous individuals in order to limit problems with null alleles and the resolution of gametic phases among primer pairs along the 3' flank. The group of 40 western *Th. sirtalis* contained only four heterozygous individuals, and of all polymorphic sites in the alignment, a proportion of 0.225 were heterozygous. For the following analyses, the heterozygous sites of these four individuals were coded as ambiguities. None of the individuals in the final alignment contained heterozygous sites in the DIV p-loop. We collapsed redundant sequences in the alignment if they were found within the same locality, but retained redundancies if they were found in multiple sampling locations. The final concatenated alignment of exon 26 (1144bp) and its 3' flank (3606bp) contained a total of 4750bp. The exon 26 fragment had 22 polymorphic sites (proportion informative=0.68), and the 3' flanking fragment had 123 polymorphic sites (proportion informative=0.66).

To account for potential differences in patterns of evolution among loci, we conducted a partitioned phylogenetic analysis and estimated separate substitution models for the exon 26 coding and 3' non-coding fragments (e.g. Castoe and Parkinson 2006; McGuire et al. 2007; Brown et al. 2009). We used JModelTest 2.1.7 (Guindon and Gascuel 2003; Darriba et al. 2012) to select the best-fit DNA substitution models for exon 26 (HKY85) and the 3' fragment (HKY85 + I). We conducted the partitioned phylogenetic analysis using Bayesian Inference (BI) in the program MrBayes 3.2 (Ronquist et al. 2012). The program implemented the separate substitution models for each partition, and also allowed for among-partition variation in evolutionary rates, which has been shown to improve branch length estimation (Marshall et al. 2006). Four simultaneous runs with six heated chains for 10,000,000 generations were performed, saving every 1,000th generation. We set the burn-in to 25,000 samples and then used the remaining samples to generate the final majority consensus tree and posterior probabilities. We confirmed stationarity in the program Tracer 1.6 by comparing fluctuating values of the likelihood from the four independent searches (Rambaut et al. 2014). We also estimated the phylogeny with a partitioned maximum likelihood (ML) analysis in RAxML 8.2.4 (Stamatakis 2014). The current version of RAxML does not allow the application of different substitution models in partitioned analyses, so we implemented the HKY + I model for both exon 26 and the 3' non-coding fragments. RAxML also only allows for optimization of a single evolutionary rate across all partitions. We estimated branch support with 1000 nonparametric bootstrap replicates. The BI and ML analyses produced identical topologies, which we visualized in the program TreeGraph2 (Stöver and Müller 2010).

We took two precautions to assess the robustness of our partitioning strategy. First, we compared these partitioned results to analogous analyses with unpartitioned data. Accounting for coding and non-coding regions in the partitioned analyses appeared to have little effect, as the partitioned and unpartitioned data produced the same tree topology. Second, to assess whether the putative convergent site in the DIV p-loop of exon 26 (I1561V) might bias results, we removed exon 26 from the alignment and reran then entire analysis with only the 3606bp of 3' non-coding sequence (Supplemental Information S6).

To further assess patterns of population structure at the *SCN4A* locus, we analyzed the full dataset in the population genetic program BAPS 6.0 (Corander et al. 2008), which allows for admixture within and among lineages. We used the sequence data from all 40 western *Th. sirtalis* to infer the optimal number of genetic groupings (*k*) without prior information of sampling locations. First, we ran the analysis assuming a mixture model to determine the most probable *k.* We set *k* to a maximum of 23, the total number of different western sampling sites in the dataset. The resulting mixture clusters were used for the admixture analysis. We used recommended admixture settings, including 200 reference individuals, and we repeated the analysis 100 times per individual. The entire analysis was repeated five times to check for convergence among different runs.

Lastly, we sought to reconstruct the historical order of substitutions to the DIV p-loop of $Na_V1.4$ in the California and Pacific Northwest hotspots. We used the *SCN4A* gene tree topology and branch lengths to reconstruct the DIV p-loop amino acid sequences of ancestral nodes using a maximum likelihood (ML) approach implemented

in the program PAML 4.9 (Yang 2007). We used the same program to calculate marginal posterior probabilities, which represent the likelihood a correct amino acid was reconstructed at a given site under the model's assumptions. We inferred ancestral DIV p-loop sequences using three different forms of ML models (amino acid-, codon-, and nucleotide-based), and then assessed congruence across the reconstructions (see Chang et al. 2002).

Contemporary patterns of DIV variation suggested the same I1561V change evolved independently in the two separate hotspots as an initial mutational step towards more TTX-resistant changes (see Results section, Figure 2). We used a likelihood-based Shimodaira-Hasegawa test (Shimodaira and Hasegawa 1999) to test the *a priori* null hypothesis that the I1561V change instead arose only once. To do so, we generated a second ML tree where all taxa with the I1561V change (from both California and the Pacific Northwest) were constrained to monophyly. We used the SH-test to compare fit of the constraint tree to that of our original unconstrained ML tree. We assessed significance with 10,000 bootstrap replicates in the package 'phangorn' in R (Schliep 2011).

## Results

### *Contemporary variation in $Na_V1.4$*

Population variation in the full $Na_V1.4$ protein-coding sequence of *Th. sirtalis* was limited almost entirely to the DIV p-loop region. Overall nucleotide variation in the full 5,625bp of *SCN4A* sequence was low for both synonymous (Bay Area, $\pi<0.0001$; Benton $\pi=0.0014$) and non-synonymous sites (Bay Area, $\pi=0.0003$; Benton $\pi=0.0002$;

Supplemental Information S4). Tajima's D values for the full sequence were negative for both the Bay Area and Benton samples, although not significant. Sliding window analyses of Tajima's D with varying widow sizes revealed a similar pattern (data not shown). We found only six polymorphic amino acid positions in the full translated sequence, all of which varied both within- and among-populations (Supplemental Information S5). Five of the six sites were the specific point mutations previously associated with TTX resistance in the DIV p-loop (i.e. those in Figure 1). The sixth site was located at amino acid position 549 in the intracellular portion of the protein, outside of the pore region (non-synonymous position 1654bp in Supplemental Information S5). We found no evidence of variation in the p-loops of Domains I-III.

Our expanded geographic sample of the DIV p-loop sequence uncovered both within- and among-population variation in the three derived alleles characterized previously by Geffeney et al. (2005) (Figure 2). The five known point mutations to the DIV p-loop occurred only in these three specific combinations. We did not find other intermediate or unique alleles, nor other novel mutations to the p-loop. Population variation in the three derived alleles was also consistent with geographic patterns of phenotypic TTX resistance. Observed frequencies of TTX-resistant alleles were tightly correlated with population estimates of phenotypic TTX resistance (Figure 3, Spearman's Rank Correlation, $r_S=0.848$, $p<0.001$); and the occurrence of TTX-resistant alleles was localized within the two hotspots. Allele frequencies were consistently out of Hardy-Weinberg Equilibrium, as expected for a locus under strong selection (Table 1).

We generated a parsimony haplotype network for the 286 individuals from which we were able to sequence the full 666bp fragment of coding sequencing in exon 26

(Figure 4 inset). The parsimony network was largely uninformative because almost all the polymorphic sites in the alignment were the non-synonymous changes in the p-loop that confer TTX resistance. Consequently, taxa grouped according to their specific DIV p-loop amino acid sequence. Despite low divergence in the protein-coding sequence, haplotypes in the network did fall into two apparent geographic groups, a California/Northwest Coast and an Intermountain group. This broad pattern of divergence was also reflected in the phylogenetic analysis (see below).

*Historical analysis of the DIV p-loop*

Tests for signatures of recombination (PHI, NSS, and Max $\chi^2$) were non-significant for our sample of western *Th. sirtalis*, so we proceeded with the phylogenetic analysis. The partitioned BI and ML *SCN4A* gene trees of the full 4750bp dataset broadly supported three geographic clades within western *Th. sirtalis*: (1) central California, (2) the Northwest Coast, and (3) an Intermountain clade that spanned the Cascade and Klamath Mountain Ranges (Figure 4). Each of the three groups had a posterior probability >0.95 and bootstrap support >70 in the BI and ML analyses, respectively. The analysis of the reduced dataset (excluding the 1144bp exon 26 fragment) produced the same three well-supported clades, but lacked the same resolution among DIV alleles within each geographic group (Supplemental Information S6).

The population genetic BAPS analysis identified four genetic clusters ($k$=4, Figure 4) as the most likely number of groupings, which were consistent with geographic patterns in the phylogeny. All individuals had posterior admixture coefficients >0.85, and no individuals showed evidence for admixture exceeding the threshold of p=0.05. BAPS

results were consistent across all five replicate runs. Individuals from the Northwest Coast and Intermountain clades formed two separate genetic groups, as in the phylogeny. The analysis did detect additional structure among DIV alleles in California, where all individuals with the ancestral sequence or I1561V change formed one group and individuals with the additional changes I1555L, D1568N, and G1569V formed a second group.

The gene tree topology supported two independent origins of the I1561V change, in the California and Northwest Coast clades. The two parallel changes were intermediate steps to more TTX-resistant, but unique, DIV alleles in each of the two lineages. The ancestral sequence reconstruction in PAML also supported this evolutionary history (Figure 4). Results from the amino acid-, codon-, and nucleotide-based models were all congruent, and all ancestral nodes were supported with posterior probabilities >0.99. Finally, the topology of our best ML tree was a significantly better fit than the constraint tree where all I1561V taxa were forced into monophyly (SH test, p=0.0187).

**Discussion**

Contemporary patterns of variation in western *Th. sirtalis* suggest the evolution of TTX-resistant mutations in $Na_V1.4$ proceeded independently in two separate lineages, yet began with the same first mutational step. An I1561V change in the DIV p-loop likely arose independently in each of the two geographic hotspots of elevated phenotypic TTX resistance. This initial mutation was followed by a small number of unique, lineage-specific changes to the DIV p-loop in each hotspot. Below, we discuss evidence for historical convergence and then potential drivers of repeated change to the DIV p-loop.

*Historical convergence in the DIV p-loop*

Patterns of population variation in the $Na_V1.4$ channel demonstrate that TTX-resistant mutations in the DIV p-loop evolved independently in two separate geographic regions. The I1561V allele was found in both hotspots; however, the I1555L-D1568N-G1569V allele was unique to California and the G1566A allele unique to the Pacific Northwest. Population frequencies of these three TTX-resistant DIV alleles were tightly correlated with population mean estimates of phenotypic TTX resistance throughout western North America (Figures 2 and 3). Outside the two hotspots, we only found the ancestral $Na_V1.4$ sequence. For example, non-resistant populations located between the two hotspots (Crescent and Parsnip) and in allopatry with *Taricha* newts (Lofton Lake and Bear Lake) were fixed for the ancestral DIV amino acid sequence.

Contemporary patterns of allelic variation provide strong evidence that TTX-resistant mutations in the DIV p-loop began with the same I1561V change in each hotspot. The I1561V change is the only point mutation to occur in *all* derived alleles in both hotspots. Prior to this study, the I1561V allele (which confers a slight increase in TTX resistance) was not known to occur in California; however, we detected the allele in both hotspots. In our sample, the other point mutations in the two highly resistant alleles (I1555L-D1568N-G1569V in California; G1566A in the Pacific Northwest) never occurred in lineages without the initial I1561V change. Our wide-ranging survey of 368 individuals from 27 localities did not uncover other intermediate or unique mutational combinations that lacked the I1561V change.

The *SCN4A* gene tree also indicated the I1561V change was the first mutation to arise in each hotspot (Figure 4). In the phylogeny, taxa sampled from the California and Pacific Northwest hotspots generally grouped within the California and Northwest Coast clades, respectively. Within each of these clades, the I1561V change was the initial mutational step towards TTX resistance, preceding the other point mutations in alleles that confer higher resistance. In addition, the phylogenetic analysis suggested the I1561V changes found in each hotspot are not identical-by-descent, but rather arose independently. Two separate I1561V changes were also supported by the ancestral sequence reconstruction, an analysis that is considered robust despite phylogenetic uncertainty (Hanson-Smith et al. 2010) and when divergence is low (Zhang and Nei 1997; Blanchette et al. 2004). The constraint tree (with forced monophyly of all I1561V taxa) was significantly less likely than our best ML topology that depicted two I1561V changes.

The three geographic groups identified from the gene tree and BAPS analysis (California, Northwest Coast, and Intermountain) were qualitatively similar to those in a mtDNA phylogeny of western *Th. sirtalis* by Janzen et al. (2002), highlighting the need to interpret $Na_V1.4$ evolution in the context of historical biogeography. The mtDNA tree supported a pattern of post-glacial population expansion in the last ~10,000 years from two separate glacial refugia: (1) a northward population expansion out of southern California and (2) a southward expansion from southwestern Canada. Populations in the two hotspots, where the I1561V changes putatively arose in parallel, appeared genetically disparate in the mtDNA phylogeny. As in the *SCN4A* tree, Janzen et al. (2002) found divergence between populations in California and the Pacific Northwest. The intersecting

mountain ranges at the California-Oregon border, located between the two hotspots, are a site of historical vicariance for not only *Th. sirtalis*, but also many other co-distributed taxa (Mahoney 2004; Mead et al. 2005; Swenson et al. 2005), including the newt *Ta. granulosa* (Kuchta and Tan 2005). This pattern of north-south divergence might help explain how genetic convergence arose if populations in California and the Northwest were historically isolated. Historical vicariance may also explain why a number of localities in our *SCN4A* gene tree contained individuals that grouped into multiple geographic clades (e.g. Howard Lake grouped in both the California and Northwest Coast clades). A number of these localities lie in regions that appear to have been influenced by vicariance (e.g. Howard Lake located in the Northern Coast Range of California), and may now represent contact zones between the three geographic clades (Janzen et al. 2002).

Although our phylogenetic analysis provides evidence for parallel, independent I1561V changes in the two hotspots, we cannot rule out alternative scenarios. We consider recombination an unlikely explanation because the 3' non-coding sequence used in the gene tree is closely linked to the DIV p-loop, and tests for recombination were non-significant. However, a more comprehensive test for recombination would involve evaluating sequence variation on both sides of the DIV p-loop, not just the 3' flanking region. A more plausible alternative may be the retention of an undetected ancestral polymorphism (e.g. Colosimo et al. 2005; Barrett and Schluter 2008). A polymorphism at position 1561 could have existed at low frequency in the ancestor of western *Th. sirtalis*, with the I1561V change subsequently increasing due to contemporary selection in each of the two hotspots. In addition, our phylogenetic analysis of the reduced dataset (excluding

exon 26 and the putatively convergent I1561V site) was ambiguous to whether the I1561V change arose twice or existed as an ancestral polymorphism (Supplemental Information S6). Retention of polymorphisms and incomplete lineage sorting could also help explain why certain localities in the *SCN4A* gene tree contained individuals that grouped in multiple geographic clades (e.g. Howard Lake).

Unfortunately, nucleotide variation in the DIV p-loop does not help to distinguish between convergence and ancestral polymorphism at the amino acid level. In the standard genetic code, the adenine-guanine mutation found in both hotspots is the only single point mutation in a codon triplet capable of generating an isoleucine-valine amino acid change. The scope of this study does not permit genome-spanning estimates of linkage disequilibrium to elucidate signatures of selection (Innan and Kim 2004; Prezeworski et al. 2005); however, an ancestral I1561V polymorphism may be less probable given contemporary patterns of DIV variation. We surveyed a total of 111 individuals from 10 populations with low phenotypic resistance surrounding the hotspots – including five sites located between the two hotspots – and did not find evidence of the I1561V allele (Figure 2). Moreover, the I1561V change has never been found in eastern populations of *Th. sirtalis* (Feldman et al. 2009; Avila 2015), which are ancestral to the California and Northwest Coast clades in our *SCN4A* phylogeny, or in other TTX-resistant *Thamnophis* species (Feldman et al. 2009, 2012; McGlothlin et al. 2016).

*Potential drivers of historical convergence*

Convergent evolution at the protein-level generally occurs for two non-exclusive reasons (reviewed in Storz 2016). In some cases, only a limited number of mutations can

produce a specific phenotypic outcome. For example, the target of selection may be highly specific and changes to only a few specialized loci can produce a requisite outcome (Gompel and Prud'homme 2009; Stern and Orgogozo 2009; Christin et al. 2010; Storz 2016). TTX resistance has repeatedly evolved in a number of unrelated taxa through specific genetic changes to the $Na_V1.4$ pore that disrupt TTX-binding (Jost et al. 2008; Feldman et al. 2009, 2012; Brodie and Brodie 2015; Hanifin and Gilly 2015; Toledo et al. 2016). Genetic convergence in the DIV p-loop of *Th. sirtalis* (and other taxa) must be due in part to the specificity of toxin binding – only a subset of residues in the four p-loops actually interact with TTX (Fozzard and Lipkind 2010; Tikhonov and Zhorov 2012). However, it seems unlikely that binding specificity alone can explain convergence in the historical order of changes to the DIV p-loop.

Convergence can also arise due to different forms of substitution biases that influence which amino acid changes contribution to phenotypic variation. Mutational biases, like transition:transversion rates, may affect the direction of molecular evolution (Yampolsky and Stoltzfus 2001; Stoltzfus and Yampolsky 2009; Storz 2016); however, recent work has focused on fixation biases and negative pleiotropy. Certain beneficial mutations may be unlikely to persist due to pleiotropic effects that disrupt some other aspect of protein structure or function. Pleiotropy can bias the identity and position of mutations, but also the number of feasible mutational routes to an adaptive phenotype (DePristo et al. 2005; Miller et al. 2006; Weinreich et al. 2006; Tokuriki and Tawfik 2009; Feldman et al. 2012; Storz 2016). Epistatic effects arise through the combinatorial interactions of each successive mutation and its predecessors, so the consequences of each mutational step depend on its current genetic background (Weinreich et al. 2005,

2006; Poelwijk et al. 2007; Bank et al. 2016; Natarajan et al. 2016; Storz 2016). Thus, the overall effect of a series of mutations may depend on the sequential order in which they occur. For example, certain function-altering changes are contingent on a genetic background where other requisite or permissive mutations have already occurred (Ortlund et al. 2007; Blount et al. 2008; Bridgham et al. 2009; Harms and Thornton 2013; Storz 2016).

Changes to the $Na_V1.4$ pore probably reflect a delicate balance between TTX-resistant properties and the maintenance of $Na_V$ channel function (Feldman et al. 2012; Toledo et al. 2016). $Na_V$ channels play the highly conserved role of signaling in muscle and nerve tissue (Goldin 2002). We found a lack of polymorphism and negative Tajima's D values in the full *SNC4A* coding sequence (Supplemental Information S4, S5), which are consistent with a history of purifying selection on the $Na_V1.4$ channel. In particular, the p-loops of $Na_V$ channels are highly conserved among vertebrates (Tikhonov and Zhorov 2005; Brodie and Brodie 2015). The p-loops form the selectivity filter at the channel pore, which is critically responsible for the selective influx of $Na^+$ ions that propagate action potentials. Many of these amino acid residues in the filter also interact with TTX (Fozzard and Lipkind 2010), and TTX-resistant changes to the p-loops can compromise signaling properties of the channel by disrupting $Na^+$ conductance (Terlau et al. 1991; Feldman et al. 2012) and increasing calcium ion permeability (Heinemann et al. 1992). Consequently, only a limited number of mutations can confer TTX resistance without disrupting $Na_V$ ion channel function (Feldman et al. 2012; Toledo et al. 2016).

In western *Th. sirtalis*, the I1561V change was clearly the first mutational step towards TTX resistance in both hotspots (regardless of whether the changes are identical-

by-state or by-descent). Other point mutations in highly resistant alleles appear to be contingent on the I1561V change, because they always occur in combination. Alone, the I1561V change only provides a slight increase in resistance (Geffeney et al. 2005), and amino acid position 1561 is not thought to directly interact with TTX (Fozzard and Lipkind 2010). However, the Ile-Val change could modify pore structure in a way that disrupts interactions between TTX and other pore residues (Tikhonov and Zhorov 2011; Toledo et al. 2016). It could also represent a permissible intermediate step towards resistance, which enables other mutations that would otherwise disrupt channel function (e.g. Ortlund et al. 2007). Unfortunately, the individual and combinatorial effects of changes in the DIV p-loop have not been functionally evaluated.

Evidence from the $Na_V$ channels of other TTX-resistant taxa implies that amino acid position 1561 does play an important role in the mutational order of changes to the channel pore. For example, a Thr-Ser change at the homologous position in the $Na_V1.4$ channel of toxic newt species is associated with TTX resistance. This change is apparently ancestral to all newts (family: Salamandridae) and preceded three other amino acid changes to the DIV p-loop that confer even greater resistance to toxic modern newts (Hanifin and Gilly 2015). Pufferfish in the genus *Arothron* have an Ile-Met change at the homologous position in the $Na_V1.4a$ channel (teleost fish have two $Na_V1.4$ paralogs due to an ancient genome duplication; Jost *et al.* 2008). In *Th. sirtalis*, the $Na_V1.6$ paralog expressed in the peripheral nervous system (PNS) has an identical Ile-Val change at the same position, which apparently arose in parallel with $Na_V1.4$ and not due to gene conversion. This change probably confers low levels of TTX resistance to PNS channels,

but the substitution is ancestral to all Natricines and may not have initially evolved in response to TTX (McGlothlin et al. 2014, 2016).

*Evolutionary loss of TTX resistance?*

Our phylogenetic analysis indicated an unexpected evolutionary loss of TTX resistance in the Intermountain clade (Figure 4). If TTX-resistant changes to the DIV p-loop do have detrimental pleiotropic effects in the pore, selection could conceivably favor a loss in populations of *Th. sirtalis* that occur in allopatry with toxic newts. Lee et al. (2011) used a cloned mammalian $Na_V1.4$ channel to assess functional consequences of the single I1561V change and the highly resistant California allele (I1561V plus I1555L, D1568N, and G1569V) in the DIV p-loop. Both alleles resulted in a shift in the voltage dependence of slow inactivation, which could ultimately cause an increase in cell excitability. But, it is unclear if such shifts in biophysical properties actually perturb channel function or translate into fitness costs at the organismal level. Brodie and Brodie (1999) found preliminary evidence for a trade-off between whole-animal TTX resistance and crawl speed in *Th. sirtalis* from the Pacific Northwest (where we found TTX-resistant DIV alleles). In our sample, we found a recurrent pattern of heterozygote deficiency and high $F_{IS}$ values in the DIV p-loop of many populations (Table 1), which could reflect balancing selection for distinctly resistant and non-resistant genotypes.

The *SCN4A* gene tree may accurately reflect an evolutionary loss of TTX resistance, but we address two other alternatives. Due to the high proportion of TTX-resistant individuals on the Northwest coast (e.g. Ten Mile and Benton), we found few homozygous individuals with the ancestral DIV sequence (unlike the California hotspot,

e.g. Willow Creek). More dense taxon sampling, focused on individuals with the ancestral DIV sequence, could help improve phylogenetic resolution and sequence reconstruction in the Pacific Northwest (i.e. Hillis 1998; Hanson-Smith et al. 2010). For example, the tree topology could erroneously portray a loss of TTX resistance because our sample did not include genotypes that help root the Intermountain clade to ancestral individuals at the base of the Northwest Coast clade. In an alternative scenario, if evolutionary loss of TTX resistance is possible, the I1561V mutation could have instead evolved once in the ancestor of all western *Th. sirtalis*, but then was lost twice in the California and Northwest Coast clades. Future studies should assess the potential for an evolutionary loss of resistance in the $Na_V1.4$ channel.

*Conclusion*

Evolution is ultimately dependent on the input of novel genetic variation, but the mutations that actually contribute to adaptation may be biased toward a predictable subset of possible alternatives. In *Th. sirtalis*, convergent genetic evolution of TTX resistance in the $Na_V1.4$ channel pore proceeded through the same mutational first-step, an I1561V change that apparently arose twice in the separate hotpots. This repeated first step implies that molecular evolution in the $Na_V1.4$ channel follows a predictable set of rules, wherein an outcome of TTX resistance cannot be achieved unless mutations occur in a particular order within the DIV p-loop. Evolution is of course not entirely deterministic, as we also found unique point mutations in each hotspot.

A growing list of empirical studies point to the importance of sequential order in the mutational route to adaptation. Increasingly, context-dependent effects and intragenic

epistasis are recognized as pervasive forces in protein evolution (Weinreich et al. 2005, 2006; Poelwijk et al. 2007; Breen et al. 2012; Natarajan et al. 2013; Storz 2016). For example, in experimental evolution of antibiotic resistance in *E. coli*, the functional consequences of first-step mutations were strong determinants of the identity and order of subsequent adaptive substitutions (Salverda et al. 2011). In vertebrate glucocorticoid receptors, the eventual evolution of cortisol specificity depended on early permissive mutations with characteristic biophysical properties (Ortlund et al. 2007; Bridgham et al. 2009; Harms and Thornton 2014). Thus, the overall "predictability" of molecular evolution may ultimately depend on patterns of contingency and epistasis that determine the identity and order of amino acid substitutions (DePristo et al. 2005; Miller et al. 2006; Weinreich et al. 2006; Tokuriki and Tawfik 2009).

In extreme cases, sign epistasis can cause a single substitution to have opposing functional or fitness consequences in different genetic backgrounds (Weinreich et al. 2005; Harms and Thornton 2013; Shah et al. 2015; Storz 2016; Ono et al. 2017). Unlike our results, Natarajan et al. (2015, 2016) found that convergence in hemoglobin-oxygen affinity in high-altitude avian species did not evolve through a repeated order of mutations to hemoglobin. However, functional analysis showed that the effects of individual mutations were still dependent on their genetic background. Molecular evolution was therefore unpredictable due to lineage-specific patterns of intragenic epistasis. On the other hand, closely related taxa are predicted to share similar genetic and developmental constraints due to their common genetic background (Wake 1991; Arthur 2001; Yoon and Baum 2004; Losos 2011). If mutations do exhibit context-dependent effects, then protein evolution may be most predictable in closely related organisms, like

populations of *Th. sirtalis* that share a very similar $Na_V1.4$ protein sequence. Although molecular evolution is deterministic in both examples, hemoglobin and the $Na_V1.4$ channel, change may only be "predictable" in organisms that share similar genetic backgrounds.

**Acknowledgements**

This work was supported by a Rosemary Grant Award from the Society for the Study of Evolution, a Grant in Aid of Research from the Society for Integrative and Comparative Biology, a Theodore Roosevelt Memorial Grant from the American Museum of Natural History, and a Doctoral Dissertation Improvement Grant from the National Science Foundation (DEB 1601296) to MTJH and EDB III, as well as NSF awards to EDB III and EDB Jr. (DEB 0922216), and to CRF (IOS 1355221). We thank CAF&W for the scientific collecting permit (SC-000814 to CRF) and IACUCs for protocols to EDB Jr. at USU (1008) and CRF at UNR (00453 and 00687). We also thank C. Alencar and E. Ely for curating our *Th. sirtalis* tissue collections, and A. Mortensen, J. Scoville, A. Wilkinson, and G. Blaustein for aid with captive animal care. We thank J. McGlothlin for help with primer design. Members of the E. Brodie and R. Cox labs at the University of Virginia provided helpful comments that improved this manuscript. The authors declare no conflict of interest with this manuscript.

**Literature Cited**

Arthur, W. 2001. Developmental drive: an important determinant of the direction of phenotypic evolution. Evol. Dev. 3:271–278.

Avila, L. A. 2015. Feeding ecology and tetrodotoxin resistance in Eastern *Thamnophis sirtalis*. University of Virginia, Charlottesville, VA.

Bank, C., S. Matuszewski, R. T. Hietpas, and J. D. Jensen. 2016. On the (un)predictability of a large intragenic fitness landscape. Proc. Natl. Acad. Sci. 201612676.

Barrett, R. D. H., and D. Schluter. 2008. Adaptation from standing genetic variation. Trends Ecol. Evol. 23:38–44.

Blanchette, M., E. D. Green, W. Miller, and D. Haussler. 2004. Reconstructing large regions of an ancestral mammalian genome in silico. Genome Res. 14:2412–2423.

Bloom, J. D., L. I. Gong, and D. Baltimore. 2010. Permissive secondary mutations enable the evolution of influenza oseltamivir resistance. Science 328:1272–1275.

Blount, Z. D., C. Z. Borland, and R. E. Lenski. 2008. Historical contingency and the evolution of a key innovation in an experimental population of *Escherichia coli*. Proc. Natl. Acad. Sci. 105:7899–7906.

Breen, M. S., C. Kemena, P. K. Vlasov, C. Notredame, and F. A. Kondrashov. 2012. Epistasis as the primary factor in molecular evolution. Nature 490:535–538.

Bridgham, J. T., E. A. Ortlund, and J. W. Thornton. 2009. An epistatic ratchet constrains the direction of glucocorticoid receptor evolution. Nature 461:515–519.

Brodie III, E. D., and E. D. Brodie, Jr. 1999. Costs of exploiting poisonous prey: evolutionary trade-offs in a predator-prey arms race. Evolution 53:626–631.

Brodie III, E. D., and E. D. Brodie, Jr. 2015. Predictably convergent evolution of sodium channels in the arms race between predators and prey. Brain. Behav. Evol. 86:48–57.

Brodie III, E. D., and E. D. Brodie, Jr. 1990. Tetrodotoxin resistance in garter snakes: an evolutionary response of predators to dangerous prey. Evolution 44:651–659.

Brodie, Jr., E. D., B. J. Ridenhour, and E. D. Brodie III. 2002. The evolutionary response of predators to dangerous prey: hotspots and coldspots in the geographic mosaic of coevolution between garter snakes and newts. Evolution 56:2067–2082.

Brown, M. W., F. W. Spiegel, and J. D. Silberman. 2009. Phylogeny of the "forgotten" cellular slime mold, *Fonticula alba*, reveals a key evolutionary branch within Opisthokonta. Mol. Biol. Evol. 26:2699–2709.

Bruen, T. C., H. Philippe, and D. Bryant. 2006. A simple and robust statistical test for detecting the presence of recombination. Genetics 172:2665–2681.

Castoe, T. A., A. P. J. de Koning, H.-M. Kim, W. Gu, B. P. Noonan, G. Naylor, Z. J. Jiang, C. L. Parkinson, and D. D. Pollock. 2009. Evidence for an ancient adaptive episode of convergent molecular evolution. Proc. Natl. Acad. Sci. 106:8986–8991.

Castoe, T. A., and C. L. Parkinson. 2006. Bayesian mixed models and the phylogeny of pitvipers (Viperidae: Serpentes). Mol. Phylogenet. Evol. 39:91–110.

Chang, B. S. W., K. Jönsson, M. A. Kazmi, M. J. Donoghue, and T. P. Sakmar. 2002. Recreating a functional ancestral archosaur visual pigment. Mol. Biol. Evol. 19:1483–1489.

Christin, P.-A., D. M. Weinreich, and G. Besnard. 2010. Causes and evolutionary significance of genetic convergence. Trends Genet. 26:400–405.

Clement, M. J., Q. Snell, P. Walker, D. Posada, and K. A. Crandall. 2002. TCS: estimating gene genealogies.

Colosimo, P. F., K. E. Hosemann, S. Balabhadra, G. Villarreal Jr, M. Dickson, J. Grimwood, J. Schmutz, R. M. Myers, D. Schluter, and D. M. Kingsley. 2005. Widespread parallel evolution in sticklebacks by repeated fixation of ectodysplasin alleles. Science 307:1928–1933.

Corander, J., P. Marttinen, J. Sirén, and J. Tang. 2008. Enhanced Bayesian modelling in BAPS software for learning genetic structures of populations. BMC Bioinformatics 9:539.

Darriba, D., G. L. Taboada, R. Doallo, and D. Posada. 2012. jModelTest 2: more models, new heuristics and parallel computing. Nat Meth 9:772–772.

DePristo, M. A., D. M. Weinreich, and D. L. Hartl. 2005. Missense meanderings in sequence space: a biophysical view of protein evolution. Nat. Rev. Genet. 6:678–687.

Dong, K. 2007. Insect sodium channels and insecticide resistance. Invert. Neurosci. 7:17.

Excoffier, L., and H. E. L. Lischer. 2010. Arlequin suite ver 3.5: a new series of programs to perform population genetics analyses under Linux and Windows. Mol. Ecol. Resour. 10:564–567.

Feldman, C. R., E. D. Brodie, Jr., E. D. Brodie III, and M. E. Pfrender. 2012. Constraint shapes convergence in tetrodotoxin-resistant sodium channels of snakes. Proc. Natl. Acad. Sci. 109:4556–4561.

Feldman, C. R., E. D. Brodie, Jr., E. D. Brodie III, and M. E. Pfrender. 2010. Genetic architecture of a feeding adaptation: garter snake (*Thamnophis*) resistance to tetrodotoxin bearing prey. Proc. R. Soc. B Biol. Sci. 277:3317–3325.

Feldman, C. R., E. D. Brodie, Jr., E. D. Brodie III, and M. E. Pfrender. 2009. The evolutionary origins of beneficial alleles during the repeated adaptation of garter snakes to deadly prey. Proc. Natl. Acad. Sci. 106:13415–13420.

Fozzard, H. A., and G. M. Lipkind. 2010. The tetrodotoxin binding site is within the outer vestibule of the sodium channel. Mar. Drugs 8:219–234.

Geffeney, S., E. D. Brodie, Jr., P. C. Ruben, and E. D. Brodie III. 2002. Mechanisms of adaptation in a predator-prey arms race: TTX-resistant sodium channels. Science 297:1336–1339.

Geffeney, S. L., E. Fujimoto, E. D. Brodie III, E. D. Brodie, Jr., and P. C. Ruben. 2005. Evolutionary diversification of TTX-resistant sodium channels in a predator-prey interaction. Nature 434:759–763.

Goldin, A. L. 2002. Evolution of voltage-gated Na+ channels. J. Exp. Biol. 205:575–584.

Gompel, N., and B. Prud'homme. 2009. The causes of repeated genetic evolution. Dev. Biol. 332:36–47.

Gong, L. I., M. A. Suchard, and J. D. Bloom. 2013. Stability-mediated epistasis constrains the evolution of an influenza protein. eLife 2:e00631.

Guindon, S., and O. Gascuel. 2003. A simple, fast, and accurate algorithm to estimate large phylogenies by Maximum Likelihood. Syst. Biol. 52:696–704.

Hanifin, C. T., and W. F. Gilly. 2015. Evolutionary history of a complex adaptation: Tetrodotoxin resistance in salamanders. Evolution 69:232–244.

Hanson-Smith, V., B. Kolaczkowski, and J. W. Thornton. 2010. Robustness of ancestral sequence reconstruction to phylogenetic uncertainty. Mol. Biol. Evol. 27:1988–1999.

Harms, M. J., and J. W. Thornton. 2013. Evolutionary biochemistry: revealing the historical and physical causes of protein properties. Nat. Rev. Genet. 14:559–571.

Harms, M. J., and J. W. Thornton. 2014. Historical contingency and its biophysical basis in glucocorticoid receptor evolution. Nature 512:203–207.

Heinemann, S. H., H. Terlau, W. Stühmer, K. Imoto, and S. Numa. 1992. Calcium channel characteristics conferred on the sodium channel by single mutations. Nature 356:441–443.

Hillis, D. M. 1998. Taxonomic sampling, phylogenetic accuracy, and investigator bias. Syst. Biol. 47:3–8.

Holm, S. 1979. A simple sequentially rejective multiple test procedure. Scand. J. Stat. 6:65–70.

Innan, H., and Y. Kim. 2004. Pattern of polymorphism after strong artificial selection in a domestication event. Proc. Natl. Acad. Sci. U. S. A. 101:10667–10672.

Jakobsen, I. B., and S. Easteal. 1996. A program for calculating and displaying compatibility matrices as an aid in determining reticulate evolution in molecular sequences. Comput. Appl. Biosci. CABIOS 12:291–295.

Janzen, F. J., J. G. Krenz, T. S. Haselkorn, E. D. Brodie, Jr., and E. D. Brodie III. 2002. Molecular phylogeography of common garter snakes (*Thamnophis sirtalis*) in western North America: implications for regional historical forces. Mol. Ecol. 11:1739–1751.

Jost, M. C., D. M. Hillis, Y. Lu, J. W. Kyle, H. A. Fozzard, and H. H. Zakon. 2008. Toxin-resistant sodium channels: Parallel adaptive evolution across a complete gene family. Mol. Biol. Evol. 25:1016–1024.

Keenan, K., P. McGinnity, T. F. Cross, W. W. Crozier, and P. A. Prodöhl. 2013. diveRsity: an R package for the estimation and exploration of population genetics parameters and their associated errors. Methods Ecol. Evol. 4:782–788.

Kuchta, S. R., and A.-M. Tan. 2005. Isolation by distance and post-glacial range expansion in the Rough-Skinned Newt, *Taricha granulosa*. Mol. Ecol. 14:225–244.

Lee, C. H., D. K. Jones, C. Ahern, M. F. Sarhan, and P. C. Ruben. 2011. Biophysical costs associated with tetrodotoxin resistance in the sodium channel pore of the garter snake, *Thamnophis sirtalis*. J. Comp. Physiol. A 197:33–43.

Leigh, J. W., and D. Bryant. 2015. popart: full-feature software for haplotype network construction. Methods Ecol. Evol. 6:1110–1116.

Li, Y., Z. Liu, P. Shi, and J. Zhang. 2010. The hearing gene Prestin unites echolocating bats and whales. Curr. Biol. 20:R55–R56.

Librado, P., and J. Rozas. 2009. DnaSP v5: a software for comprehensive analysis of DNA polymorphism data. Bioinformatics 25:1451–1452.

Losos, J. B. 2011. Convergence, adaptation, and constraint. Evolution 65:1827–1840.

Mahoney, M. J. 2004. Molecular systematics and phylogeography of the *Plethodon elongatus* species group: combining phylogenetic and population genetic methods to investigate species history. Mol. Ecol. 13:149–166.

Marshall, D. C., C. Simon, T. R. Buckley, and A. Baker. 2006. Accurate branch length estimation in partitioned Bayesian analyses requires accommodation of among-partition rate variation and attention to branch length priors. Syst. Biol. 55:993–1003.

McGlothlin, J. W., J. P. Chuckalovcak, D. E. Janes, S. V. Edwards, C. R. Feldman, E. D. Brodie, Jr., M. E. Pfrender, and E. D. Brodie III. 2014. Parallel evolution of tetrodotoxin resistance in three voltage-gated sodium channel genes in the garter snake *Thamnophis sirtali*s. Mol. Biol. Evol. 31:2836–2846.

McGlothlin, J. W., M. E. Kobiela, C. R. Feldman, T. A. Castoe, S. L. Geffeney, C. T. Hanifin, G. Toledo, F. J. Vonk, M. K. Richardson, E. D. Brodie, Jr., M. E. Pfrender, and E. D. Brodie III. 2016. Historical contingency in a multigene family facilitates adaptive evolution of toxin resistance. Curr. Biol. 26:1616–1621.

McGuire, J. A., C. C. Witt, D. L. Altshuler, J. V. Remsen, K. Zamudio, and J. Sullivan. 2007. Phylogenetic systematics and biogeography of hummingbirds: Bayesian and Maximum Likelihood analyses of partitioned data and selection of an appropriate partitioning strategy. Syst. Biol. 56:837–856.

Mead, L. S., D. R. Clayton, R. S. Nauman, D. H. Olson, and M. E. Pfrender. 2005. Newly discovered populations of salamanders from Siskiyou County California represent a species distinct from *Plethodon stormi*. Herpetologica 61:158–177.

Miller, S. P., M. Lunzer, and A. M. Dean. 2006. Direct demonstration of an adaptive constraint. Science 314:458–461.

Natarajan, C., F. G. Hoffmann, R. E. Weber, A. Fago, C. C. Witt, and J. F. Storz. 2016. Predictable convergence in hemoglobin function has unpredictable molecular underpinnings. Science 354:336–339.

Natarajan, C., N. Inoguchi, R. E. Weber, A. Fago, H. Moriyama, and J. F. Storz. 2013. Epistasis among adaptive mutations in deer mouse hemoglobin. Science 340:1324–1327.

Natarajan, C., J. Projecto-Garcia, H. Moriyama, R. E. Weber, V. Muñoz-Fuentes, A. J. Green, C. Kopuchian, P. L. Tubaro, L. Alza, M. Bulgarella, M. M. Smith, R. E. Wilson, A. Fago, K. G. McCracken, and J. F. Storz. 2015. Convergent evolution of hemoglobin function in high-altitude Andean waterfowl involves limited parallelism at the molecular sequence level. PLOS Genet 11:e1005681.

Ono, J., A. C. Gerstein, and S. P. Otto. 2017. Widespread genetic incompatibilities between first-step mutations during parallel adaptation of Saccharomyces cerevisiae to a common environment. PLOS Biol. 15:e1002591.

Ortlund, E. A., J. T. Bridgham, M. R. Redinbo, and J. W. Thornton. 2007. Crystal structure of an ancient protein: Evolution by conformational epistasis. Science 317:1544–1548.

Payandeh, J., T. Scheuer, N. Zheng, and W. A. Catterall. 2011. The crystal structure of a voltage-gated sodium channel. Nature 475:353–358.

Poelwijk, F. J., D. J. Kiviet, D. M. Weinreich, and S. J. Tans. 2007. Empirical fitness landscapes reveal accessible evolutionary paths. Nature 445:383–386.

Prezeworski, M., G. Coop, and J. D. Wall. 2005. The signature of positive selection on standing genetic variation. Evolution 59:2312–2323.

R Core Team. 2016. R: A language and environment for statistical computing. R Foundation for Statistical Computing, Vienna, Austria.

Rambaut, A., M. Suchard, D. Xie, and A. Drummond. 2014. Tracer.

Raymond, M., and F. Rousset. 1995. GENEPOP (Version 1.2): Population genetics software for exact tests and ecumenicism. J. Hered. 86:248–249.

Ridenhour, B. 2004. The coevolutionary process: The effects of population structure on a predator-prey system. Indiana University, Bloomington, IN.

Ridenhour, B. J., E. D. Brodie III, and E. D. Brodie, Jr. 2004. Resistance of neonates and field-collected garter snakes (*Thamnophis* spp.) to tetrodotoxin. J. Chem. Ecol. 30:143–154.

Ronquist, F., M. Teslenko, P. van der Mark, D. L. Ayres, A. Darling, S. Höhna, B. Larget, L. Liu, M. A. Suchard, and J. P. Huelsenbeck. 2012. MrBayes 3.2: Efficient Bayesian phylogenetic inference and model choice across a large model space. Syst. Biol. 61:539–542.

Rousset, F. 2008. genepop'007: a complete re-implementation of the genepop software for Windows and Linux. Mol. Ecol. Resour. 8:103–106.

Salverda, M. L. M., E. Dellus, F. A. Gorter, A. J. M. Debets, J. van der Oost, R. F. Hoekstra, D. S. Tawfik, and J. A. G. M. de Visser. 2011. Initial mutations direct alternative pathways of protein evolution. PLOS Genet. 7:e1001321.

Schliep, K. P. 2011. phangorn: phylogenetic analysis in R. Bioinformatics 27:592–593.

Shah, P., D. M. McCandlish, and J. B. Plotkin. 2015. Contingency and entrenchment in protein evolution under purifying selection. Proc. Natl. Acad. Sci. 112:E3226–E3235.

Shi, Y., and S. Yokoyama. 2003. Molecular analysis of the evolutionary significance of ultraviolet vision in vertebrates. Proc. Natl. Acad. Sci. 100:8308–8313.

Shimodaira, H., and M. Hasegawa. 1999. Multiple comparisons of log-likelihoods with applications to phylogenetic inference. Mol. Biol. Evol.

Smith, J. M., and N. H. Smith. 2002. Recombination in animal mitochondrial DNA. Mol. Biol. Evol. 19:2330–2332.

Stamatakis, A. 2014. RAxML Version 8: A tool for phylogenetic analysis and post-analysis of large phylogenies. Bioinformatics 30:1312–1313.

Stephens, M., N. J. Smith, and P. Donnelly. 2001. A new statistical method for haplotype reconstruction from population data. Am. J. Hum. Genet. 68:978–989.

Stern, D. L., and V. Orgogozo. 2009. Is genetic evolution predictable? Science 323:746–751.

Stoltzfus, A., and L. Y. Yampolsky. 2009. Climbing mount probable: Mutation as a cause of nonrandomness in evolution. J. Hered. 100:637–647.

Storz, J. F. 2016. Causes of molecular convergence and parallelism in protein evolution. Nat. Rev. Genet. 17:239–250.

Stöver, B. C., and K. F. Müller. 2010. TreeGraph 2: Combining and visualizing evidence from different phylogenetic analyses. BMC Bioinformatics 11:7.

Swenson, N. G., D. J. Howard, A. E. M. E. Hellberg, and E. J. B. Losos. 2005. Clustering of contact zones, hybrid zones, and phylogeographic breaks in North America. Am. Nat. 166:581–591.

Tajima, F. 1983. Evolutionary relationship of DNA sequences in finite populations. Genetics 105:437–460.

Tajima, F. 1989. The effect of change in population size on DNA polymorphism. Genetics 123:597–601.

Templeton, A. R., K. A. Crandall, and C. F. Sing. 1992. A cladistic analysis of phenotypic associations with haplotypes inferred from restriction endonuclease mapping and DNA sequence data. III. Cladogram estimation. Genetics 132:619–633.

Terlau, H., S. H. Heinemann, W. Stühmer, M. Pusch, F. Conti, K. Imoto, and S. Numa. 1991. Mapping the site of block by tetrodotoxin and saxitoxin of sodium channel II. FEBS Lett. 293:93–96.

Tikhonov, D. B., and B. S. Zhorov. 2012. Architecture and pore block of Eukaryotic voltage-gated sodium channels in view of NavAb bacterial sodium channel structure. Mol. Pharmacol. 82:97–104.

Tikhonov, D. B., and B. S. Zhorov. 2005. Modeling p-loops domain of sodium channel: Homology with potassium channels and interaction with ligands. Biophys. J. 88:184–197.

Tikhonov, D. B., and B. S. Zhorov. 2011. Possible roles of exceptionally conserved residues around the selectivity filters of sodium and calcium channels. J. Biol. Chem. 286:2998–3006.

Tokuriki, N., and D. S. Tawfik. 2009. Stability effects of mutations and protein evolvability. Curr. Opin. Struct. Biol. 19:596–604.

Toledo, G., C. Hanifin, S. Geffeney, and E. D. Brodie III. 2016. Convergent evolution of tetrodotoxin-resistant sodium channels in predators and prey. Pp. 87–113 *in* R. J. F. and S. Y. Noskov, ed. Current Topics in Membranes. Academic Press.

Wake, D. B. 1991. Homoplasy: The result of natural selection, or evidence of design limitations? Am. Nat. 138:543–567.

Watterson, G. 1975. On the number of segregating sites in genetical models without recombination. Theor Popul Biol 7:256–276.

Weinreich, D. M., N. F. Delaney, M. A. DePristo, and D. L. Hartl. 2006. Darwinian evolution can follow only very few mutational paths to fitter proteins. Science 312:111–114.

Weinreich, D. M., R. A. Watson, and L. Chao. 2005. Perspective: Sign epistasis and genetic constraint on evolutionary trajectories. Evolution 59:1165–1174.

Woods, R., D. Schneider, C. L. Winkworth, M. A. Riley, and R. E. Lenski. 2006. Tests of parallel molecular evolution in a long-term experiment with *Escherichia coli*. Proc. Natl. Acad. Sci. 103:9107–9112.

Yampolsky, L. Y., and A. Stoltzfus. 2001. Bias in the introduction of variation as an orienting factor in evolution. Evol. Dev. 3:73–83.

Yang, Z. 2007. PAML 4: Phylogenetic Analysis by Maximum Likelihood. Mol. Biol. Evol. 24:1586–1591.

Yokoyama, S., and F. B. Radlwimmer. 2001. The molecular genetics and evolution of red and green color vision in vertebrates. Genetics 158:1697–1710.

Yoon, H.-S., and D. A. Baum. 2004. Transgenic study of parallelism in plant morphological evolution. Proc. Natl. Acad. Sci. U. S. A. 101:6524–6529.

Zhang, J., and M. Nei. 1997. Accuracies of ancestral amino acid sequences inferred by the parsimony, likelihood, and distance methods. J. Mol. Evol. 44:S139–S146.

## Tables and Figures

**Table 1.** Population estimates of phenotypic TTX resistance and DIV p-loop allele variation.

| Population | County | 50% MAMU dose | No. of individuals | $N_A$ | $H_O$ | $H_E$ | $F_{IS}$ | HWE Exact Test |
|---|---|---|---|---|---|---|---|---|
| Bear Lake | Bear Lake Co., ID | 3.6 | 14 | 1 | - | - | - | - |
| Benton | Benton Co., OR | 34.1 | 43 | 3 | 0.233 | 0.498 | 0.536 | 0.0002* |
| Carmel Valley † | Monterey Co., CA | 451.0 | 27 | 2 | 0.148 | 0.492 | 0.703 | 0.0003* |
| Clallam | Clallam Co., WA | 4.5 | 12 | 1 | - | - | - | - |
| Cresecent | Del Norte Co., CA | 4.2 | 12 | 1 | - | - | - | - |
| Dupont | Pierce Co., WA | 27.9 | 19 | 2 | 0.158 | 0.508 | 0.695 | 0.0040* |
| East Bay | Contra Costa Co., CA | 945.1 | 4 | 1 | - | - | - | - |
| Feather Lake † | Lassen Co., CA | 3.1 | 9 | 1 | - | - | - | - |
| Gilroy | Santa Cruz Co., CA | 18.4 | 33 | 3 | 0.303 | 0.514 | 0.415 | 0.0015* |
| Hoquiam | Grays Harbor Co., WA | 7.0 | 4 | 2 | 0.000 | 0.429 | 1.000 | 0.1436 |
| Howard Lake † | Mendocino Co., CA | 22.7 | 6 | 1 | - | - | | - |
| Ledson Marsh | Sonoma Co., CA | 10.4 | 11 | 2 | 0.455 | 0.506 | 0.107 | 1.0000 |
| Lofton Lake | Lake Co., OR | 2.2 | 13 | 1 | - | - | - | - |
| Lost Lake | Hood River Co., OR | 4.6 | 7 | 1 | - | - | - | - |
| Mill City | Marion Co., OR | 15.9 | 6 | 3 | 0.167 | 0.712 | 0.783 | 0.0132 |
| Omo | El Dorado Co., CA | 560.0 | 5 | 1 | - | - | - | - |
| Orick | Humboldt Co., CA | 4.6 | 8 | 1 | - | - | - | - |
| Parsnip | Jackson Co., OR | 4.7 | 10 | 1 | - | - | - | - |
| Potter's Slough | Pacific Co., WA | 19.6 | 15 | 3 | 0.267 | 0.674 | 0.613 | 0.0087 |
| Priest Lake | Texada Island, BC | 4.3 | 10 | 1 | - | - | - | - |
| San Simeon | San Luis Obispo Co., CA | 5.6 | 7 | 2 | 0.000 | 0.264 | 1.000 | 0.0739 |
| Skagit | Skagit Co., WA | 4.4 | 17 | 1 | - | - | - | - |
| Stayton | Marion Co., OR | 22.2 | 11 | 3 | 0.091 | 0.602 | 0.855 | 0.0006* |
| Ten Mile | Lane Co., OR | 52.2 | 7 | 2 | 0.000 | 0.440 | 1.000 | 0.0204 |
| Warrenton | Clatsop Co., OR | 15.2 | 22 | 3 | 0.045 | 0.210 | 0.788 | 0.0014* |
| Willits | Mendocino Co., CA | 6.7 | 16 | 2 | 0.063 | 0.175 | 0.651 | 0.0970 |
| Willow Creek | Sonoma Co., CA | 729.7 | 20 | 2 | 0.000 | 0.185 | 1.000 | 0.0019* |

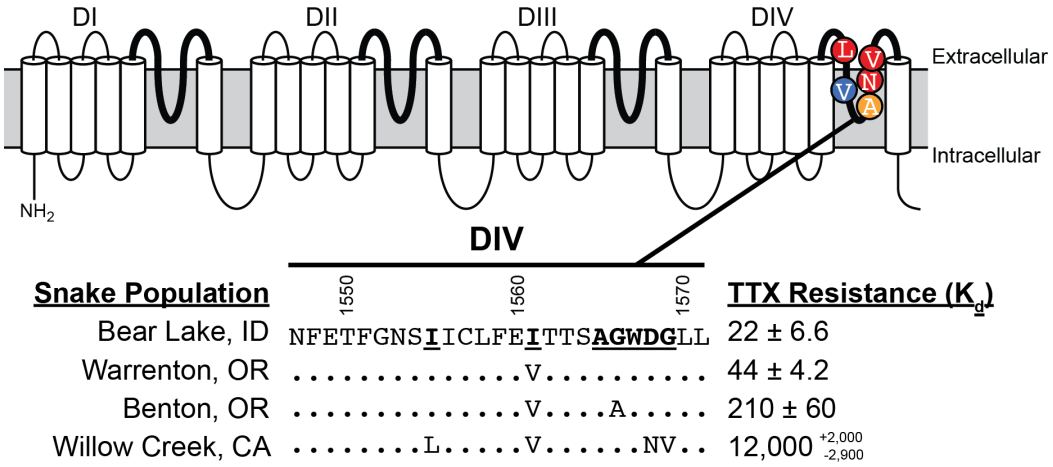


**Figure 1.** Schematic of the $Na_V1.4$ skeletal muscle sodium channel in *Th. sirtalis*. Each domain (DI-IV) is shown above with the extracellular pore loops (p-loops) in solid black lines. Specific amino acid changes in the DIV p-loop are show in their relative positions in the pore. Below, the ancestral DIV p-loop sequence is listed (collected from Bear Lake, ID), as well as derived changes identified in three other individuals from TTX-resistant populations. The TTX resistance of each allele ($K_d$ ±95% C.I.) was previously evaluated in cloned $Na_V1.4$ channels, measured as the concentration of TTX (nM) that blocks 50% of cloned channels (Geffeney et al. 2005).

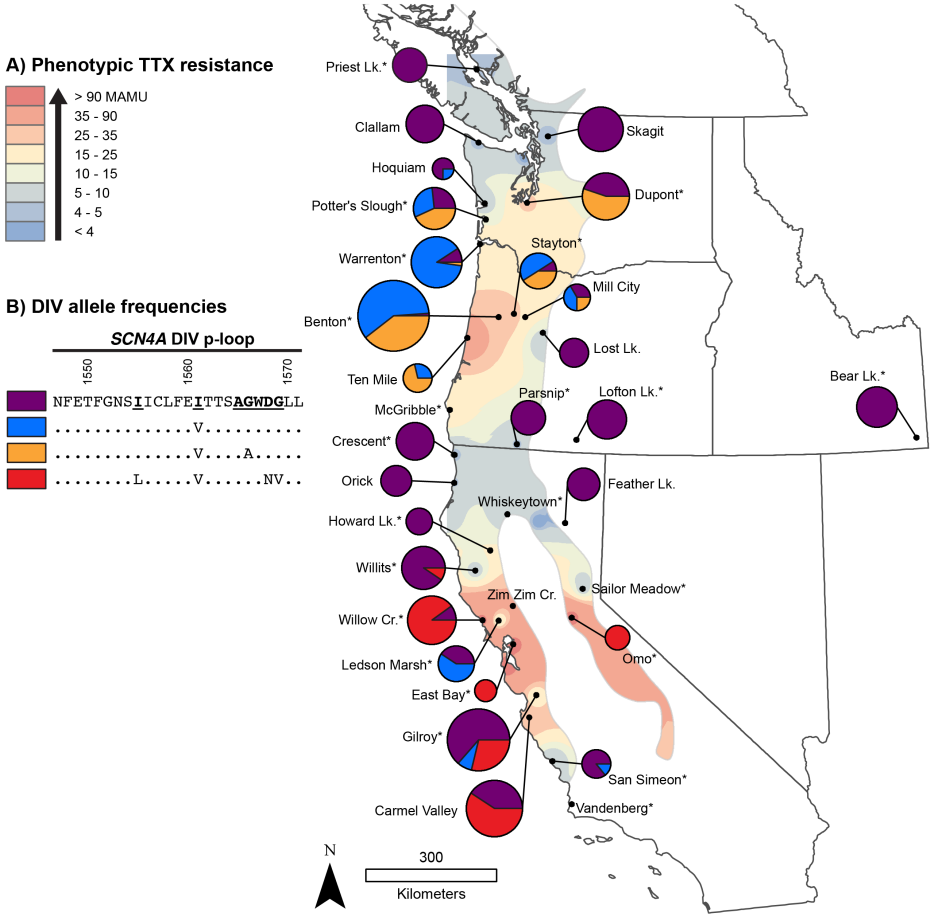


**Figure 2. A)** Average phenotypic TTX resistance (50% MAMU) in populations of *Th. sirtalis* in western North America. Estimates are interpolated across the geographic range wherein *Th. sirtalis* occur in sympatry with *Taricha* newts (recreated from Brodie et al. 2002). **B)** Pie charts indicate observed population frequencies of the four unique DIV alleles identified in this study. Chart size is proportional to the sample size at each location. All localities used in the phylogenetic analysis are marked with an asterisk (*).

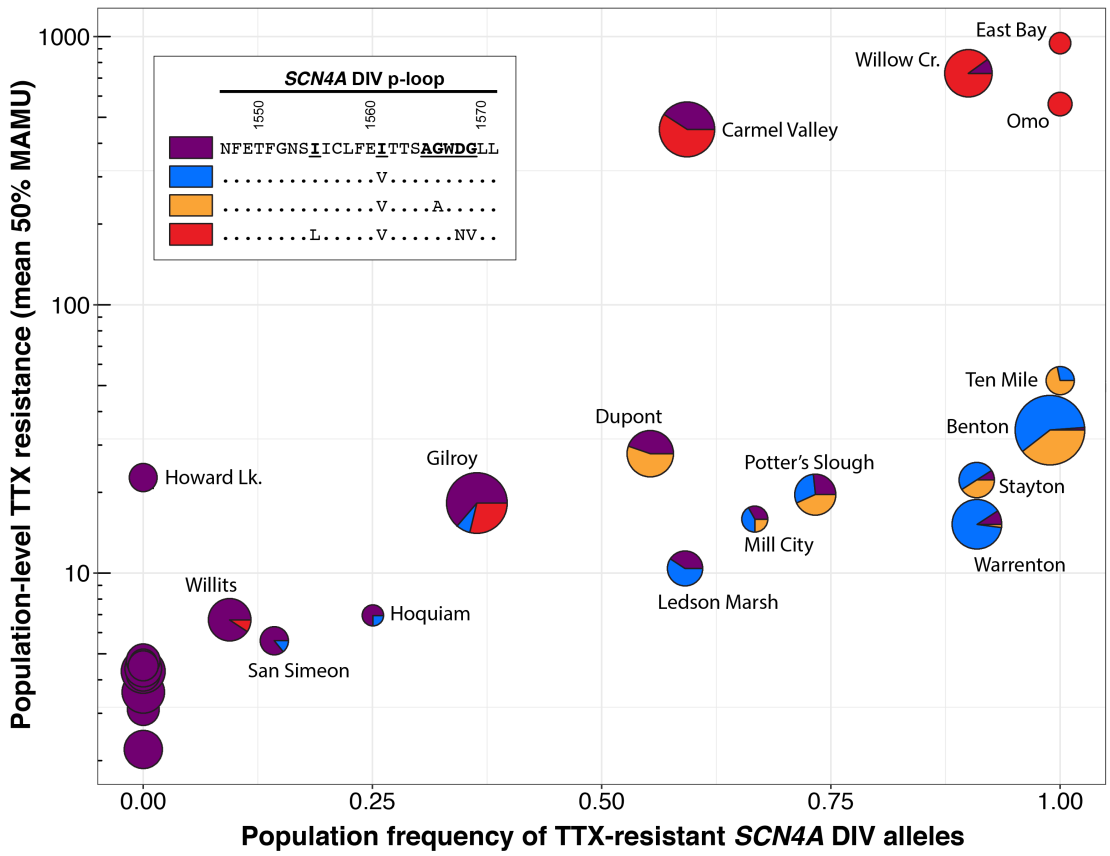


**Figure 3.** Relationship between the frequency of TTX-resistant DIV alleles and the phenotypic TTX resistance (50% MAMU) of each population. Each locality is represented by its pie chart from Figure 2. All alleles that differ from the ancestral DIV sequence have been demonstrated to be TTX resistant. All unlabeled localities clustered in the lower left-hand corner have <5 MAMU estimates of TTX resistance.

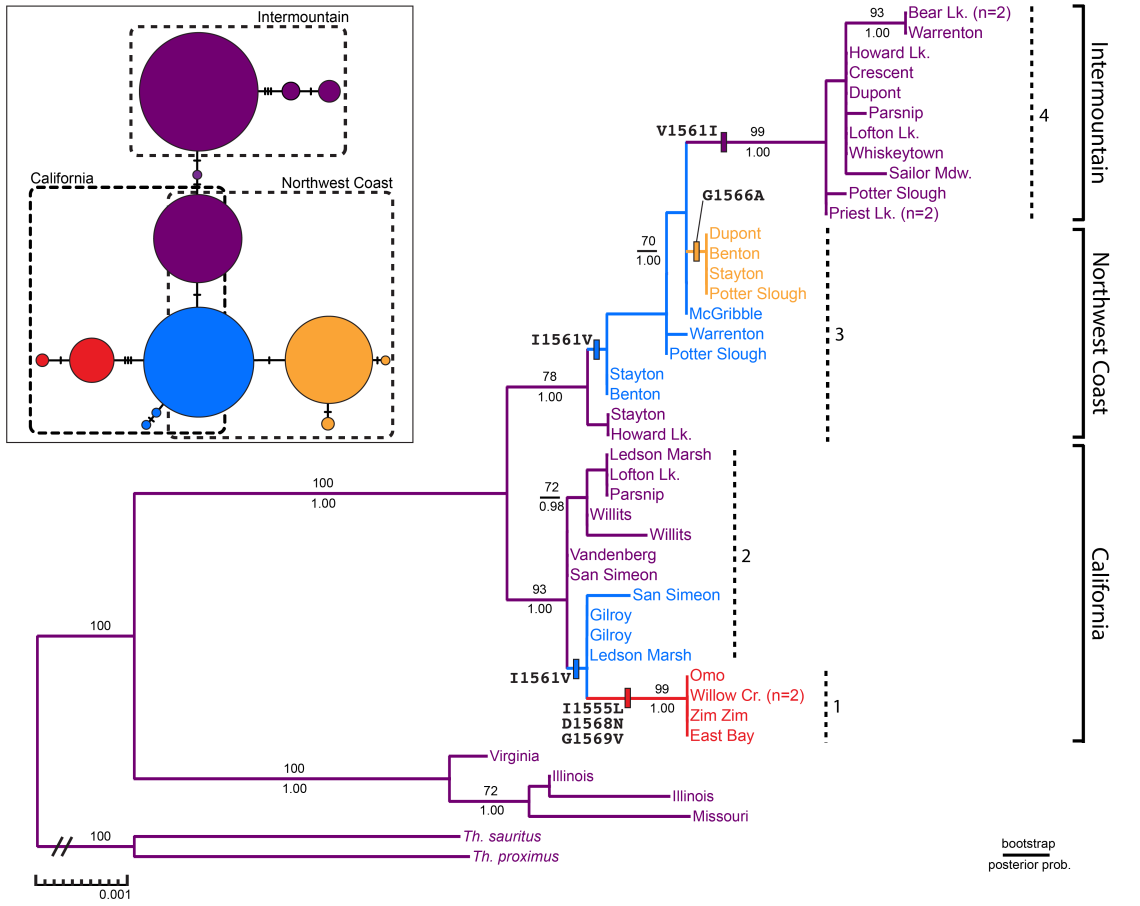


**Figure 4.** Evolutionary relationships among DIV sequences. Inset shows the haplotype network of the 666bp of exon 26 protein-coding sequence that includes the DIV p-loop. Circles represent unique observed haplotypes with size proportional to their frequency in the sample. Intermediate mutational steps are represented by dashes along the lines connecting haplotypes. Each haplotype is color-coded by its DIV p-loop amino acid sequence, as in Figure 2. Approximate geographic groupings are shown with dashed boxes. Below, the *SCN4A* gene tree is shown with ML bootstrap support and BI posterior probabilities. Each individual taxon is labeled according to its sampling location and color-coded by its DIV p-loop sequence. Branches are labeled to reflect the identify of mutational changes from the PAML ancestral sequence reconstruction of the DIV p-loop.

Vertical dashed lines to the right of taxa (labeled 1-4) identify the four genetic groups from the BAPS analysis.

**Supplemental Information**

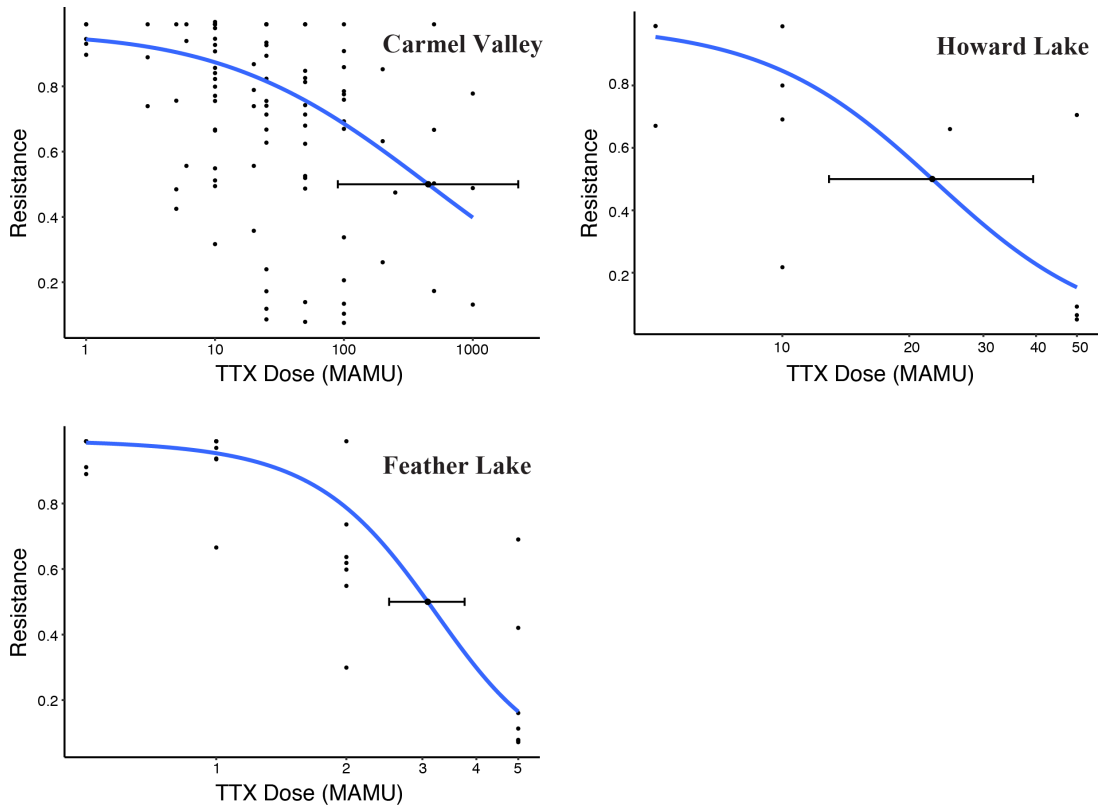


**Supplemental Information S1.** Dose-response curves of phenotypic TTX resistance for populations of *Th. sirtalis* assayed in this study. Curves were estimated with curvilinear regression, in accordance with Brodie *et al.* 2002 and Ridenhour *et al.* 2004.

For each population, the estimated 50% MAMU dose is marked with 95% confidence intervals. All statistics were performed in R (R Core Team 2016).

**Supplemental Information S2.** Population estimates of phenotypic TTX resistance for populations assayed for the first time in this study. N is the number of individuals assayed and $N_i$ is the total number of TTX injections given to the group. The estimated 50% MAMU dose of each population is shown, including 95% confidence intervals, the intercept (α) and slope (β) of the curvilinear regression, and the significance level (p-value).

| **Population** | **N** | **$N_i$** | **Estimated 50% dose** | **Lower 95% CI** | **Upper 95% CI** | **α** | **β** | **p-value** |
|---|---|---|---|---|---|---|---|---|
| Carmel Valley | 26 | 97 | 451.0 | 89.7 | 2252.4 | -3.18 | 0.52 | 0.0003 |
| Feather Lake | 24 | 31 | 3.1 | 2.5 | 3.8 | -5.96 | 4.23 | 0.0000 |
| Howard Lake | 4 | 12 | 22.7 | 12.9 | 39.4 | -7.06 | 2.23 | 0.0066 |

**Supplemental S3.** Primer sequences

| **Full *SCN4A* protein-coding sequence** | |
|---|---|
| Exon.1.F | 5'-CAGAAGCACCATGGACGAGT-3' |
| Exon.1.R | GAAGCTGTTCCGAGCAAAGC |
| Exon.2.F | AGCTGACCAACTGCATAACCA |
| Exon.2.R | CCACACACCTTCCTCTGCTT |
| Exon.3.F | AACAAGCACAAGCCCAAAGC |
| Exon.3.R | TACCTCCCCTGCTGATGTCA |
| Exon.4.F | TGTAGGCCTTTTTGGGGGTG |
| Exon.4.R | CCCCATTCAATTTCCCATGGC |
| Exon.5.F | ATTGGCCAGGATCCCAACAG |
| Exon.5.R | GCTTTAGCTTTGTCATCCCCA |
| Exon.6.F | AGACTTGGGCAACGTCTCTG |
| Exon.6.R | CACACACACACGGTTGCTTT |
| Exon.7.F | ACAAGTCTGGCTCTCCTCCT |
| Exon.7.R | GGTTTCGGCCAGCTTTCATG |
| Exon.8.F | CCAGTCATTCCCTCTCAGCC |
| Exon.8.R | CTGGGTTGCTACACCCTGTT |
| Exon.9.F | TTCCAGGTACCAAGGAGGGT |
| Exon.9.R | CTCCCCGACACCCAAAATGA |
| Exon.10a.F | TTGGCTATCCTGTTGGCTGG |
| Exon.10a.R | GGTTCCTGGTGCATGGAGAA |
| Exon.10b.F | GCCTAACTCTAACCCTAGCCC |
| Exon.10b.R | ATGCTGGACTGAGGTGGTTG |
| Exon.13.F | CAACCACCTCAGTCCAGCAT |
| Exon.13.R | TTGGAATCAGAGGCACCACC |
| Exon.14.F | AATAATTTGGGGGCGGAGGG |
| Exon.14.R | CCCTGGCTGATGGCACTTAT |
| Exon.15.F | ATTTGGGGAGGGATGCTTCC |
| Exon.15.R | GCAGTTGGCAACTTGTGACC |
| Exon.16.F | GGGCTGAAAGGCAAAAGTGG |
| Exon.16.R | TCCAGCCAGATGCATCTCTG |
| Exon.17.F | TATGGCGAACGCTTTGGACA |
| Exon.17.R | TAGCCAGCTTGGTGTGACTG |
| Exon.18.F | CAGCAAGGCGACTCTTCTGT |
| Exon.18.R | GAGGCACTGGAGCTATCTGG |
| Exon.19.F | TCTGTCCCCTCCCGAATGAT |
| Exon.19.R | AGCTGGGGAGAAAAGCAGTT |

| | |
|---|---|
| Exon.20.F | GCTGCTGAGCATCCTTCTGA |
| Exon.20.R | TGGTAACCTCTGCGGCAAAT |
| Exon.21.F | TGATCATTGCTCTGGCTGCA |
| Exon.21.R | GGTCAAAGGGCAAGCTGAGA |
| Exon.22-23.F | CCCAAATCCCACTCATGGCT |
| Exon.22-23.R | GAAGGCTGCACTGTACCCTT |
| Exon.24.F | AATTGGAGCCCTTGGAGCAA |
| Exon.24.R | GGGGTGTTTCTGAGGGGAAC |
| Exon.25.F | TGTCTTGCACCCTTCCTGTC |
| Exon.25.R | GGCTGGGTGAAGCAAGAGAA |
| Exon.26a.F | GCACCTTTTTGTATCCTTTCTGC |
| Exon.26a.R | TGCTTCAGGGCATCCATTTCTCCA |
| Exon.26b.F | AAGAGCCGCTGAGAATTGCT |
| Exon.26b.R | CCAGAAGAGGAGATGCTGCA |

| ***SCN4A* 3' flanking non-coding sequence** | |
|---|---|
| Seg1.1F | ATTTCTGGCTTGTTTGCTTG |
| Seg1.2F | ATGTGCAGCATCTCCTCTTC |
| Seg1.1R | TGCACCCATACTGTACATGC |
| Seg1.2R | GACATTGCAGTTTTGTGTTCC |
| Seg2.1F | TATGGGTGCAAAATGAATGG |
| Seg2.2F | TGGCTGGAAGTCCAATTAAG |
| Seg2.1R | GCAGGTGCTTCTATGCCTAC |
| Seg2.2R | ATGGAAAGGAAGATGTGCTC |
| Seg3.1F | AAAAGTGGTGAGGACAGCAG |
| Seg3.2F | CCCTGGGTCTTTTAACTTTATG |
| Seg3.1R | AGGTGTTGAGGTTGTCCATC |
| Seg3.2R | GTGATTTCACCAGGCATTG |
| Seg5.1F | TCCTAATGGGAGATTGGGTAG |
| Seg5.2F | GATAGTCCAATTTGGGTTGG |
| Seg5.1R | CCTGGACTGACTAAACCTTGC |
| Seg5.2R | TGACAAAACATCCTACGAAGC |
| Seg6.1F | TGTTTACTTTCCCTCCAGTCC |
| Seg6.2F | CACTTGAGTTTCCCAGGTTG |
| Seg6.1R | CACATCACCCCATAGACTGC |
| Seg6.2R | AGTGAGTGGGAGACTGATGC |

**Supplemental Information S4.** Nucleotide variation in the full *SCN4A* protein-coding sequence in two focal populations of *Th. sirtalis* from the geographically distinct hotspots. The number of segregating sites, estimates of Nei's and Watterson's θ (π and θ, respectively), and Tajima's D values for the full *SNC4A* sequence are shown for each population. Estimates of π and θ are shown for all nucleotide sites, and for only synonymous (S) and non-synonymous (NS) positions.

| Location | No. of individuals | No. of seg. sites | π (all sites) | π (S) | π (NS) | θ (all sites) | θ (S) | θ (NS) | Tajima's D |
|---|---|---|---|---|---|---|---|---|---|
| Bay Area | 10 | 4 | 0.00021 | 0.00000 | 0.00027 | 0.00031 | 0.00000 | 0.00040 | -0.950 |
| Benton | 10 | 10 | 0.00051 | 0.00137 | 0.00023 | 0.00071 | 0.00194 | 0.00027 | -0.970 |

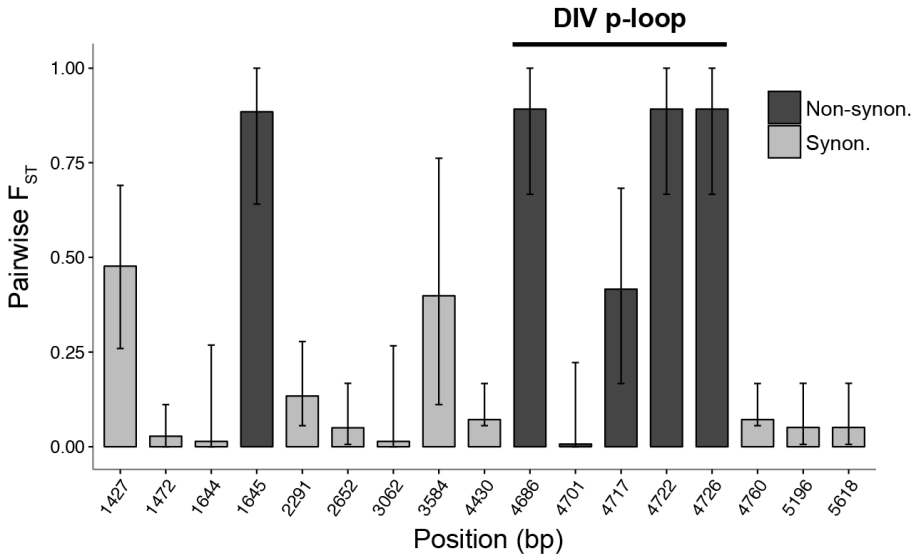


**Supplemental Information S5.** Pairwise $F_{ST}$ estimates for all polymorphic synonymous and non-synonymous positions in the full *SCN4A* protein-coding sequence. The location of each polymorphic nucleotide position along the *SCN4A* coding-sequence is shown on the x-axis. Invariant sites were removed from the analysis. To visualize among-population variation between the Bay Area and Benton sites, we calculated individual $F_{ST}$ values for each polymorphic nucleotide position. Positions are color-coded as either non-synonymous or synonymous, and those located in the DIV p-loop are identified above.

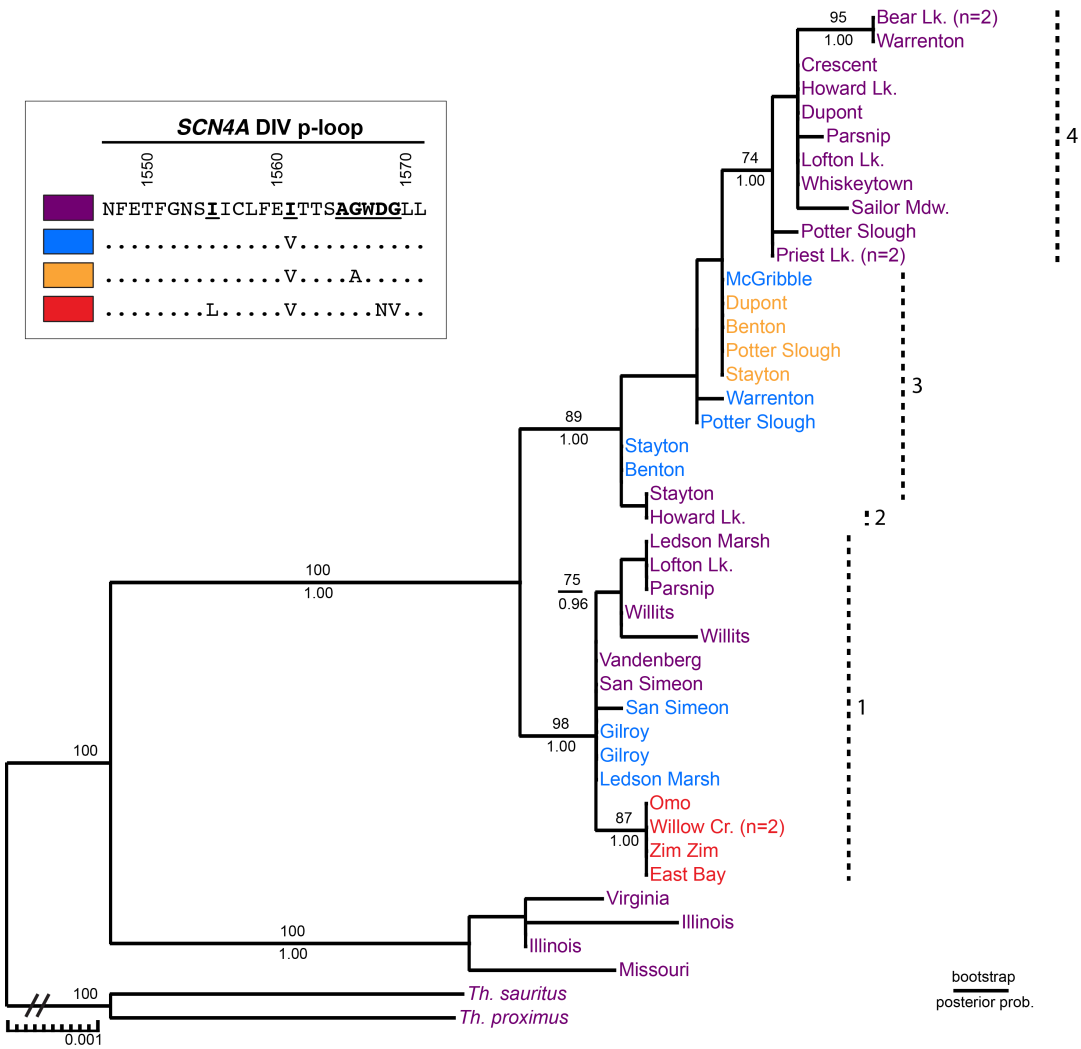


**Supplemental Information S6.** Phylogenetic and BAPS analyses of the reduced dataset (excluding the 1144bp fragment of exon 26 coding sequence). Vertical dashed lines to the right of taxa (labeled 1-4) identify the four genetic groups from the BAPS analysis. The reduced analysis produced geographic groups that were largely consistent with the full partitioned analysis, with one exception. The Howard Lk. individual in the Northwest Coast clade formed its own cluster in the BAPS analysis. This perhaps occurred because the Howard Lk. individual contained five heterozygous sites coded as ambiguities, which may have confounded cluster assignment. Like the full partitioned analysis, the topology of the best ML tree was a significantly better fit than the constraint tree where all I1561V

taxa were forced into monophyly (Shimodaira-Hasegawa test, p=0.0002). We were unable to conduct the ancestral sequence reconstruction in PAML, because taxa with different DIV p-loop alleles (e.g. Gilroy and Vandenberg) were collapsed down in polytomies.

# CHAPTER 2:

Large-effect mutations generate trade-off between predatory and locomotor ability during arms race coevolution with deadly prey[2]

[2]As published: Hague, MTJ, G Toledo, SL Geffeney, CT Hanifin, ED Brodie, Jr., ED Brodie III. 2018. Large-effect mutations generate trade-off between predatory and locomotor ability during arms race coevolution with deadly prey. *Evolution Letters*, 2: 406-416.

**Abstract**

Adaptive evolution in response to one selective challenge may disrupt other important aspects of performance. Such evolutionary trade-offs are predicted to arise in the process of local adaptation, but it is unclear if these phenotypic compromises result from the antagonistic effects of simple amino acid substitutions. We tested for trade-offs associated with beneficial mutations that confer tetrodotoxin (TTX) resistance in the voltage-gated sodium channel ($Na_V1.4$) in skeletal muscle of the common garter snake (*Thamnophis sirtalis*). Separate lineages in California and the Pacific Northwest independently evolved TTX-resistant changes to the pore of $Na_V1.4$ as a result of arms race coevolution with toxic prey, newts of the genus *Taricha*. Snakes from the California lineage that were homozygous for an allele known to confer large increases in toxin resistance ($Na_V1.4^{LVNV}$) had significantly reduced crawl speed compared to individuals with the ancestral TTX-sensitive channel. Heterologous expression of native snake $Na_V1.4$ proteins demonstrated that the same $Na_V1.4^{LVNV}$ allele confers a dramatic increase in TTX resistance and a correlated decrease in overall channel excitability. Our results suggest the same mutations that accumulate during arms race coevolution and beneficially interfere with toxin-binding also cause changes in electrophysiological function of the channel that may affect organismal performance. This trade-off was only evident in the predator lineage where coevolution has led to the most extreme resistance phenotype, determined by four critical amino acid substitutions. If these biophysical changes also translate to a fitness cost—for example, through the inability of *T. sirtalis* to quickly escape predators—then pleiotropy at this single locus could contribute to

observed variation in levels of TTX resistance across the mosaic landscape of coevolution.

**Impact Summary**

Evolutionary trade-offs are commonly expected to arise during the process of adaptation. As populations diverge and adapt to local conditions, compromises can develop between related traits, like virulence and spore production in pathogens, or microbial resistance and growth in plants. At a mechanistic level, it is almost entirely unclear how genetic changes mediate these higher level ecological trade-offs. This study bridges that gap by linking specific mutations that evolved in response to one selective challenge, deadly prey, to consequences for protein function and organismal performance that present an ecological cost. Garter snakes in western North America evolved TTX resistance as a result of arms race coevolution with their toxic prey, newts of the genus *Taricha*. We found that trade-offs at multiple levels of biological organization occur due to beneficial mutations that confer tetrodotoxin (TTX) resistance in the skeletal muscle sodium channel ($Na_V1.4$) of the common garter snake (*Thamnophis sirtalis*). Snakes with toxin-resistant mutations in $Na_V1.4$ had significantly reduced crawl speed, a whole-animal measure of muscle performance. The same set of TTX-resistant mutations reduces the overall excitability of voltage-gated sodium channels, a critical component of the vertebrate nervous system. These results suggest that the antagonistic effects of just a small number of amino acid substitutions at a single locus have the potential to influence broader ecological trade-offs and drive mosaic patterns of adaptation across the landscape.

## Introduction

The evolutionary process occurs in the context of economic limitations, such that adaptations in one phenotypic dimension can compromise structure or function in another (Lynch and Gabriel 1987; Whitlock 1996; Brodie and Brodie 1999; Ghalambor et al. 2004; Kawecki and Ebert 2004; Bono et al. 2017). Specialization for a specific task is predicted to reduce overall performance in others (i.e. a jack-of-all-trades is a master of none; Huey and Hertz 1984; Thompson 1986, 1994; Futuyma and Moreno 1988; Remold 2012). Consequently, as populations diverge and adapt to local conditions, compromises can arise at the phenotypic level, for example, between virulence and spore production in pathogens (Thrall and Burdon 2003), or microbial resistance and growth in plants (Todesco et al. 2010). But, at an underlying molecular level, these trade-offs must be driven to a degree by specific changes in protein function and biomechanics, such that the biophysical changes of a single mutation may be beneficial in one sense, but disruptive to other important aspects of performance (Wang et al. 2002; DePristo et al. 2005; Weinreich et al. 2006; Harms and Thornton 2013; Natarajan et al. 2016; Storz 2016). In this respect, pleiotropy is thought to be an important driver of broader phenotypic patterns of adaptation; however, a functional link between changes in the structure of individual proteins and population variation in phenotypic trade-offs remains tenuous (Hall et al. 2010; Anderson et al. 2011, 2013; Savolainen et al. 2013; Ågren et al. 2013, 2017; Bono et al. 2017). We predict that as beneficial mutations accrue in response to one selective challenge, their pleiotropic effects will generate trade-offs observable in landscape patterns of phenotypic variation.

In this study, we examined whether functional trade-offs develop as a result of the stepwise mutational changes that accumulate en route to an escalated adaptation. We tested whether alleles that confer tetrodotoxin (TTX) resistance in the common garter snake (*Thamnophis sirtalis*) also reduce other aspects of whole-animal performance and underlying protein function. Populations of *T. sirtalis* in western North America evolved resistance to the neurotoxin TTX as a result of arms race coevolution with deadly prey, newts of the genus *Taricha* (Brodie et al. 2002; Hanifin et al. 2008). Throughout their sympatric range, garter snakes prey occasionally on newts along with other amphibians. Individual differences in snake resistance and newt toxicity predict whether a given predator-prey interaction goes to completion, ending with the consumption of prey and/or incapacitation of predator (Williams et al. 2003, 2010). Population patterns of predator resistance and prey toxicity vary by several orders of magnitude across the spatial landscape, creating a geographic mosaic of coevolving traits with roughly matched abilities in both species. Snakes from two distinct coevolutionary "hotspots", California and the Pacific Northwest, independently evolved resistance through convergent amino acid changes to the skeletal muscle voltage-gated sodium channel ($Na_V1.4$) that disrupt TTX-binding at the molecular level (Figure 1A; Geffeney et al. 2005; Hague et al. 2017).

The deadly effects of TTX occur because the toxin binds to the outer pore of voltage-gated sodium channels ($Na_V$) in muscle and nerve tissue, blocking the influx of sodium ions and preventing action potential propagation (Fozzard and Lipkind 2010; Tikhonov and Zhorov 2012). The channels comprise four homologous domains (DI-DIV), each of which contains a pore-loop (p-loop) that together form the outer pore of the channel where TTX molecules bind (Terlau et al. 1991; Fozzard and Lipkind 2010;

Payandeh et al. 2011; Tikhonov and Zhorov 2012; Toledo et al. 2016). TTX-resistant mutations to the DIV p-loop of $Na_V1.4$ arose in a stepwise fashion within each phylogenetically distinct lineage of *T. sirtalis* (Figure 1A). An I1561V change (i.e. $Na_V1.4^V$) was the first resistant substitution to arise in both California and the Pacific Northwest, followed later by more resistant mutations to the DIV p-loop that are unique within each lineage (Hague et al. 2017). Functional expression of derived alleles from California ($Na_V1.4^V$ and $Na_V1.4^{LVNV}$) and the Pacific Northwest ($Na_V1.4^V$ and $Na_V1.4^{VA}$) confirms they confer increasing levels of TTX resistance to $Na_V1.4$ (Geffeney et al. 2005). Channel-level TTX resistance conferred by each DIV allele is tightly correlated with muscle and whole-animal levels of resistance (Geffeney et al. 2002, 2005; Feldman et al. 2010; Hague et al. 2017). Across western populations of *T. sirtalis*, TTX-resistant alleles occur at high frequency within each of the two hotspots sympatric with toxic newts, but are largely absent in surrounding "coldspots" where newts are non-toxic (Brodie et al. 2002; Hanifin et al. 2008; Hague et al. 2017).

Within a few populations of garter snakes, it appears that TTX resistance is negatively correlated with locomotor performance—individuals with higher resistance crawl slower—suggesting a possible tradeoff associated with the evolution of resistance (Brodie and Brodie 1999). Crawl speed is an important measure of performance in reptiles (e.g. Shine et al. 2000; Aubret et al. 2007) and is under positive survival selection in some populations of garter snakes (Jayne and Bennett 1990). This relationship suggests that adaptation to toxic prey might come at a cost of reduced organismal performance, which also may be important in structuring broader mosaic patterns of

coevolution (e.g. hotspots and coldspots). We investigated the underlying molecular basis for a putative trade-off between TTX resistance and locomotor performance.

Some amino acid residues in the pore of $Na_V1.4$ that determine TTX resistance also play a conserved role in electrical signaling in skeletal muscle tissue (Goldin 2002; Tikhonov and Zhorov 2005; Lee et al. 2011; Brodie and Brodie 2015; Toledo et al. 2016). Therefore, we predicted that mutations to the DIV p-loop that disrupt toxin-binding would generate a functional trade-off between TTX resistance and other phenotypes related to muscle performance. Because resistance of the $Na_V1.4$ channel evolved twice—in California and separately in the Pacific Northwest—we were able to conduct two evolutionarily independent tests for costs associated with TTX resistance. In each lineage, we tested for a relationship between DIV p-loop genotype and phenotypic variation in crawl speed, a whole-animal measure of muscle performance. Then, to evaluate the presumed underlying mechanism, we functionally expressed snake $Na_V1.4$ channels in *Xenopus* oocytes and tested whether derived alleles in the DIV p-loop caused pleiotropic changes to electrophysiological properties of the channel.

## Methods

### *Crawl speed assay*

If TTX-resistant mutations to $Na_V1.4$ also disrupt skeletal muscle function, then we expected snakes with derived genotypes in the DIV p-loop to have reduced crawl speed compared to those with the ancestral, non-resistant channel. To test for a relationship between DIV genotype and crawl speed, we collected genotypic information from neonate snakes for which phenotypic variation in TTX resistance and crawl speed

were previously collected (Brodie et al. 2002; Feldman et al. 2010; Hague et al. 2017). The final datasets included 77 neonate snakes from seven populations in California and 95 neonates from 11 populations in the Pacific Northwest at sites that co-occur with *Taricha* newts (Figure 1B, Table S1). These neonates were born in the lab to wild-caught females, providing a uniformly aged sample of variation in crawl speed that was largely unexposed yet to postnatal selection.

Females were collected from the wild between 1985-2001 and 2004-2005 and returned to the laboratory at Utah State University. Within 24 hours of parturition, neonates were measured for mass (g), snout-vent length (SVL; mm), and total length (mm), and then housed individually in 15x10.5 cm plastic tubs. Each neonate was stimulated to crawl for 2 m on a 4 x 0.1 m linear racetrack lined with indoor-outdoor carpet. The racetrack was equipped with infrared sensors to electronically record sprint speed over 0.5 m intervals. Crawl speed was measured as the maximum velocity (m/s) over any 0.5 m interval. We raced each individual twice, and used the average as our crawl speed estimate. A single observer (EDB, Jr.) conducted all crawl speed trials in order to limit variance among observers. Previous work has shown that crawl speed estimates from this protocol are highly repeatable (Brodie and Brodie 1999; Brodie et al. 2002; Ridenhour et al. 2004; Feldman et al. 2010).

The neonates were also genotyped for their amino acid sequence in the DIV p-loop of the $Na_V1.4$ channel. Methods for DNA extraction from tail tip tissue and Sanger sequencing are described in Hague et al. 2017. For each individual, we sequenced a 666 bp fragment that includes the DIV p-loop region of $Na_V1.4$. Heterozygous positions on chromatograms were identified by eye and confirmed in both directions with sequencing.

The haplotype phase of the DIV p-loop sequence for each individual was inferred computational with the program PHASE (Stephens et al. 2001) and then translated into the amino acid sequence. We detected few subjects with a heterozygous DIV p-loop, or from the California lineage with the $Na_V1.4^{V/V}$ genotype (see Table S1), so these individuals were removed from the dataset due to insufficient power.

We used R version 3.4.1 (R Core Team 2018) to test for a relationship between the response variable (neonate crawl speed [m/s]) and the independent variable, genotype of the DIV p-loop in $Na_V1.4$. We used a mixed modeling approach with the "lmer" function implemented in the *lme4* package (Bates et al. 2015). The DIV p-loop genotype of each neonate was coded as a categorical fixed effect, with each unique genotype as a different level. We included SVL and mass in the model as fixed effects, because crawl speed in garter snakes scales with body length and mass (Arnold and Bennett 1988; Garland 1988; Brodie 1992, 1993). We also included the latitude of the population where each neonate originated in the wild as a fixed effect, because mean body size varies among populations in *T. sirtalis* (Brodie et al. 2002), and personal observations suggest that size varies along a latitudinal gradient. Finally, the population where each neonate originated was included as a random effect. Statistical significance of fixed effects was determined by an ANOVA using a Wald Chi-Square test with type III sum of squares and one degree of freedom, implemented in the *car* R package (Fox and Weisberg 2011).

Our goal was to conduct a replicated test for trade-offs with crawl speed in two monophyletic lineages of *T. sirtalis*, California and the Pacific Northwest, so we analyzed data from the two regions in separate statistical models. Populations in California and the Pacific Northwest are geographically separated and genetically divergent according to

autosomal and mitochondrial loci (Janzen et al. 2002; Hague et al. 2017). Moreover, a gene tree of the $Na_V1.4$ protein, based on genomic DNA from neonates in this study, indicates that TTX resistance in the DIV p-loop evolved independently in the two lineages (Hague et al. 2017). Therefore, we assigned neonates to either the California or Pacific Northwest lineage based on the $Na_V1.4$ tree. As a precaution, we did not include populations located in between the two lineages, along the California/Oregon border, because it is an apparent region of historical vicariance, and may now represent a contact zone between southern and northern lineages. Populations in this region all lack variation in $Na_V1.4$, such that only the ancestral, non-resistant sequence ($Na_V1.4^{+}$) is found (Hague et al. 2017).

*Heterologous expression of $Na_V1.4$ mutants*

We tested whether changes in the biophysical function of the channel might underlie locomotor trade-offs by evaluating the function of snake $Na_V1.4$ channels expressed in heterologous *Xenopus* oocytes. We generated clones of $Na_V1.4$ with the ancestral DIV p-loop sequence ($Na_V1.4^{+}$) and two derived alleles ($Na_V1.4^{V}$ and $Na_V1.4^{LVNV}$), expressed each channel variant, and then measured TTX binding affinity ($K_d$). We also recorded the voltage-dependence of activation and fast-inactivation ($V_{1/2}$) in order to visualize channel excitability—the window current for which each channel is available to open and initiate action potentials in skeletal muscle tissue (Ketelaars et al. 2001; Remy et al. 2003; Barker et al. 2016).

The three different alleles were constructed in the background of a native, non-resistant $Na_V1.4$ channel sampled from *T. sirtalis* in Illinois, outside the range of *Taricha*

newts. Populations in Illinois are closely related and ancestral to western *T. sirtalis*, and contain the non-resistant p-loop sequence of $Na_V1.4$ (Janzen et al. 2002; Hague et al. 2017). All evidence suggests that western *T. sirtalis* and the Illinois sample share very high sequence similarity in $Na_V1.4$ (99.7%) throughout the full 1,875 amino acid sequence of the protein (Hague et al. 2017). Our Illinois construct improves upon previous expression work, which measured the effects of TTX-resistant mutations from *T. sirtalis* in the divergent genetic background of mammalian $Na_V1.4$ proteins (e.g. Geffeney et al. 2005; Lee et al. 2011). Due to resource constraints, we were only able to assess a limited number of mutants. We chose to focus our analysis on the two most common derived alleles in the wild ($Na_V1.4^{V}$ and $Na_V1.4^{LVNV}$).

The native $Na_V1.4$ construct was generated using Gibson assembly (Gibson et al. 2009). We first used Sanger sequencing to generate the full protein-coding sequence of $Na_V1.4$ from an individual in Illinois (Hague et al. 2017). The synthetic $Na_V1.4$ cDNA sequence (1,875 aa, 5,625 bp) was codon optimized (IDT) for expression in *Xenopus laevis* oocytes. Two silent EcoRV cut sites were included at positions 4,482 and 5,211 to allow for mutagenesis. We used a commercial supplier (IDT) to generate four synthetic oligonucleotides (≈1,400 bp each) that corresponded to the codon-optimized cDNA. The blocks included 20 bp overlapping regions with each other and the target vector to enable Gibson assembly. We assembled gene fragments with a linearized (SmaI, NEB) vector (pGEMHE, courtesy of J. Rosenthal) that included a T7 promotor for in vitro mRNA synthesis, 3' and 5' *Xenopus* globin UTRs, and a poly-A tail using standard Gibson assembly protocols (NEB). The product of this reaction was transformed into competent JM109 cells (Promega, USA) and selectively screened using standard protocols. Positive

clones were sequenced using Sanger sequencing (Sequetech; USA) to ensure correct assembly and orientation of the $Na_V1.4$ sequence. We chose one correct clone, which was re-transformed and sequence verified for further expression and mutagenesis.

The three channel variants were then constructed using Gibson assembly. Sequence-verified plasmids with the complete $Na_V1.4$ insert were digested with EcoRV (NEB) and purified in agarose gel (0.8%) to isolate the 8.5 kb fragment. The fragment was further purified and concentrated using standard Phenol:Choloroform protocols and $Na^+$ acetate precipitation. The resulting linearized plasmid was identical to the native $Na_V1.4$ construct with approximately 700 bp removed from the DIV region of the protein. We constructed all three DIV alleles ($Na_V1.4^+$, $Na_V1.4^V$, and $Na_V1.4^{LVNV}$) with the same approach. The three different constructs were then linearized with a Nhe1 digestion (NEB). We used a T7 ultra mMessage mMachine kit (Life Technologies) to synthesize capped and tailed mRNAs and then injected 5-30 ng of each channel clone mRNA into stage 5 *Xenopus* oocytes (EcoCyte Bioscience).

Ionic currents were measured at room temperature (22-25°C) 2-7 days after mRNA injection using the cut-open oocyte Vaseline gap voltage-clamp technique (Stefani and Bezanilla 1998) with a CA-1B High Performance Oocyte Clamp (Dagan Instruments). Recordings were made in an external solution containing (in mM): 120 Na-Mes, 10 Hepes-Na, 1.8 $CaCl_2$, pH 7.2 and an internal solution containing (in mM): 110 K-Mes, 10 Na-Mes, 10 Hepes-K, 1 EGTA-K, pH 7.2. Current records were acquired using Axon pClamp software (version 10, Molecular Devices), sampling at 100 kHz and filtering at 20 kHz. The holding potential for all experiments was -100 mV. Leak subtraction was performed with the use of a *p*/4 protocol.

We first measured TTX binding affinity to assess the TTX resistance of each channel clone. Peak currents were evoked at 0.05 Hz with 20-ms pulses to 0 mV following a 500 ms prepulse to -150 mV. Peak current amplitudes were measured offline with Igor Pro (Wavemetrics). The ratio of peak currents in the presence and absence of TTX over a range of TTX concentrations were calculated with peak currents recorded before and after perfusing the selected TTX concentration into the external bath solution for 5 minutes. To estimate the TTX concentration that blocked 50% of the expressed channels, the data were fitted to an equation derived from a single-site Langmuir adsorption isotherm, current ratio = 1/1+[TTX]/$K_d$ in which [TTX] is the concentration of toxin and $K_d$ is the concentration of TTX at which half of the channels are bound to the toxin. $K_d$ and its 95% confidence limits were estimated from the curve using Igor Pro (Wavemetrics).

We next measured the voltage-dependence of activation and fast-inactivation to assess the gating properties of each cloned channel. The voltage-dependence of activation was measured from the peak inward current during a 20 ms test pulse to voltages ranging from -100 to 80 mV in 10 mV steps following a 500-ms prepulse to -150 mV. The voltage-dependence of fast-inactivation was measured from the peak inward current during a 20 ms pulse to 0 mV after a 500 ms, conditioning prepulse ranging from -150 to -10 mV in 10 mV increments. Peak current amplitudes were measured during test pulses offline with Igor Pro (Wavemetrics). Conductance-voltage relationships were derived using the following equation: $G_{Na} = I_{peak}/(V_M - E_{Na})$ where $G_{Na}$ represents sodium conductance, $I_{peak}$ is the peak-test-pulse current, $V_M$ is the test-pulse voltage, and $E_{Na}$ is the measured sodium equilibrium potential. Activation and fast-inactivation curves were

fitted by a Boltzmann distribution with the following equation: Normalized conductance or current amplitude = $1/(1+ \exp(-ze_0(V_M - V_{1/2})/kT))$ where $z$ is the apparent valence, $e_0$ is the elementary charge, $V_{1/2}$ is the midpoint voltage, $k$ is the Boltzmann constant, and $T$ is the temperature in degrees Kelvin. $V_{1/2}$ and its 95% confidence limits were estimated from the curve using Igor Pro (Wavemetrics). Finally, for each cloned variant, we visualized channel window current as the area below the normalized overlapping activation and fast-inactivation curves.

**Results and Discussion**

*Resistance mutations are linked to reduced crawl speed*

In the Pacific Northwest lineage, we did not find a significant relationship between DIV p-loop genotype and crawl speed. Body mass was the only significant fixed effect in the model (Table 1; Wald $\chi^2$ =4.02, p=0.045), which is consistent with previous work that shows locomotor ability depends on mass and SVL in *Thamnophis* species (Arnold and Bennett 1988; Garland 1988; Brodie 1992, 1993). Unlike in the Pacific Northwest, in California we found that the DIV p-loop genotype accounted for significant variance in crawl speed of neonate snakes (Wald $\chi^2$ =6.09, p=0.014). Animals with the highly TTX-resistant $Na_V1.4^{LVNV/LVNV}$ genotype had a slower mean crawl speed than individuals with the ancestral wildtype channel (Figure 2). SVL also significantly affected crawl speed in the California lineage (Wald $\chi^2$ =16.10, p<0.001).

The pattern observed in the California lineage suggests a compromise between two phenotypes linked to the function of $Na_V1.4$ in skeletal muscle tissue: TTX resistance and crawl speed. The four amino acid substitutions in the $Na_V1.4^{LVNV}$ allele, shown

previously to confer large increases in whole-animal resistance (Geffeney et al. 2002, 2005; Feldman et al. 2010; Hague et al. 2017), appear to disrupt muscle performance to an extent that is detectable at the organismal level. It is unlikely the reduction in crawl speed is due to unaccounted for changes in other regions of $Na_V1.4$ linked to the DIV p-loop, because the majority of protein-coding sequence is extremely conserved in *T. sirtalis*. Of the 1,875 residues in the $Na_V1.4$ channel, only one other amino acid position in western *T. sirtalis* exhibits polymorphism outside of the substitutions in the DIV p-loop examined here. That single change is distantly located in the intracellular portion of the protein, such that it is unlikely to influence channel biophysics or occur in linkage with substitutions in the DIV p-loop (Hague et al. 2017).

The changes found in the $Na_V1.4^{LVNV}$ allele represent a late escalatory stage of TTX resistance in the arms race with toxic newts. Of all derived alleles in either California and the Pacific Northwest, $Na_V1.4^{LVNV}$ contains the most amino acid changes to the channel pore and confers the largest increase in phenotypic TTX resistance (Hanifin et al. 2008; Hague et al. 2017). The $Na_V1.4^{LVNV}$ channel is an order of magnitude more resistant than any other known variant in *T. sirtalis* (see below; Geffeney et al. 2005), and snakes with even one copy of $Na_V1.4^{LVNV}$ have extremely high levels of phenotypic TTX resistance (Feldman et al. 2010). In fact, *T. sirtalis* in the California lineage are so resistant they appear to have escaped the arms race and can consume sympatric newts with little or no consequence (Hanifin et al. 2008). This level of escalation has not occurred in the Pacific Northwest lineage. Reduced crawl speed in California, but not in less-resistant populations from the Pacific Northwest, implies that

negative trade-offs only arise late in the adaptive trajectory of the TTX-resistant $Na_V1.4$ channel.

We tested for categorical differences in crawl speed among DIV p-loop genotypes, but previous work suggests a trade-off between whole-animal TTX resistance and crawl speed may also occur on a continuous scale at the individual level. In populations from the Pacific Northwest, Brodie and Brodie (1999) found that individual variation in phenotypic TTX resistance was negatively associated with crawl speed (although the DIV genotype of each individual was unknown). Our model did not find evidence for a trade-off in the Pacific Northwest; however, mutations to the pore of $Na_V1.4$ are not the sole determinant of whole-animal TTX resistance (McGlothlin et al. 2014, 2016; Feldman et al. 2015). Consequently, there may be other unknown mechanisms that contribute to a trade-off between physiological resistance and crawl speed.

*Resistance mutations alter channel function*

Heterologous expression of cloned $Na_V1.4$ variants demonstrated the $Na_V1.4^{V}$ channel had a small increase in TTX resistance compared to the ancestral wildtype ($K_d$=65 nM; Figure 3A), which was coupled with a 7 mV shift in the voltage-dependence of fast-inactivation towards more depolarized potentials ($V_{1/2}$=-49.2 mV; Table 2, Figure S1). These changes resulted in a slight overall increase in the window current of the channel (Figure 3B). The $Na_V1.4^{LVNV}$ channel, in contrast, generated a dramatic 260-fold increase in TTX resistance ($K_d$=13,000 nM; Figure 3A) coupled with a large 20 mV shift in the voltage-dependence of activation towards more depolarized potentials ($V_{1/2}$=-16.4

mV; Table 2, Figure S1). The depolarized shift in activation led to a clear reduction in the window current of the $Na_V1.4^{LVNV}$ channel (Figure 3C).

Our results indicate that TTX-resistant mutations to the channel pore have pleiotropic effects on important aspects of protein function. The large shifts in voltage-dependence of activation and window current found in the $Na_V1.4^{LVNV}$ clone suggest that TTX-resistant mutations cause a reduction in the excitability of $Na_V1.4$ channels in skeletal muscle tissue. These shifts were not observed in past experiments that expressed the same TTX-resistant substitutions in the foreign genetic background of a mammalian $Na_V1.4$ channel (Lee et al. 2011). Mutations to the DIV p-loop disrupt toxin-binding at the outer pore, but they also occur in an important region for gating and ion conductance in voltage-gated ($Na_V$) sodium channels (Vilin and Ruben 2001; Hilber et al. 2005; Xiong et al. 2006; Lee et al. 2011). The p-loop sequences are otherwise highly conserved in vertebrates (Goldin 2002; Tikhonov and Zhorov 2005; Brodie and Brodie 2015; Toledo et al. 2016; Hague et al. 2017) and $Na_V1.4$ is thought to be under strong purifying selection for the maintenance of its important role in electrical signaling of muscle tissue (Brodie and Brodie 2015). The changes to excitability we observed in the $Na_V1.4^{LVNV}$ clone are consistent with a trade-off between TTX resistance and muscle performance in the crawl speed assay. Similar depolarizing shifts in the voltage-dependence of activation, for example, occur in humans with a congenital myopathy that causes general muscle weakness and delays in developmental milestones like walking (Zaharieva et al. 2016). A number of mutations to $Na_V1.4$ in humans are linked to comparable muscle pathologies like paralysis and weakness (Cannon 1996; Lehmann-Horn and Jurkat-Rott

1999; Vilin and Ruben 2001; Jurkat-Rott et al. 2015; Nicole and Fontaine 2015; Zaharieva et al. 2016; Hinard et al. 2017).

Ultimately, evolution of the pore sequence of $Na_V1.4$ must strike a balance between TTX-resistant properties and the maintenance of channel function (Feldman et al. 2012; Brodie and Brodie 2015; Toledo et al. 2016). Our results are consistent with other work that shows TTX-resistant mutations in the DIV p-loop affect a range of biophysical properties in $Na_V$ channels. Slow-inactivation, a more prolonged form of $Na_V$ inactivation, is also altered by changes to the pore of the channel. TTX-resistant mutations in the $Na_V1.4^{LVNV}$ allele have been shown to alter the voltage-dependence of slow-inactivation towards more depolarized membrane potentials (Lee et al. 2011; Toledo et al. *unpubl. data*). In addition to gating, amino acid residues in the pore are critically responsible for the selective influx of $Na^+$ ions that propagate action potentials. TTX-resistant mutations to the pore can disrupt $Na^+$ conductance (Terlau et al. 1991; Feldman et al. 2012) and increase calcium ion permeability (Heinemann et al. 1992). For example, the D1568N amino acid substitution in $Na_V1.4^{LVNV}$ removes a negative charge that interacts with TTX, but also causes a decrease in ion conductance (Terlau et al. 1991; Toledo et al. 2016).

TTX-resistant mutations in the California lineage clearly affect important electrophysiological properties of $Na_V1.4$ and correlate with reductions in organismal performance of crawl speed. However, the mechanistic link between changes to $Na_V1.4$ function and reduced organismal performance still remains untested. To unequivocally demonstrate a functional link between TTX-resistant mutations, their electrophysiological effects, and locomotor performance would require direct recordings

from muscle fibers of snakes with known genotypes. Only then could we establish whether the reduced excitability we observed in $Na_V1.4^{LVNV}$ causes changes to threshold and speed of action potential conductance in skeletal muscle tissue. Therefore, we cannot rule out alternative explanations for the relationships we detected between DIV genotype, channel function, and organismal performance. For example, compensatory effects in the muscle cells of TTX-resistant snakes, like changes to $Na_V1.4$ expression or the sodium-potassium pump, could ameliorate reduced excitability in $Na_V1.4^{LVNV}$. In addition, the four mutations in the DIV p-loop of $Na_V1.4^{LVNV}$ might have different functional consequences depending on their genetic background. We inserted the DIV allele into an $Na_V1.4$ background based on an Illinois snake, which differs in sequence identity from western populations by no more than five other amino acids substitutions. However, the sequences are otherwise 99.7% identical throughout the 1,875 amino acid positions of the channel (Hague et al. 2017), and the five differences occur in regions that do not regulate activation or fast-inactivation. Thus, we consider it unlikely that this small number of differences would dramatically confound our interpretations.

*Conclusion*

As a population evolves towards a new adaptive peak, phenotypic compromises are expected to arise if an underlying allele impacts multiple aspects of organismal performance (Felsenstein 1976; Hedrick et al. 1976; Hedrick 1986, 2006; Kawecki and Ebert 2004; Bono et al. 2017). In the arms race with toxic newts, populations of *T. sirtalis* that evolved exaggerated TTX resistance experience an apparent trade-off as mutations accumulate in the otherwise conserved pore region of $Na_V1.4$. These costs are not clear at

every mutational step, such as the single substitution we examined from the Pacific Northwest, but they become evident where coevolution has led to extreme phenotypes and the largest number of substitutions at the underlying level. The trade-off we observed may ultimately limit coevolutionary dynamics if snakes experience a fitness cost. Garter snakes must avoid their own predators, including birds and mammals, and crawl speed in *T. sirtalis* has previously been shown to influence survival (Jayne and Bennett 1990; Shine et al. 2000). A phenotypic trade-off between resistance and locomotion has important implications for landscape-level patterns of coevolution. For example, TTX-resistant alleles like $Na_V1.4^{LVNV}$ may be favored in localities where toxic newts represent strong reciprocal selection, but disfavored in areas with non-toxic newts where reduced crawl speed and anti-predator ability are more important contributors to survival.

Geographic patterns of $Na_V1.4$ polymorphism appear to support balancing selection for such a trade-off in the arms race. In wild populations, TTX-resistant alleles occur at high frequency in geographic "hotspots" with toxic newts, but at low frequency in neighboring "coldspots" where newts have little or no toxin (Hanifin et al. 2008; Hague et al. 2017). This mosaic pattern implies the existence of spatial variation in selection on $Na_V1.4$ alleles. In California, allele frequencies shift from predominantly TTX-resistant ($Na_V1.4^{LVNV}$) to non-resistant ($Na_V1.4^{+}$) over the short geographic distance of about 150 km (Hague et al. 2017). For alleles with pleiotropic effects, like $Na_V1.4^{LVNV}$, balancing selection is expected to maintain genetic polymorphism across a heterogeneous landscape of selection, like a mosaic of variably toxic newt populations (Turelli and Barton 2004; Charlesworth 2006; Mitchell-Olds et al. 2007). At conserved loci of large effect, like the $Na_V1.4$ channel, maintenance of polymorphism may be

predicted because single mutations result in trade-offs that alter whole-animal measures of performance.

**Acknowledgements**

This work was supported by a Rosemary Grant Award from the Society for the Study of Evolution, a Grant-in-Aid of Research from the Society for Integrative and Comparative Biology, a Theodore Roosevelt Memorial Grant from the American Museum of Natural History, and a Doctoral Dissertation Improvement Grant from the National Science Foundation (DEB 1601296) to MTJH, as well as an NSF award to EDB III (DEB 0922216). Work at USU was supported by a New Faculty Success and Scholarship Grant (USU) to CTH. We thank IACUC for the protocol to EDB Jr. at USU (1008). R. Cox, R. Costello, P. Cook, and E. Butterfield at UVA provided helpful comments that improved this manuscript. The authors declare no conflict of interest with this manuscript.

**Literature Cited**

Ågren, J., C. G. Oakley, S. Lundemo, and D. W. Schemske. 2017. Adaptive divergence in flowering time among natural populations of *Arabidopsis thaliana*: Estimates of selection and QTL mapping. Evolution 71:550–564.

Ågren, J., C. G. Oakley, J. K. McKay, J. T. Lovell, and D. W. Schemske. 2013. Genetic mapping of adaptation reveals fitness tradeoffs in *Arabidopsis thaliana*. Proc. Natl. Acad. Sci. 110:21077–21082.

Anderson, J. T., C.-R. Lee, C. A. Rushworth, R. I. Colautti, and T. Mitchell-Olds. 2013. Genetic trade-offs and conditional neutrality contribute to local adaptation. Mol. Ecol. 22:699–708.

Anderson, J. T., J. H. Willis, and T. Mitchell-Olds. 2011. Evolutionary genetics of plant adaptation. Trends Genet. 27:258–266.

Arnold, S. J., and A. F. Bennett. 1988. Behavioural variation in natural populations. V. morphological correlates of locomotion in the garter snake (*Thamnophis radix*). Biol. J. Linn. Soc. 34:175–190.

Aubret, F., X. Bonnet, and R. Shine. 2007. The role of adaptive plasticity in a major evolutionary transition: early aquatic experience affects locomotor performance of terrestrial snakes. Funct. Ecol. 21:1154–1161.

Barker, B. S., M. Ottolini, J. L. Wagnon, R. M. Hollander, M. H. Meisler, and M. K. Patel. 2016. The SCN8A encephalopathy mutation p.Ile1327Val displays elevated sensitivity to the anticonvulsant phenytoin. Epilepsia 57:1458–1466.

Bates, D., M. Mächler, B. Bolker, and S. Walker. 2015. Fitting linear mixed-effects models using lme4. J. Stat. Softw. 67:1–48.

Bono, L. M., L. B. Smith, D. W. Pfennig, and C. L. Burch. 2017. The emergence of performance trade-offs during local adaptation: insights from experimental evolution. Mol. Ecol. 26:1720–1733.

Brodie III, E. D. 1993. Consistency of individual differences in anti-predator behaviour and colour pattern in the garter snake, *Thamnophis ordinoides*. Anim. Behav. 45:851–861.

Brodie III, E. D. 1992. Correlational selection for color pattern and antipredator behavior in the garter snake *Thamnophis ordinoides*. Evolution 46:1284–1298.

Brodie III, E. D., and E. D. Brodie, Jr. 1999. Costs of exploiting poisonous prey: evolutionary trade-offs in a predator-prey arms race. Evolution 53:626–631.

Brodie III, E. D., and E. D. Brodie, Jr. 2015. Predictably convergent evolution of sodium channels in the arms race between predators and prey. Brain. Behav. Evol. 86:48–57.

Brodie, Jr., E. D., B. J. Ridenhour, and E. D. Brodie III. 2002. The evolutionary response of predators to dangerous prey: hotspots and coldspots in the geographic mosaic of coevolution between garter snakes and newts. Evolution 56:2067–2082.

Cannon, S. C. 1996. Ion-channel defects and aberrant excitability in myotonia and periodic paralysis. Trends Neurosci. 19:3–10.

Charlesworth, D. 2006. Balancing selection and its effects on sequences in nearby genome regions. PLOS Genet. 2:e64.

DePristo, M. A., D. M. Weinreich, and D. L. Hartl. 2005. Missense meanderings in sequence space: a biophysical view of protein evolution. Nat. Rev. Genet. 6:678–687.

Feldman, C. R., E. D. Brodie, Jr., E. D. Brodie III, and M. E. Pfrender. 2012. Constraint shapes convergence in tetrodotoxin-resistant sodium channels of snakes. Proc. Natl. Acad. Sci. 109:4556–4561.

Feldman, C. R., E. D. Brodie, Jr., E. D. Brodie III, and M. E. Pfrender. 2010. Genetic architecture of a feeding adaptation: garter snake (*Thamnophis*) resistance to tetrodotoxin bearing prey. Proc. R. Soc. B Biol. Sci. 277:3317–3325.

Feldman, C. R., A. M. Durso, C. T. Hanifin, M. E. Pfrender, P. K. Ducey, A. N. Stokes, K. E. Barnett, E. D. Brodie Iii, and E. D. Brodie, Jr. 2015. Is there more than one way to skin a newt? Convergent toxin resistance in snakes is not due to a common genetic mechanism. Heredity, doi: 10.1038/hdy.2015.73.

Felsenstein, J. 1976. The theoretical population genetics of variable selection and migration. Annu. Rev. Genet. 10:253–280.

Fox, J., and S. Weisberg. 2011. An R companion to applied regression. Second. Sage, Thousand Oaks CA.

Fozzard, H. A., and G. M. Lipkind. 2010. The tetrodotoxin binding site is within the outer vestibule of the sodium channel. Mar. Drugs 8:219–234.

Futuyma, D. J., and  and G. Moreno. 1988. The evolution of ecological specialization. Annu. Rev. Ecol. Syst. 19:207–233.

Garland, T. 1988. Genetic basis of activity metabolism. I. Inheritance of speed, stamina, and antipredator displays in the garter snake *Thamnophis sirtalis*. Evolution 42:335–350.

Geffeney, S., E. D. Brodie, Jr., P. C. Ruben, and E. D. Brodie III. 2002. Mechanisms of adaptation in a predator-prey arms race: TTX-resistant sodium channels. Science 297:1336–1339.

Geffeney, S. L., E. Fujimoto, E. D. Brodie III, E. D. Brodie, Jr., and P. C. Ruben. 2005. Evolutionary diversification of TTX-resistant sodium channels in a predator-prey interaction. Nature 434:759–763.

Ghalambor, C. K., D. N. Reznick, and J. A. Walker. 2004. Constraints on adaptive evolution: the functional trade-off between reproduction and fast-start swimming performance in the Trinidadian Guppy (*Poecilia reticulata*). Am. Nat. 164:38–50.

Gibson, D. G., L. Young, R.-Y. Chuang, J. C. Venter, C. A. H. Iii, and H. O. Smith. 2009. Enzymatic assembly of DNA molecules up to several hundred kilobases. Nat. Methods 6:343.

Goldin, A. L. 2002. Evolution of voltage-gated Na+ channels. J. Exp. Biol. 205:575–584.

Hague, M. T. J., C. R. Feldman, E. D. Brodie, Jr., and E. D. Brodie III. 2017. Convergent adaptation to dangerous prey proceeds through the same first-step mutation in the garter snake *Thamnophis sirtalis*. Evolution 71:1504–1518.

Hall, M. C., D. B. Lowry, and J. H. Willis. 2010. Is local adaptation in *Mimulus guttatus* caused by trade-offs at individual loci? Mol. Ecol. 19:2739–2753.

Hanifin, C. T., E. D. Brodie, Jr., and E. D. Brodie III. 2008. Phenotypic mismatches reveal escape from arms-race coevolution. PLoS Biol 6:e60.

Harms, M. J., and J. W. Thornton. 2013. Evolutionary biochemistry: revealing the historical and physical causes of protein properties. Nat. Rev. Genet. 14:559–571.

Hedrick, P. W. 1986. Genetic polymorphism in heterogeneous environments: a decade later. Annu. Rev. Ecol. Syst. 17:535–566.

Hedrick, P. W. 2006. Genetic polymorphism in heterogeneous environments: the age of genomics. Annu Rev Ecol Evol Syst 37:67–93.

Hedrick, P. W., M. E. Ginevan, and E. P. Ewing. 1976. Genetic polymorphism in heterogeneous environments. Annu. Rev. Ecol. Syst. 7:1–32.

Heinemann, S. H., H. Terlau, W. Stühmer, K. Imoto, and S. Numa. 1992. Calcium channel characteristics conferred on the sodium channel by single mutations. Nature 356:441–443.

Hilber, K., W. Sandtner, T. Zarrabi, E. Zebedin, O. Kudlacek, H. A. Fozzard, and H. Todt. 2005. Selectivity filter residues contribute unequally to pore stabilization in voltage-gated sodium channels. Biochemistry (Mosc.) 44:13874–13882.

Hinard, V., A. Britan, M. Schaeffer, M. Zahn-Zabal, U. Thomet, J.-S. Rougier, A. Bairoch, H. Abriel, and P. Gaudet. 2017. Annotation of functional impact of voltage-gated sodium channel mutations. Hum. Mutat. 38:485–493.

Huey, R. B., and P. E. Hertz. 1984. Is a jack-of-all-temperatures a master of none? Evolution 38:441–444.

Janzen, F. J., J. G. Krenz, T. S. Haselkorn, E. D. Brodie, Jr., and E. D. Brodie III. 2002. Molecular phylogeography of common garter snakes (*Thamnophis sirtalis*) in western North America: implications for regional historical forces. Mol. Ecol. 11:1739–1751.

Jayne, B. C., and A. F. Bennett. 1990. Selection on locomotor performance capacity in a natural population of garter snakes. Evolution 44:1204–1229.

Jurkat-Rott, K., R. Rüdel, and F. Lehmann-Horn. 2015. Muscle channelopathies: myotonias and periodic paralyses. Pp. 719–734 *in* B. T. Darras, H. R. Jones, M. M. Ryan, and D. C. D. Vivo, eds. Neuromuscular Disorders of Infancy, Childhood, and Adolescence (Second Edition). Academic Press, San Diego.

Kawecki, T. J., and D. Ebert. 2004. Conceptual issues in local adaptation. Ecol. Lett. 7:1225–1241.

Ketelaars, S. O. M., J. A. Gorter, E. A. van Vliet, F. H. Lopes da Silva, and W. J. Wadman. 2001. Sodium currents in isolated rat CA1 pyramidal and dentate granule neurones in the post-status epilepticus model of epilepsy. Neuroscience 105:109–120.

Lee, C. H., D. K. Jones, C. Ahern, M. F. Sarhan, and P. C. Ruben. 2011. Biophysical costs associated with tetrodotoxin resistance in the sodium channel pore of the garter snake, *Thamnophis sirtalis*. J. Comp. Physiol. A 197:33–43.

Lehmann-Horn, F., and K. Jurkat-Rott. 1999. Voltage-gated ion channels and hereditary disease. Physiol. Rev. 79:1317–1372.

Lynch, M., and W. Gabriel. 1987. Environmental tolerance. Am. Nat. 129:283–303.

McGlothlin, J. W., J. P. Chuckalovcak, D. E. Janes, S. V. Edwards, C. R. Feldman, E. D. Brodie, Jr., M. E. Pfrender, and E. D. Brodie III. 2014. Parallel evolution of tetrodotoxin resistance in three voltage-gated sodium channel genes in the garter snake *Thamnophis sirtalis*. Mol. Biol. Evol. 31:2836–2846.

McGlothlin, J. W., M. E. Kobiela, C. R. Feldman, T. A. Castoe, S. L. Geffeney, C. T. Hanifin, G. Toledo, F. J. Vonk, M. K. Richardson, E. D. Brodie, Jr., M. E.

Pfrender, and E. D. Brodie III. 2016. Historical contingency in a multigene family facilitates adaptive evolution of toxin resistance. Curr. Biol. 26:1616–1621.

Mitchell-Olds, T., J. H. Willis, and D. B. Goldstein. 2007. Which evolutionary processes influence natural genetic variation for phenotypic traits? Nat. Rev. Genet. 8:845–856.

Natarajan, C., F. G. Hoffmann, R. E. Weber, A. Fago, C. C. Witt, and J. F. Storz. 2016. Predictable convergence in hemoglobin function has unpredictable molecular underpinnings. Science 354:336–339.

Nicole, S., and B. Fontaine. 2015. Skeletal muscle sodium channelopathies. Curr. Opin. Neurol. 28:508.

Payandeh, J., T. Scheuer, N. Zheng, and W. A. Catterall. 2011. The crystal structure of a voltage-gated sodium channel. Nature 475:353–358.

R Core Team. 2018. R: A Language and Environment for Statistical Computing. R Foundation for Statistical Computing, Vienna, Austria.

Remold, S. 2012. Understanding specialism when the jack of all trades can be the master of all. Proc. R. Soc. Lond. B Biol. Sci. rspb20121990.

Remy, S., B. W. Urban, C. E. Elger, and H. Beck. 2003. Anticonvulsant pharmacology of voltage-gated Na+ channels in hippocampal neurons of control and chronically epileptic rats. Eur. J. Neurosci. 17:2648–2658.

Ridenhour, B. J., E. D. Brodie III, and E. D. Brodie, Jr. 2004. Resistance of neonates and field-collected garter snakes (*Thamnophis* spp.) to tetrodotoxin. J. Chem. Ecol. 30:143–154.

Savolainen, O., M. Lascoux, and J. Merilä. 2013. Ecological genomics of local adaptation. Nat. Rev. Genet. 14:807.

Shine, R., M. M. Olsson, M. P. Lemaster, I. T. Moore, and R. T. Mason. 2000. Effects of sex, body size, temperature, and location on the antipredator tactics of free-ranging gartersnakes (*Thamnophis sirtalis*, Colubridae). Behav. Ecol. 11:239–245.

Stefani, E., and F. Bezanilla. 1998. [17] Cut-open oocyte voltage-clamp technique. Pp. 300–318 *in* Methods in Enzymology. Academic Press.

Stephens, M., N. J. Smith, and P. Donnelly. 2001. A new statistical method for haplotype reconstruction from population data. Am. J. Hum. Genet. 68:978–989.

Storz, J. F. 2016. Causes of molecular convergence and parallelism in protein evolution. Nat. Rev. Genet. 17:239–250.

Terlau, H., S. H. Heinemann, W. Stühmer, M. Pusch, F. Conti, K. Imoto, and S. Numa. 1991. Mapping the site of block by tetrodotoxin and saxitoxin of sodium channel II. FEBS Lett. 293:93–96.

Thompson, J. N. 1986. Constraints on arms races in coevolution. Trends Ecol. Evol. 1:105–107.

Thompson, J. N. 1994. The coevolutionary process. University of Chicago Press.

Thrall, P. H., and J. J. Burdon. 2003. Evolution of virulence in a plant host-pathogen metapopulation. Science 299:1735–1737.

Tikhonov, D. B., and B. S. Zhorov. 2012. Architecture and pore block of Eukaryotic voltage-gated sodium channels in view of NavAb bacterial sodium channel structure. Mol. Pharmacol. 82:97–104.

Tikhonov, D. B., and B. S. Zhorov. 2005. Modeling p-loops domain of sodium channel: homology with potassium channels and interaction with ligands. Biophys. J. 88:184–197.

Todesco, M., S. Balasubramanian, T. T. Hu, M. B. Traw, M. Horton, P. Epple, C. Kuhns, S. Sureshkumar, C. Schwartz, C. Lanz, R. A. E. Laitinen, Y. Huang, J. Chory, V. Lipka, J. O. Borevitz, J. L. Dangl, J. Bergelson, M. Nordborg, and D. Weigel. 2010. Natural allelic variation underlying a major fitness trade-off in *Arabidopsis thaliana*. Nature 465:632.

Toledo, G., C. Hanifin, S. Geffeney, and E. D. Brodie III. 2016. Convergent evolution of tetrodotoxin-resistant sodium channels in predators and prey. Pp. 87–113 *in* R. J. F. and S. Y. Noskov, ed. Current Topics in Membranes. Academic Press, Cambridge, MA.

Turelli, M., and N. H. Barton. 2004. Polygenic variation maintained by balancing selection: pleiotropy, sex-dependent allelic effects and G × E interactions. Genetics 166:1053–1079.

Vilin, Y. Y., and P. C. Ruben. 2001. Slow inactivation in voltage-gated sodium channels. Cell Biochem. Biophys. 35:171–190.

Wang, X., G. Minasov, and B. K. Shoichet. 2002. Evolution of an antibiotic resistance enzyme constrained by stability and activity trade-offs. J. Mol. Biol. 320:85–95.

Weinreich, D. M., N. F. Delaney, M. A. DePristo, and D. L. Hartl. 2006. Darwinian evolution can follow only very few mutational paths to fitter proteins. Science 312:111–114.

Whitlock, M. C. 1996. The red queen beats the jack-of-all-trades: the limitations on the evolution of phenotypic plasticity and niche breadth. Am. Nat. 148:S65–S77.

Williams, B. L., E. D. Brodie, Jr., and E. D. Brodie III. 2003. Coevolution of deadly toxins and predator resistance: self-assessment of resistance by garter snakes leads to behavioral rejection of toxic newt prey. Herpetologica 59:155–163.

Williams, B. L., C. T. Hanifin, E. D. Brodie, Jr., and E. D. Brodie III. 2010. Tetrodotoxin affects survival probability of rough-skinned newts (*Taricha granulosa*) faced with TTX-resistant garter snake predators (*Thamnophis sirtalis*). Chemoecology 20:285–290.

Xiong, W., Y. Z. Farukhi, Y. Tian, D. DiSilvestre, R. A. Li, and G. F. Tomaselli. 2006. A conserved ring of charge in mammalian Na+ channels: a molecular regulator of the outer pore conformation during slow inactivation. J. Physiol. 576:739–754.

Zaharieva, I. T., M. G. Thor, E. C. Oates, C. van Karnebeek, G. Hendson, E. Blom, N. Witting, M. Rasmussen, M. T. Gabbett, G. Ravenscroft, M. Sframeli, K. Suetterlin, A. Sarkozy, L. D'Argenzio, L. Hartley, E. Matthews, M. Pitt, J. Vissing, M. Ballegaard, C. Krarup, A. Slørdahl, H. Halvorsen, X. C. Ye, L.-H. Zhang, N. Løkken, U. Werlauff, M. Abdelsayed, M. R. Davis, L. Feng, R. Phadke, C. A. Sewry, J. E. Morgan, N. G. Laing, H. Vallance, P. Ruben, M. G. Hanna, S. Lewis, E.-J. Kamsteeg, R. Männikkö, and F. Muntoni. 2016. Loss-of-function mutations in SCN4A cause severe fetal hypokinesia or 'classical' congenital myopathy. Brain 139:674–691.

**Tables and Figures**

**Table 1.** Results of linear mixed models (LMMs) testing effects on crawl speed for each garter snake lineage.

| | **Pacific Northwest** | | **California** | |
|---|---|---|---|---|
| **Fixed-effect** | **Wald $\chi^2$** | **p-value** | **Wald $\chi^2$** | **p-value** |
| DIV p-loop genotype | 0.16 | 0.924 | 6.09 | 0.014* |
| SVL | 3.66 | 0.056 | 16.1 | 0.000* |
| Mass | 4.02 | 0.045* | 0.01 | 0.92 |
| Latitude | 0.51 | 0.477 | 0.64 | 0.423 |

**Table 2.** TTX resistance and channel function as measured on cut-open voltage clamp recording. For each channel type, TTX resistance was measured as the TTX concentration that blocked 50% of channels ($K_d$ ± 95% confidence intervals). The voltage values (mV) are shown for which 50% of channels are open due to activation and closed due to fast-inactivation ($V_{1/2}$ ± 95% C.I.).

| **$Na_V1.4$ mutant** | **n** | **TTX resistance $K_d$ ± C.I. (nM)** | **n** | **Activation $V_{1/2}$ ± C.I. (mV)** | **n** | **Fast-inactivation $V_{1/2}$ ± C.I. (mV)** |
|---|---|---|---|---|---|---|
| $Na_V1.4^{+}$ | 13 | 50 ± 5.2 | 7 | -36.2 ± 1.0 | 9 | -56.6 ± 0.7 |
| $Na_V1.4^{V}$ | 11 | 65 ± 11 | 8 | -34.7 ± 1.9 | 8 | -49.2 ± 0.8 |
| $Na_V1.4^{LVNV}$ | 11 | 13000 ± 1800 | 7 | -16.4 ± 0.5 | 10 | -54.7 ± 0.7 |

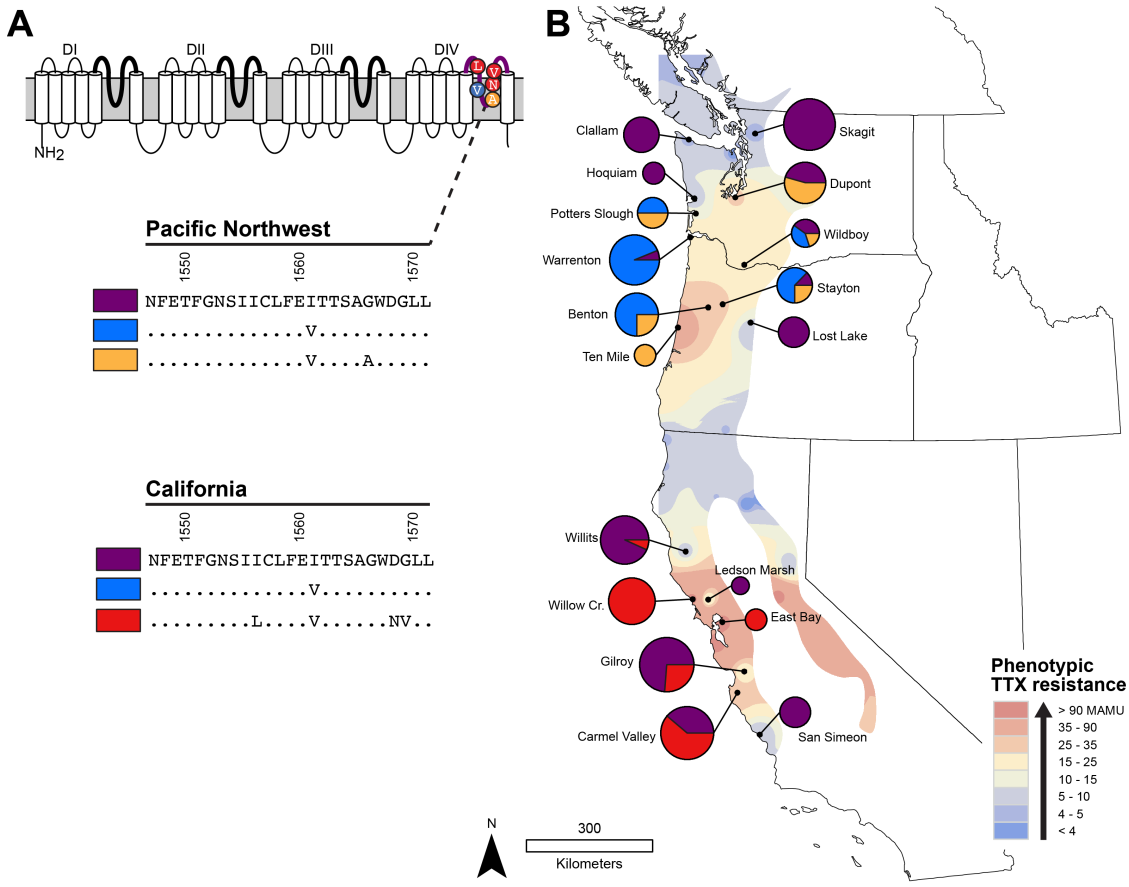


**Figure 1. Substitutions in $Na_V1.4$ arose independently in California and the Pacific Northwest. (A)** Schematic of the $Na_V1.4$ skeletal muscle sodium ion channel in *T. sirtalis*. Each domain (DI–DIV) is shown with the extracellular pore loops (p-loops) highlighted with bold lines. Specific amino acid changes in the DIV p-loop are show in their relative positions within the pore. Below, the TTX-sensitive ancestral sequence (purple) is listed for each lineage of *T. sirtalis*, in California and the Pacific Northwest, followed by other alleles found in each region that are known to confer stepwise increases in channel resistance. **(B)** Pie charts indicate the frequencies of different homozygous neonates for each population sampled from the two lineages. Chart size is proportional to sample size. On the map background, population-level average

phenotypic TTX resistance (50% MAMU) of *T. sirtalis* is interpolated across the geographic range of sympatry with *Taricha* newts (figure adapted from Hague et al. 2017).

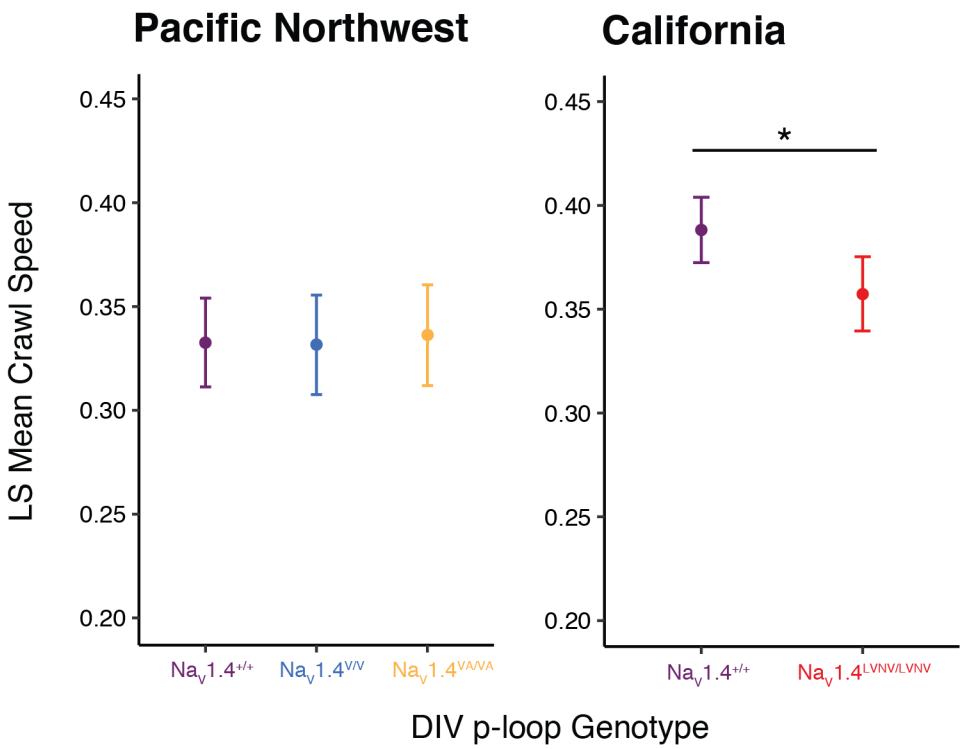


**Figure 2. Neonates from California with a TTX-resistant genotype show reductions in crawl speed.** Least square (LS) mean velocity (± 95% C.I.) of neonates with different homozygous DIV genotypes (colors as in Figure 1). LS means for the Pacific Northwest and California datasets were derived from separate LMMs. $Na_V1.4^{V/V}$ homozygotes from California and all heterozygotes were not included in the analyses because they were so rare (see Table S1).

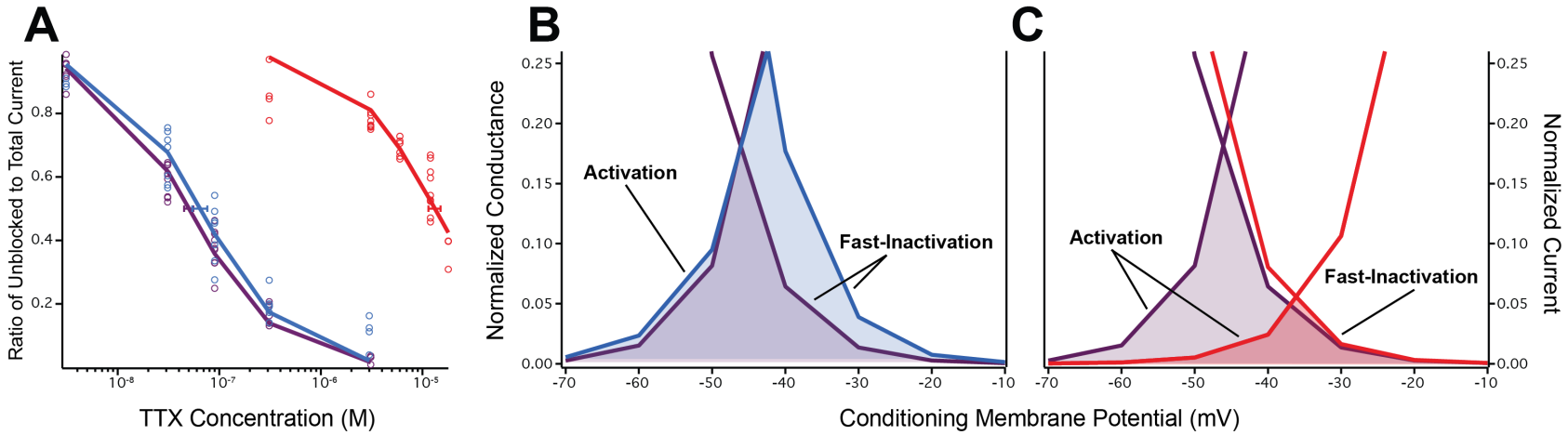


**Figure 3. TTX-resistant alleles change functional measures of $Na_V1.4$ channel activity. (A)** TTX resistance of three cloned $Na_V1.4$ channels from *T. sirtalis*. Each channel is color-coded according to its DIV sequence in Figure 1. The TTX concentration that blocked 50% of the channels ($K_d$) for each channel type was calculated from pooled channel data. Lines represent the equations fitted to the data for each channel and $K_d$ values (± 95% C.I.) are shown with a horizontal bar. Next, the window currents for the **(B)** $Na_V1.4^V$ and **(C)** $Na_V1.4^{LVNV}$ channels are shown as the shaded area below the normalized overlapping activation and fast-inactivation curves. Each channel is shown in comparison to the ancestral $Na_V1.4^+$ channel (in purple). The voltage-dependence of activation and fast-inactivation (including $V_{1/2}$ ± 95% C.I.) were measured by fitting the data with a Boltzmann function (see Figure S1).

**Supplemental Information**

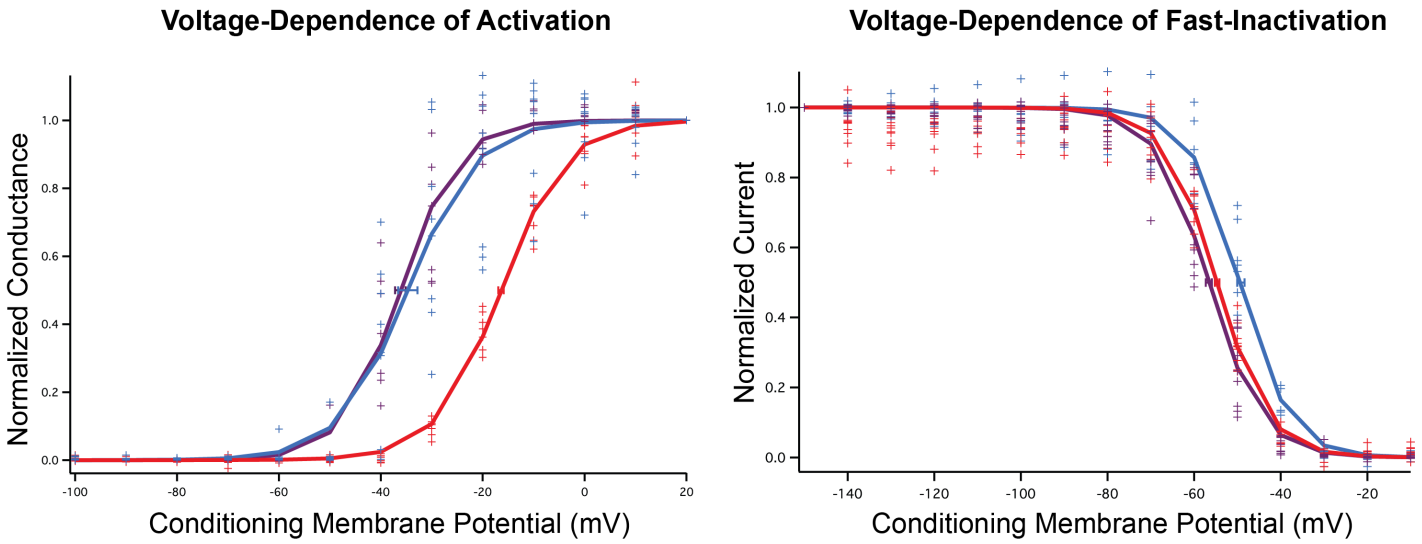


**Figure S1 related to Figure 3.** Estimated curves for the voltage-dependence of activation and fast-inactivation. Each mutant channel is color-coded according to its DIV sequence in Figure 1 (i.e. purple = $Na_V1.4^+$, etc.). The membrane voltage at which 50% of the channels are activated or inactivated ($V_{1/2}$) for each channel was calculated by fitting pooled channel data with a Boltzmann function. $V_{1/2}$ values (± 95% C.I.) are shown with a horizontal bar.

**Table S1 related to Figure 1.** Sampling information for populations from the California and Pacific Norwest datasets. Individual sample sizes are show for each DIV p-loop genotype. $Na_V1.4^{V/V}$ homozygotes from California and all heterozygotes were removed from the analyses due to low sample sizes and a lack of power.

California lineage

| Population | **County** | **Latitude** | **Longitude** | **$Na_V1.4^{+/+}$** | **$Na_V1.4^{V/+}$** | **$Na_V1.4^{V/V}$** | **$Na_V1.4^{LVNV/+}$** | **$Na_V1.4^{LVNV/LVNV}$** |
|---|---|---|---|---|---|---|---|---|
| **Carmel Valley** | Monterey, CA | 36.482112 | -121.717191 | 7 | - | - | 2 | 11 |
| **East Bay** | Contra Costa, CA | 37.977521 | -122.228124 | - | - | - | - | 3 |
| **Gilroy** | Santa Cruz, CA | 36.946163 | -121.563676 | 14 | 1 | 2 | 9 | 5 |
| **Ledson Marsh** | Sonoma, CA | 38.446913 | -122.647488 | 2 | 4 | 1 | - | - |
| **San Simeon** | San Luis Obispo, CA | 35.603385 | -121.079395 | 6 | - | 1 | - | - |
| **Willits** | Mendocino, CA | 39.44217 | -123.35263 | 14 | - | - | 1 | 1 |
| **Willow Cr.** | Sonoma, CA | 38.431705 | -123.06943 | 0 | - | - | - | 14 |
| | | | **Total** | **43** | **5** | **4** | **12** | **34** |

Pacific Northwest lineage

| Population | **County** | **Latitude** | **Longitude** | **$Na_V1.4^{+/+}$** | **$Na_V1.4^{V/+}$** | **$Na_V1.4^{V/V}$** | **$Na_V1.4^{VA/V}$** | **$Na_V1.4^{VA/+}$** | **$Na_V1.4^{VA/VA}$** |
|---|---|---|---|---|---|---|---|---|---|
| **Benton** | Benton., OR | 44.699936 | -123.221014 | - | - | 9 | 6 | - | 3 |
| **Clallam** | Clallam, WA | 48.25144 | -124.26268 | 8 | - | - | - | - | - |
| **Dupont** | Pierce, WA | 47.0972 | -122.63454 | 5 | - | - | - | 3 | 6 |
| **Hoquiam** | Grays Harbor, WA | 47.009425 | -123.911207 | 3 | - | - | - | - | - |
| **Lost Lake** | Hood River, OR | 44.442778 | -121.918611 | 6 | - | - | - | - | - |
| **Potters Slough** | Pacific, WA | 46.68519 | -123.82902 | - | 1 | 3 | 2 | 1 | 3 |
| **Skagit** | Skagit, WA | 48.49134 | -122.15052 | 17 | - | - | - | - | - |
| **Stayton** | Marion, OR | 44.792182 | -122.794489 | 1 | - | 5 | 1 | - | 2 |
| **Ten Mile** | Lane, OR | 44.222224 | -124.075364 | - | - | - | - | - | 3 |
| **Warrenton** | Clatsop, OR | 46.16807 | -123.93873 | 1 | - | 15 | 1 | - | - |
| **Wildboy** | Skaminia, WA | 45.671883 | -122.216926 | 2 | - | 2 | 1 | - | 1 |
| | | | **Total** | **43** | **1** | **34** | **11** | **4** | **18** |

# CHAPTER THREE:

Toxicity and population structure of the Rough-Skinned Newt (*Taricha granulosa*) outside the range of an arms race with resistant predators[3]

[3]As published: Hague, MTJ, LA Avila, CT Hanifin, WA Snedden, AN Stokes, ED Brodie, Jr., ED Brodie III. 2016. Toxicity and population structure of the Rough-Skinned Newt (*Taricha granulosa*) outside the range of an arms race with resistant predators. *Ecology & Evolution*, 6: 2714-2724.

**Abstract**

Species interactions, and their fitness consequences, vary across the geographic range of a coevolutionary relationship. This spatial heterogeneity in reciprocal selection is predicted to generate a geographic mosaic of local adaptation, wherein coevolutionary traits are phenotypically variable from one location to the next. Under this framework, allopatric populations should lack variation in coevolutionary traits due to the absence of reciprocal selection. We examine phenotypic variation in tetrodotoxin (TTX) toxicity of the Rough-Skinned Newt (*Taricha granulosa*) in regions of allopatry with its TTX-resistant predator, the Common Garter Snake (*Thamnophis sirtalis*). In sympatry, geographic patterns of phenotypic exaggeration in toxicity and toxin-resistance are closely correlated in prey and predator, implying that reciprocal selection drives phenotypic variation in coevolutionary traits. Therefore, in allopatry with TTX-resistant predators, we expect to find uniformly low levels of newt toxicity. We characterized TTX toxicity in northwestern North America, including the Alaskan panhandle where *Ta. granulosa* occur in allopatry with *Th. sirtalis*. First we used microsatellite markers to estimate population genetic structure and determine if any phenotypic variation in toxicity might be explained by historical divergence. We found northern populations of *Ta. granulosa* generally lacked population structure in a pattern consistent with northern range expansion after the Pleistocene. Next we chose a cluster of sites in Alaska, which uniformly lacked genetic divergence, to test for phenotypic divergence in toxicity. As predicted, overall levels of newt toxicity were low; however, we also detected unexpected among- and within-population variation in toxicity. Most notably, a small number of individuals contained large doses of TTX that rival means of toxic populations in

sympatry with *Th. sirtalis*. Phenotypic variation in toxicity, despite limited neutral genetic divergence, suggests that factors other than reciprocal selection with *Th. sirtalis* likely contribute to geographic patterns of toxicity in *Ta. granulosa*.

**Introduction**

Coevolution occurs across a heterogeneous landscape of reciprocal selection, where species interactions and their fitness consequences vary from one location to the next (Thompson 2005). Reciprocal selection drives adaptive evolution at the phenotypic interface of coevolution – the set of traits that mediate the coevolutionary interaction (Brodie and Brodie 1999; Brodie and Ridenhour 2003). Consequently, spatial variation in the form and intensity of reciprocal selection is predicted to generate a geographic mosaic of local adaptation to coevolutionary dynamics (Thompson 2005; e.g. Thompson 1997; Brodie et al. 2002; Nash et al. 2008). If among-population phenotypic variation in coevolutionary traits is determined entirely by the heterogeneity of reciprocal selection, then allopatric populations should have limited phenotypic variation because of the absence of reciprocal selection. In antagonistic interactions, phenotypic exaggeration of traits like parasite virulence or prey toxicity should be uniformly limited in regions of allopatry with a natural enemy, because exaggerated trait values are predicted to come at a physiological cost or trade-off with other fitness components (Vermeij 1994; Abrams 2000; Rigby and Jokela 2000).

Here we characterize variation in toxicity of the Rough-Skinned Newt (*Taricha granulosa*) in allopatry with its toxin-resistant predator, the Common Garter Snake (*Thamnophis sirtalis*), to test the hypothesis that phenotypic variation in a coevolutionary trait is limited in the absence of reciprocal selection with a natural enemy. *Taricha granulosa* and other congeners possess tetrodotoxin (TTX), a lethal neurotoxin that deters most predators. However, multiple species of garter snake, including *Th. sirtalis*, independently evolved resistance to the toxin (Geffeney et al. 2002, 2005; Feldman et al.

2009). Geographic patterns of phenotypic exaggeration in newt toxicity and snake TTX resistance are closely correlated across the co-occurring range of the species in western North America, implying the existence of strong reciprocal selection (Hanifin et al. 2008). TTX resistance in western *Th. sirtalis* is clearly a derived trait (Motychak et al. 1999), and western populations in allopatry with *Taricha* generally lack exaggerated resistance (Brodie et al. 2002; Hanifin et al. 2008). However, the degree to which toxicity of *Taricha* varies in allopatry with *Th. sirtalis* is unknown.

We examine newt toxicity in northwestern North America, one of the few geographic regions where *Ta. granulosa* occur outside the range of any known TTX-resistant predator, including *Th. sirtalis*. The range of *Ta. granulosa* extends north through the Alaskan panhandle (Nussbaum and Brodie 1981), whereas *Th. sirtalis* has been documented only as far north as central British Columbia (Figure 1; Rossman et al. 1996). Despite anecdotal accounts, there are no photographs or voucher specimen of *Th. sirtalis* in Alaska (Neuman-Lee et al. 2011). In this study, we were able to confirm the presence of *Th. sirtalis* as far north as the tip of Vancouver Island and Kitmat, BC, but we found no evidence of any natural populations of *Thamnophis* in Alaska.

First, we use neutral microsatellites to characterize population structure of *Ta. granulosa* in British Columbia and Alaska, because biogeography provides an important context for which to understand geographic patterns of phenotypic variation (Thompson 2005; Knowles and Carstens 2007). For example, comparisons of toxicity among phylogenetically divergent populations would potentially be confounded by historical relationships. To avoid the confounding effects of phylogeny, we examine variation in

toxicity among a geographic cluster of sites in Alaska where populations of *Ta. granulosa* lack neutral genetic subdivision.

We expect selection in the absence of a TTX-resistant predator to favor reduced toxicity, particularly if TTX production comes at a physiological cost or trade-off, as is predicted for increasing trait values in arms races (Vermeij 1994; Abrams 2000; Rigby and Jokela 2000). Alternatively, if the toxicity of *Ta. granulosa* varies significantly among Alaskan sites (despite a lack of neutral genetic divergence), factors other than reciprocal selection with *Th. sirtalis* likely contribute to variation in toxicity.

## Material and Methods

### *Sampling*

*Taricha granulosa* were sampled in April and May of 2004. We sampled from ponds in Bella Coola, British Columbia (within the range of *Th. sirtalis*) and on coastal islands of the Alaskan panhandle, including Revillagigedo, Wrangell, Mitkoff, and Prince of Wales islands (Table 1, Figure 1). The following methods were conducted using an approved Institutional Animal Care and Use Committee protocol. We removed tail tip tissue from each newt for the genetic analysis and then used a human biopsy skin punch (Acuderm® Inc.) to collect a 5mm diameter dorsal skin punch for the TTX assay. In addition to the northern samples, we also collected genetic data from from a population of *Ta. granulosa* at Ledson Marsh in Sonoma County, California. These samples were used in the analysis of geographic population structure to provide a comparison of genetic variation with a population located in the southern portion of the range of *Ta. granulosa* (see Discussion).

*Genetic Analysis*

We extracted and purified genomic DNA from tail tissue using the DNeasy Blood & Tissue kit (Qiagen, Inc.). A total of six microsatellite loci – Tgr01, Tgr02, Tgr04, Tgr06, Tgr10, and Tgr14 – were amplified by adapting protocols from Jones et al. (2001). Microsatellites were run on a 3730xl 96-Capillary Genetic Analyzer at the DNA Analysis Facility at Yale University and scored using GeneMarker v. 2.2.0 (SoftGenetics, State College, PA, USA). We were unable to amplify Tgr04 in the samples from Ledson Marsh, CA. We first estimated the frequency of null alleles for each locus using FREENA (Chapuis and Estoup 2007). GENEPOP (Raymond and Rousset 1995) was used to test for linkage disequilibrium between pairs of loci in each population using a log likelihood ratio test. The same program was used to test for departures from Hardy-Weinberg equilibrium (HWE) for each locus and population. We adjusted p-values with a sequential-Bonferroni correction (Holm 1979). Next, we estimated population genetic diversity, including observed heterozygosity ($H_O$), expected heterozygosity ($H_E$), and number of alleles ($N_A$) in ARLEQUIN 3.5.1.3 (Excoffier and Lischer 2010). We also used FSTAT (Goudet 1995) to estimate allelic richness (A) for each population.

To assess population structure, we used ARLEQUIN to estimate pairwise $F_{ST}$ values between sampling sites. Statistical significance was obtained by permuting the samples 1000 times, and p-values were adjusted with a sequential-Bonferroni correction. We chose to use $F_{ST}$, as opposed to $R_{ST}$, because it tends to produce more accurate estimates of genetic subdivision when population structure is weak (as expected in Alaskan populations) and when the sample sizes and number of loci are limited (Gaggiotti et al. 1999; Balloux and Goudet 2002). We also used an analysis of molecular

variance (AMOVA; Excoffier et al. 1992) implemented in ARLEQUIN, which assigns genetic variation to different geographic levels (within and among populations) to obtain global $F_{ST}$ values. We estimated genetic subdivision among individuals grouped in two different manners: (1) by sampling location and (2) by the presence/absence of detectable TTX. We used the R package "adegenet" to test for the presence of isolation by distance (IBD) by plotting pairwise $F_{ST}/(1 - F_{ST})$ against the logarithm of pairwise geographic distance (Rousset 1997). Significance was assessed with permutation-based Mantel tests.

To further investigate population structure in northern populations, we used a Bayesian clustering analysis to estimate the optimal number of genetic clusters (*K*), implemented in STRUCTURE v. 2.3.4 (Pritchard et al. 2000; Falush et al. 2003). We used the sampling locations as prior information and assumed a model with population admixture and correlated allele frequencies (Falush et al. 2003). The analysis ran with 500,000 iterations as burn-in and we collected data from the following 1,000,000 iterations of MCMC in 10 independent runs for values of *K* ranging from 1 to 8 (8 being the total number of northern sampling locations). STRUCTURE HARVESTER (Earl and vonHoldt 2012) was used to detect the most probable number of clusters using the Evanno's method ( $\Delta K$ ; Evanno et al. 2005). Membership probabilities (*Q*-values) of the 10 runs for each value of the most probable *K* ($K = 2$) were averaged using CLUMPP v. 1.1.2 (Jakobsson and Rosenberg 2007) and graphed using DISTRUCT v. 1.1 (Rosenberg 2004).

*Phenotypic Analysis*

Tetrodotoxin was extracted from the dorsal skin punches as described by Hanifin et al. (2002, 2004, 2008). For each skin punch, we quantified the amount of TTX in 20µl

of extract using fluorometric high performance liquid chromatography (HPLC). We then estimated dorsal skin concentration of TTX (mg/cm$^2$ of skin), along with whole animal toxicity (mg) based on each individual's total skin area. TTX is uniformly distributed throughout the dorsal skin and dorsal levels of TTX are strongly predictive of toxicity in other skin regions (Hanifin et al. 2004). For each geographic location, we quantified mean whole animal TTX (mg) as well as the proportion of newts with any detectable TTX from the HPLC analysis (> 0.001 mg of TTX).

To test for among-site differences in TTX toxicity, we used a non-parametric Kruskal-Wallis test. We also used a multiple logistic regression to test for among-site differences in the proportion of newts with any detectable TTX (i.e., presence vs. absence of TTX). We included sex in the model to account for potential differences in toxicity among males and females (Hanifin et al. 2002). We used the 'glm' function in *R* (R Core Team 2014) with the proportion of toxic newts as the dependent variable, and population, sex, and the population*sex interaction as predictor variables. Significance of predictor variables was tested through comparisons with reduced models using likelihood ratio tests. We also generated distance matrices describing among-site differences in mean toxicity (mg TTX/cm$^2$) and the proportion of detectably toxic newts. We then used Mantel tests and Redundancy Analysis (RDA) to test for correlations between phenotypic divergence, neutral genetic divergence, and geographic distance, and then used permutation-based methods to assess significance.

## Results

*Geographic Population Structure*

We did not detect linkage disequilibrium for any pair of loci in any of the populations. We did find evidence for departures from HWE for locus Tgr10 in the Highbush populations, but we included Tgr10 in our analyses because this pattern was not consistent across all populations. These two populations also had null allele frequency estimates of 21% and 20% respectively, suggesting that deviations from HWE may be due to the presence of null alleles. The other five loci also showed infrequent evidence of null alleles, but these patterns were inconsistent across populations so we included all loci in our analyses. Genetic diversity statistics are summarized in Table 1. The California population of *Ta. granulosa* had the highest level of within-population genetic diversity, whereas northern sites in British Columbia and Alaska all had low-to-moderate levels of diversity.

Measures of population differentiation generally revealed low levels of genetic subdivision among northern sites, particularly within Alaska. Nearly all the pairwise $F_{ST}$ estimates among the geographically clustered Alaskan sites were not significantly different from zero (Table 2). Almost all Alaskan sites were significantly differentiated from the more geographically distant Bella Coola site in British Columbia. In the AMOVA including Alaska and British Columbia, the partition of among-site variation was moderate and significant ($F_{ST}$ = 0.0705, p = <0.001); however, $F_{ST}$ was lower when British Columbia was excluded from the analysis ($F_{ST}$ = 0.0185, p = 0.016). Even when Alaskan individuals were grouped by island (rather than by sampling location), $F_{ST}$ was still low ($F_{ST}$ = 0.024, and p <0.001). Alternatively, when Alaska individuals were grouped according to their presence/absence of detectable TTX, we found a non-significant $F_{ST}$ value ($F_{ST}$ = -0.0011, p = 0.478). The test for IBD revealed a significant

positive correlation between genetic differentiation and geographic distance (Mantel test: $r = 0.703$, $p = 0.022$), but this relationship disappeared when Bella Coola was removed from the analysis ($r = 0.232$, $p = 0.175$).

The STRUCTURE analysis revealed a similar pattern of population structure (Figure 2). Both the Evanno's method ($\Delta K$) and $\text{Ln}Pr(X|K)$ supported a value of $K = 2$. All Alaska individuals showed a high membership probability to one cluster, while British Columbia individuals predominantly grouped into another. To avoid overlooking fine scale population structure in Alaskan sites, we also ran a STRUCTURE analysis excluding individuals from British Columbia. The $\text{Ln}Pr(X|K)$ values indicated $K = 1$ as the most likely number of clusters and the bar plot of $K = 2$ (not shown) identified all individuals across all populations as roughly equally admixed, indicating a lack of population structure.

*Phenotypic Analysis*

We detected significant among-site differences in size-adjusted estimates of skin TTX (Kruskal-Wallis $\chi^2 = 44.62$, $p < 0.001$, $df = 7$) and whole animal toxicity (Kruskal-Wallis $\chi^2 = 40.40$, $p < 0.001$, $df = 7$). The logistic regression also revealed a significant effect of collection site on the proportion of newts with detectable TTX (likelihood ratio $\chi^2 = 29.88$, $p < 0.001$, $df = 5$). Sex and the sex*population interaction were not significant predictors in the model. We found large differences in the proportion of toxic newts across short geographic distances in Alaska, for example, the Pat's Lake site was devoid of newts with detectable levels of TTX, but only 15 km away at the Highbush site (on the same island), 94.7% of newts possessed detectable levels of TTX, with a mean toxicity of 0.2554 mg (Figure 3). Several sites also had a small number of highly toxic individuals.

One newt at Beaver Made Hole had an estimated total of 2.6 mg of TTX and three newts from Highbush had doses that exceeded 1 mg. For context, the lethal intraperitoneal dose of TTX required to kill a 20 g laboratory mouse in 30 minutes (i.e. a "mouse unit") is roughly 0.2 μg (Noguchi and Ebesu 2001). Thus, a newt with 2.6 mg of TTX contains enough toxin to kill approximately 13,000 mice.

The Mantel tests and RDA produced similar results, so here we only report Mantel test results (Table 3). We did not find a significant relationship between phenotypic divergence and neutral genetic divergence, which was unsurprising given the near complete lack of genetic divergence among Alaskan sites. The relationship between among-site differences in the proportion of toxic newts and geographic distance was marginally significant in the Mantel test after a Bonferroni correction ($r$ = -0.397, p = 0.0497), but not in the RDA. This pattern likely reflects the fact that the proportion of toxic newts at a given site can change drastically over short geographic distances.

## Discussion

Northern populations of *Ta. granulosa* generally lacked geographic population structure, particularly in Alaska. As predicted, overall population levels of newt toxicity were low outside the geographic range of TTX-resistant predators. However, we found unexpected among- and within-site variance in toxicity, which suggests that natural selection by resistant predators does not fully explain phenotypic variation in toxicity. First, we assess biogeographic structure in northern populations as context for interpreting geographic patterns of newt toxicity.

### *Geographic Population Structure*

Compared to California populations, *Ta. granulosa* in British Columbia and Alaska had reduced levels of genetic diversity. Estimates of pairwise $F_{ST}$, the AMOVA, and the STRUCTURE analysis all suggest an overall lack of population structure in northern populations, particularly within Alaska. Jones et al. (2001) and Ridenhour et al. (2007) also reported low estimates of population subdivision among sites in Oregon and Washington, suggesting that *Ta. granulosa* may exhibit low site fidelity. We detected a genetic pattern consistent with IBD, but this reflects the fact that nearly all the Alaskan sites were significantly genetically differentiated from Bella Coola (Table 2, Figure 2). Although newts from Bella Coola also had higher levels of heterozygosity than those from Alaska, these values were still low in comparison to the California sample.

The general lack of neutral genetic diversity in the northern samples is consistent with a northern post-glacial range expansion after the Pleistocene (Hewitt and Ibrahim 2001). The low levels of genetic subdivision among island sites in Alaska, despite salt-water barriers to dispersal, suggest the region was likely colonized recently by *Ta. granulosa*. Southeastern Alaska, Canada, and much of northwestern North America was either covered in ice or tundra-like habitat during the Pleistocene (Barnosky et al. 1987; Josenhans et al. 1995; Mann and Hamilton 1995). Subsequently, *Ta. granulosa* and other co-distributed taxa colonized northwestern North America in the last 10,000 years as the ice sheets retreated north (Kuchta and Tan 2005).

Elevated genetic diversity at the Bella Coola site relative to the Alaskan sites may result from a number of demographic processes. Populations of *Ta. granulosa* in Alaska sit near the northern limit of the species' range. A recent population bottleneck or extinction and re-colonization event in Alaska could result in reduced population genetic

variation compared to southern populations in Bella Coola. The Haida Gwaii region of coastal British Columbia (located proximate to Bella Coola) also has been proposed as a northern refugium for flora and fauna during the height of Pleistocene glaciation (Byun et al. 1997; Janzen et al. 2002; Shafer et al. 2010). A northern post-glacial population expansion of *Ta. granulosa* out from the Haida Gwaii region could generate a pattern of lower genetic variation in Alaska compared to Bella Coola. A previous biogeographic analysis of allozymes and mitochondrial loci in *Ta. granulosa* suggested Alaskan populations were recently colonized as early as 10,000 years ago from Oregon or Washington (Kuchta and Tan 2005); however, the study lacked population sampling in British Columbia and could have missed cryptic refugia. Ultimately, more thorough sampling in British Columbia and Alaska is required to effectively discern among competing biogeographic hypotheses of post-glacial expansion.

*Phenotypic Analyses*

As predicted, levels of newt toxicity among the genetically similar Alaskan sites were low. Mean toxicity values in Alaska were similar to those observed in populations that co-occur with non-resistant populations of *Th. sirtalis* (Hanifin et al. 2008). The low levels of TTX observed in the majority of Alaskan samples may represent an evolutionary loss of toxicity. Brodie and Brodie (1991) suggested a similar loss of toxicity in *Ta. granulosa* on Vancouver Island, BC, where non-toxic newts were still found to be resistant to TTX. The TTX-bearing phenotype appears to be ancestral in modern newts (family Salamandridae), a monophyletic group that includes *Ta. granulosa* (Hanifin and Gilly 2015). However, the evolutionary lability of TTX toxicity is unclear because genes associated with TTX biosynthesis have yet to be discovered and the newts

may ultimately sequester the toxin through their diet or a bacterial symbiont (reviewed in Hanifin 2010). Although the ultimate source of TTX is unknown in *Ta. granulosa*, the apparent loss of toxicity in allopatry with a TTX-resistant predator suggests that TTX synthesis or sequestration imposes a physiological cost. If TTX production requires a complicated biosynthetic pathway, selection may favor the loss of toxicity in the absence of a resistant predator (Williams 2010). For example, biosynthesis of a similar neurotoxin found in puffer fish, saxitoxin (STX), involves gene expression in a cluster of up to 26 genes (Moczydlowski 2013).

Despite low average levels of TTX toxicity throughout Alaska, we detected significant among-site differences. The marginally significant inverse relationship between the proportion of toxic newts and geographic distance (Table 3) highlighted how differences in toxicity occur over short geographic distances, even on the same island (e.g. PLW and HBW on Wrangell Island). In addition, a small number of newts contained surprisingly large doses of TTX. These whole animal estimates of TTX (> 1 mg per individual) rival the mean toxicity of populations of *Ta. granulosa* found in regions that co-occur with TTX-resistant *Th. sirtalis* (e.g. 1.628 mg of TTX in Tenmile, OR and 3.803 mg in McGribble, OR; Hanifin et al. 2008). The patterns of phenotypic variation in toxicity were incongruent with patterns of neutral microsatellite variation in Alaska, where populations were found to lack genetic subdivision. No evidence for a relationship between neutral genetic divergence and the presence/absence of TTX was apparent from the Mantel tests, RDA, or AMOVA.

The majority of sampled newts contained low or undetectable doses of TTX that are unlikely to be lethal to potential predators. Mean values of whole animal TTX in

Alaskan populations were similar to those observed in newt populations in southern regions that co-occur with non-resistant populations of *Th. sirtalis* (e.g. 0.011 mg in Skagit River, WA and 0.001 mg in Bear Ridge, CA; Hanifin et al. 2008). Although selection to deter TTX-sensitive predators could conceivably maintain low levels of TTX in Alaskan newts, the large doses of TTX observed in a few individuals are extreme. *Thamnophis* species are the only known predators resistant enough to consume such large doses of TTX and there are no confirmed reports of sympatric garter snakes in Alaska. Consumption of *Taricha* by avian predators, including Western Grebes (*Aechmophorus occidentalis*; McAllister et al. 1997), a Mallard (*Anas platyrhynchos*; Storm 1948), domestic fowl (Pimentel 1952), and a Great Horned Owl (*Bubo virginianus*; Mobley and Stidham 2000) have resulted in death of the predators. Stokes et al. (2011) reported evisceration of *Taricha* by an unconfirmed avian predator at Ledson Marsh in California; however, local newts at the site have low levels of TTX. Successful consumption of a *Taricha* newt was reported for great blue herons (*Ardea herodias*; Fellers et al. 2008) and bullfrogs (*Rana catesbeiana*; Jennings and Cook 1998); however, both reports also came from regions where *Taricha* were non-toxic (Hanifin et al. 2008) and a separate study found that *Ta. granulosa* from toxic populations were lethal to both these predators (Brodie 1968). Small mammals may be another potential predator of *Ta. granulosa* in Alaska, but previous tests found ten genera of mammals to be highly sensitive to TTX, including rats (*Rattus rattus*), a stoat (*Mustela erminea*), a muskrat (*Ondatra zibethicus*), and a bobcat (*Lynx rufus*) (Brodie 1968). Adult newt toxicity may reflect selection for defense against predators at an earlier life stage. Egg toxicity of *Ta. granulosa* is positively correlated with maternal toxicity (Hanifin et al. 2003, Gall et al. 2012a).

Moreover, caddisfly larvae (*Limnephilus flavastellus*) in Oregon are capable of preying on the eggs of *Ta. granulosa*, and appear to harbor some degree of resistance to TTX (Gall et al. 2011, 2012b).

The variance in toxicity of *Ta. granulosa* in allopatry with *Th. sirtalis* suggests that factors other than the coevolutionary interaction with resistant predators contribute to geographic patterns of phenotypic variation in toxicity. External factors, such as abiotic conditions, may affect the ability of newts to sequester or synthesize TTX. For example, marine taxa are generally thought to obtain TTX through the food chain or a bacterial symbiont, and high individual and regional variation in toxicity has been cited as evidence of an exogenous source of TTX in puffer fish (reviewed in Noguchi and Arakawa 2008). However, the source of TTX in newts is more controversial (Hanifin et al. 2008). When fed a non-toxic diet, captive *Ta. granulosa* can maintain and regenerate levels of TTX for extended periods (Hanifin et al. 2002; Cardall et al. 2004), but analogous tests in the fire-bellied newt (*Cynops pyrrhogaster*) and the red-spotted newt (*Notophthalmus viridescens*) appeared to result in a loss of toxicity (Yotsu-Yamashita et al. 2012; Kudo et al. 2015).

Variation in toxicity in Alaska could also result from increased variance in TTX synthesis genes and genetic drift in the absence of selection for exaggerated toxicity. This alternative may be less likely, given the lack of neutral genetic variation and subdivision in Alaskan sites. The incongruence between phenotypic variation and the lack of neutral microsatellite variation suggests that among-site variance in toxicity is not solely due to neutral drift. Admittedly, we cannot rule out the importance of genetic drift because the genetic basis of TTX synethesis is unknown. Presumably TTX toxicity in *Ta. granulosa*

has some heritable genetic component that is susceptible to drift, because southern populations have apparently evolved extreme toxicity in response to escalatory reciprocal selection with *Th. sirtalis* (Hanifin et al. 2008).

*Conclusion*

As predicted, levels of toxicity were generally low in populations of *Ta. granulosa* in allopatry with TTX-resistant predators. However, we also found evidence for among- and within-population variation in toxicity, a pattern that appears to be inconsistent with neutral genetic population structure. The limited number of samples and microsatellite markers in this study may restrict our power to detect microgeographic population structure in Alaska, thus our results should be interpreted with caution. Nevertheless, estimates of $F_{ST}$, tests for IBD, and the STRUCTURE analysis all suggest an overall pattern of limited population stucture among the geographic cluster of sites in Alaska, which decreases the likelihood that our population comparisons of TTX toxicity are confounded by deep phylogenetic divergence.

Characterizing toxicity of *Ta. granulosa* in allopatry with *Th. sirtalis* represents a critical step in inferrering how exogenous forces might influence coevolution in sympatry. These data emphasize that reciprocal selection is likely not the sole determinant of geographic patterns of toxicity in *Ta. granulosa*. Focusing only on phenotypic variation in sympatric populations would otherwise lead to a myopic interpretation of coevolutionary dynamics. The coevolutionary process occurs across space and time, which inevitability span variable ecologial and abiotic conditions. Factors unrelated to the interaction, like environmental conditions (Johnson et al. 2007; Williams

2010), physiological trade-offs (Brodie and Brodie 1999; Rigby and Jokela 2000), or selection from interactions with other organisms (Zangerl and Berenbaum 2003; Siepielski and Benkman 2004) can alter the evolutionary trajectory of coevolutionary traits. The contribution of exogenous factors should not be overlooked in the context of geographic patterns of adaptation at the phenotypic interface of coevolution.

**Acknowledgements**

This work was supported by the National Geographic Society under grant 7531-03. Members of the E. Brodie and R. Cox labs at the University of Virginia provided helpful comments that improved this manuscript. We thank B. Sanderson and C. Alencar for guidance with molecular work. We also appreciate the comments from two anonymous reviewers.

**Literature Cited**

Abrams, P. A. 2000. The evolution of predator-prey interactions: theory and evidence. Annu. Rev. Ecol. Syst.

AmphibiaWeb: Information on amphibian biology and conservation. 2016. Berkeley, California: AmphibiaWeb. Available: http://amphibiaweb.org/. Accessed: Feb 11, 2016.

Balloux, F., and J. Goudet. 2002. Statistical properties of population differentiation estimators under stepwise mutation in a finite island model. Mol. Ecol. 11:771–783.

Barnosky, C. W., P. M. Anderson, and P. J. Bartlein. 1987. The northwestern US during deglaciation; vegetational history and paleoclimatic implications. N. Am. Adjac. Oceans Last Deglaciation 3:289–321.

Brodie III, E. D., and E. D. Brodie, Jr. 1999. Costs of exploiting poisonous prey: evolutionary trade-offs in a predator-prey arms race. Evolution 53:626–631.

Brodie III, E. D., and E. D. Brodie, Jr. 1991. Evolutionary response of predators to dangerous prey: reduction of toxicity of newts and resistance of garter snakes in island populations. Evolution 45:221–224.

Brodie III, E. D., and E. D. Brodie, Jr. 1999. Predator-prey arms races. BioScience 49:557–568.

Brodie III, E. D., and B. J. Ridenhour. 2003. Reciprocal selection at the phenotypic interface of coevolution. Integr. Comp. Biol. 43:408–418.

Brodie, Jr., E. D. 1968. Investigations on the skin toxin of the adult rough-skinned newt, *Taricha granulosa*. Copeia 1968:307.

Brodie, Jr., E. D., B. J. Ridenhour, and E. D. Brodie III. 2002. The evolutionary response of predators to dangerous prey: hotspots and coldspots in the geographic mosaic of coevolution between garter snakes and newts. Evolution 56:2067–2082.

Byun, S. A., B. F. Koop, and T. E. Reimchen. 1997. North American black bear mtDNA phylogeography: Implications for morphology and the Haida Gwaii glacial refugium controversy. Evolution 51:1647–1653.

Cardall, B. L., E. D. Brodie, Jr., E. D. Brodie III, and C. T. Hanifin. 2004. Secretion and regeneration of tetrodotoxin in the rough-skin newt (*Taricha granulosa*). Toxicon 44:933–938.

Chapuis, M.-P., and A. Estoup. 2007. Microsatellite null alleles and estimation of population differentiation. Mol. Biol. Evol. 24:621–631.

Earl, D. A., and B. M. vonHoldt. 2012. STRUCTURE HARVESTER: a website and program for visualizing STRUCTURE output and implementing the Evanno method. Conserv. Genet. Resour. 4:359–361.

Evanno, G., S. Regnaut, and J. Goudet. 2005. Detecting the number of clusters of individuals using the software structure: a simulation study. Mol. Ecol. 14:2611–2620.

Excoffier, L., and H. E. L. Lischer. 2010. Arlequin suite ver 3.5: a new series of programs to perform population genetics analyses under Linux and Windows. Mol. Ecol. Resour. 10:564–567.

Excoffier, L., P. E. Smouse, and J. M. Quattro. 1992. Analysis of molecular variance inferred from metric distances among DNA haplotypes: application to human mitochondrial DNA restriction data. Genetics 131:479–491.

Falush, D., M. Stephens, and J. K. Pritchard. 2003. Inference of population structure using multilocus genotype data: linked loci and correlated allele frequencies. Genetics 164:1567–1587.

Feldman, C. R., E. D. Brodie, Jr., E. D. Brodie III, and M. E. Pfrender. 2009. The evolutionary origins of beneficial alleles during the repeated adaptation of garter snakes to deadly prey. Proc. Natl. Acad. Sci. 106:13415–13420.

Fellers, G., J. Reynolds-Taylor, and S. Farrar. 2008. *Taricha granulosa* predation. Herpetol Rev 38:317–318.

Frost, D.R., G.A. Hammerson, and G. Santos-Barrera. 2015. *Thamnophis sirtalis*. The IUCN Red List of Threatened Species 2015: e.T62240A68308267.http://dx.doi.org/10.2305/IUCN.UK.2015-2.RLTS.T62240A68308267.en. Accessed: Feb 11, 2016.

Gaggiotti, O. E., O. Lange, K. Rassmann, and C. Gliddon. 1999. A comparison of two indirect methods for estimating average levels of gene flow using microsatellite data. Mol. Ecol. 8:1513–1520.

Gall, B. G., E. D. Brodie III, and E. D. Brodie, Jr. 2011. Survival and growth of the caddisfly Limnephilus flavastellus after predation on toxic eggs of the rough-skinned newt (*Taricha granulosa*). Can. J. Zool. 89:483–489.

Gall, B. G., A. N. Stokes, S. S. French, E. D. Brodie III, and E. D. Brodie, Jr. 2012a. Female newts (*Taricha granulosa*) produce tetrodotoxin laden eggs after long term captivity. Toxicon 60:1057–1062.

Gall, B. G., A. N. Stokes, S. S. French, E. D. Brodie III, and E. D. Brodie, Jr. 2012b. Predatory caddisfly larvae sequester tetrodotoxin from their prey, eggs of the rough-skinned newt (*Taricha granulosa*). J. Chem. Ecol. 38:1351–1357.

Geffeney, S., E. D. Brodie, Jr., P. C. Ruben, and E. D. Brodie III. 2002. Mechanisms of adaptation in a predator-prey arms race: TTX-resistant sodium channels. Science 297:1336–1339.

Geffeney, S. L., E. Fujimoto, E. D. Brodie III, E. D. Brodie, Jr., and P. C. Ruben. 2005. Evolutionary diversification of TTX-resistant sodium channels in a predator-prey interaction. Nature 434:759–763.

Goudet, J. 1995. FSTAT (Version 1.2): A computer program to calculate F-statistics. J. Hered. 86:485–486.

Hanifin, C. T. 2010. The chemical and evolutionary ecology of tetrodotoxin (TTX) toxicity in terrestrial vertebrates. Mar. Drugs 8:577–593.

Hanifin, C. T., E. D. Brodie III, and E. D. Brodie, Jr. 2004. A predictive model to estimate total skin tetrodotoxin in the newt *Taricha granulosa*. Toxicon 43:243–249.

Hanifin, C. T., E. D. Brodie III, and E. D. Brodie, Jr. 2003. Tetrodotoxin levels in eggs of the rough-skin newt, *Taricha granulosa*, are correlated with female toxicity. J. Chem. Ecol. 29:1729–1739.

Hanifin, C. T., E. D. Brodie III, and E. D. Brodie, Jr. 2002. Tetrodotoxin levels of the rough-skin newt, *Taricha granulosa*, increase in long-term captivity. Toxicon 40:1149–1153.

Hanifin, C. T., E. D. Brodie, Jr., and E. D. Brodie III. 2008. Phenotypic mismatches reveal escape from arms-race coevolution. PLoS Biol 6:e60.

Hanifin, C. T., and W. F. Gilly. 2015. Evolutionary history of a complex adaptation: Tetrodotoxin resistance in salamanders. Evolution 69:232–244.

Hewitt, G., and K. Ibrahim. 2001. Inferring glacial refugia and historical migrations with molecular phylogenies. *in* Integrating Ecology and Evolution in a Spatial Context. Blackwell Science, Oxford.

Holm, S. 1979. A simple sequentially rejective multiple test procedure. Scand. J. Stat. 6:65–70.

Jakobsson, M., and N. A. Rosenberg. 2007. CLUMPP: a cluster matching and permutation program for dealing with label switching and multimodality in analysis of population structure. Bioinformatics 23:1801–1806.

Janzen, F. J., J. G. Krenz, T. S. Haselkorn, E. D. Brodie, Jr., and E. D. Brodie III. 2002. Molecular phylogeography of common garter snakes (*Thamnophis sirtalis*) in western North America: implications for regional historical forces. Mol. Ecol. 11:1739–1751.

Jennings, M., and D. Cook. 1998. Natural history notes: *Taricha torosa torosa* (Coast Range newt). Predation. Herpetol. Rev. 29:230.

Johnson, S. G., C. D. Hulsey, and F. J. G. de Leon. 2007. Spatial mosaic evolution of snail defensive traits. BMC Evol. Biol. 7.

Jones, A. G., M. S. Blouin, and S. J. Arnold. 2001. Genetic variation in two populations of the rough-skinned newt (*Taricha granulosa*) assessed using novel tetranucleotide microsatellite loci. Mol. Ecol. Notes 1:293–296.

Josenhans, H. W., D. W. Fedje, K. W. Conway, and J. V. Barrie. 1995. Post glacial sea levels on the Western Canadian continental shelf: evidence for rapid change, extensive subaerial exposure, and early human habitation. Mar. Geol. 125:73–94.

Knowles, L. L., and B. C. Carstens. 2007. Estimating a geographically explicit model of population divergence. Evolution 61:477–493.

Kuchta, S. R., and A.-M. Tan. 2005. Isolation by distance and post-glacial range expansion in the rough-skinned newt, *Taricha granulosa*. Mol. Ecol. 14:225–244.

Kudo, Y., C. Chiba, K. Konoki, Y. Cho, and M. Yotsu-Yamashita. 2015. Confirmation of the absence of tetrodotoxin and its analogues in the juveniles of the Japanese fire-bellied newt, *Cynops pyrrhogaster*, captive-reared from eggs in the laboratory using HILIC-LC-MS. Toxicon 101:101–105.

Mann, D. H., and T. D. Hamilton. 1995. Late Pleistocene and Holocene paleoenvironments of the North Pacific coast. Quat. Sci. Rev. 14:449–471.

McAllister, K., J. Skriletz, B. Hall, and M. Garner. 1997. *Taricha granulosa* (rough-skin newt) toxicity. Herpetol Rev 28:82.

Mobley, J. A., and T. A. Stidham. 2000. Great Horned Owl death from predation of a toxic California newt. Wilson Bull. 112:563–564.

Moczydlowski, E. G. 2013. The molecular mystique of tetrodotoxin. Toxicon 63:165–183.

Motychak, J. E., E. D. Brodie, Jr., and E. D. Brodie III. 1999. Evolutionary response of predators to dangerous prey: preadaptation and the evolution of tetrodotoxin resistance in garter snakes. Evolution 53:1528–1535.

Nash, D. R., T. D. Als, R. Maile, G. R. Jones, and J. J. Boomsma. 2008. A mosaic of chemical coevolution in a large blue butterfly. Science 319:88–90.

Neuman-Lee, L. A., S. E. McGaugh, M. Pfrender, and F. J. Janzen. 2011. Using mitochondrial DNA to determine the identity and origin of a gartersnake found in Alaska. J. Herpetol. 45:63–65.

Noguchi, T., and O. Arakawa. 2008. Tetrodotoxin–distribution and accumulation in aquatic organisms, and cases of human intoxication. Mar. Drugs 6:220–242.

Noguchi, T., and J. S. M. Ebesu. 2001. Puffer Poisoning: Epidemiology and Treatment. J. Toxicol. Toxin Rev. 20:1–10.

Nussbaum, R., and E. D. Brodie, Jr. 1981. *Taricha granulosa*. Cat. Am. Amphib. Reptil. 272–1.

Pimentel, R. A. 1952. Studies on the biology of *Triturus granulosus*. Oregon State University, Corvallis, OR.

Pritchard, J. K., M. Stephens, and P. Donnelly. 2000. Inference of population structure using multilocus genotype data. Genetics 155:945–959.

Raymond, M., and F. Rousset. 1995. GENEPOP (Version 1.2): Population Genetics Software for Exact Tests and Ecumenicism. J. Hered. 86:248–249.

R Core Team. 2014. R: A language and environment for statistical computing. R Foundation for Statistical Computing, Vienna, Austria.

Rigby, M. C., and J. Jokela. 2000. Predator avoidance and immune defence: costs and trade-offs in snails. Proc. R. Soc. B Biol. Sci. 267:171–176.

Rosenberg, N. A. 2004. distruct: a program for the graphical display of population structure. Mol. Ecol. Notes 4:137–138.

Rossman, D. A. 1996. The Garter Snakes: Evolution and Ecology. University of Oklahoma Press.

Rossman, D. A., N. B. Ford, and R. A. Seigel. 1996. The Garter Snakes: Evolution and Ecology. 1st Edition. edition. University of Oklahoma Press, Norman.

Rousset, F. 1997. Genetic differentiation and estimation of gene flow from F-statistics under isolation by distance. Genetics 145:1219–1228.

Shafer, A. B. A., C. I. Cullingham, S. D. Côté, and D. W. Coltman. 2010. Of glaciers and refugia: a decade of study sheds new light on the phylogeography of northwestern North America. Mol. Ecol. 19:4589–4621.

Siepielski, A. M., and C. W. Benkman. 2004. Interactions among moths, crossbills, squirrels, and lodgepole pine in a geographic selection mosaic. Evolution 58:95–101.

Stokes, A. N., D. G. Cook, C. T. Hanifin, E. D. Brodie, and E. D. Brodie. 2011. Sex-biased predation on newts of the genus *Taricha* by a novel predator and its relationship with tetrodotoxin toxicity. Am. Midl. Nat. 165:389–399.

Storm, R. M. 1948. The herpetology of Benton County, Oregon. Oregon State University, Corvallis, OR.

Thompson, J. N. 1997. Evaluating the dynamics of coevolution among geographically structured populations. Ecology 78:1619–1623.

Thompson, J. N. 2005. The Geographic Mosaic of Coevolution. University of Chicago Press, Chicago.

Vermeij, G. J. 1994. The evolutionary interaction among species: selection, escalation, and coevolution. Annu. Rev. Ecol. Syst.

Williams, B. L. 2010. Behavioral and chemical ecology of marine organisms with respect to tetrodotoxin. Mar. Drugs 8:381–398.

Yotsu-Yamashita, M., J. Gilhen, R. W. Russell, K. L. Krysko, C. Melaun, A. Kurz, S. Kauferstein, D. Kordis, and D. Mebs. 2012. Variability of tetrodotoxin and of its analogues in the red-spotted newt, *Notophthalmus viridescens* (Amphibia: Urodela: Salamandridae). Toxicon 59:257–264.

Zangerl, A. R., and M. R. Berenbaum. 2003. Phenotype matching in wild parsnip and parsnip webworms: causes and consequences. Evolution 57:806–815.

## Tables and Figures

**Table 1**. Sample locality details and microsatellite genetic diversity statistics for sites sampled in Alaska (*AK*), British Columbia (*BC*), and California (*CA*). The number of individuals collected (N) and successfully genotyped (n), mean observed heterozygosity ($H_O$), expected heterozygosity ($H_E$), number of alleles ($N_A$), and allelic richness (A), along with standard deviations (SD) are reported.

| | | | | | Microsatellite Diversity | | | | |
|---|---|---|---|---|---|---|---|---|---|
| **Locality (Island)** | **Code** | **Latitude** | **Longitude** | **N** | **n** | **$H_O$ ±SD** | **$H_E$ ±SD** | **$N_A$ ±SD** | **A ±SD** |
| *AK* | | | | | | | | | |
| Beaver Made Hole (Mitkof) | BMM | 55.47 | -131.61 | 16 | 15 | 0.34 ±0.36 | 0.35 ±0.25 | 3.17 ±1.60 | 2.31 ±0.97 |
| Ohmer Creek (Mitkof) | OCM | 56.33 | -132.09 | 6 | 6 | 0.31 ±0.35 | 0.29 ±0.33 | 2.33 ±1.37 | 2.25 ±1.30 |
| Pat's Lake (Wrangell) | PLW | 56.35 | -132.34 | 12 | 12 | 0.32 ±0.30 | 0.32 ±0.30 | 2.83 ±1.47 | 2.27 ±1.12 |
| Highbush (Wrangell) | HBW | 56.65 | -132.68 | 19 | 16 | 0.29 ±0.23 | 0.37 ±0.27 | 2.67 ±1.21 | 2.30 ±0.95 |
| Revilla Road (Revillagigedo) | RRR | 56.6 | -132.75 | 19 | 19 | 0.39 ±0.22 | 0.42 ±0.25 | 4.00 ±1.55 | 2.71 ±1.00 |
| Staney Creek (Prince of Wales) | SCP | 55.72 | -132.51 | 16 | 16 | 0.37 ±0.27 | 0.37 ±0.25 | 3.50 ±1.64 | 2.49 ±1.08 |
| Thorne Bay (Prince of Wales) | TBP | 55.81 | -133.04 | 20 | 20 | 0.32 ±0.23 | 0.31 ±0.21 | 3.00 ±0.89 | 2.08 ±0.65 |
| *BC* | | | | | | | | | |
| Bella Coola | BCB | 52.38 | -126.58 | 32 | 32 | 0.53 ±0.19 | 0.49 ±0.16 | 3.50 ±1.23 | 2.71 ±0.74 |
| *CA* | | | | | | | | | |
| Ledson Marsh | LMG | 38.45 | -122.65 | 20 | 20 | 0.65 ±0.16 | 0.75 ±0.13 | 7.60 ±3.78 | 4.65 ±1.61 |

**Table 2**. Pairwise $F_{ST}$ values from six microsatellite loci (or five in California populations, indicated in italics). Sampling sites are grouped by island. Significant values after a sequential-Bonferroni correction are shown in bold.

| **Island** | **Island Population** | Mitkof BMM | Mitkof OCM | Wrangell PLW | Wrangell HBW | Revillagigedo RRR | Prince of Wales SCP | Prince of Wales TBP | BCB | LMG | LMT |
|---|---|---|---|---|---|---|---|---|---|---|---|
| Mitkof | BMM | - | | | | | | | | | |
| | OCM | -0.024 | - | | | | | | | | |
| Wrangell | PLW | 0.029 | 0.052 | - | | | | | | | |
| | HBW | 0.037 | 0.026 | -0.004 | - | | | | | | |
| Revillagigedo | RRR | 0.040 | 0.004 | -0.037 | 0.000 | - | | | | | |
| Prince of Wales | SCP | **0.119** | **0.122** | 0.015 | 0.006 | 0.036 | - | | | | |
| | TBP | 0.041 | -0.004 | -0.032 | -0.016 | -0.013 | 0.004 | - | | | |
| | BCB | **0.123** | 0.062 | **0.121** | **0.135** | **0.107** | **0.133** | **0.117** | - | | |
| | LMG | ***0.346*** | ***0.312*** | ***0.357*** | ***0.306*** | ***0.319*** | ***0.348*** | ***0.372*** | ***0.308*** | - | |
| | LMT | ***0.455*** | ***0.431*** | ***0.460*** | ***0.421*** | ***0.423*** | ***0.452*** | ***0.472*** | ***0.390*** | ***0.242*** | - |

**Table 3.** Results from Mantel tests for correlations among distance matrices from Alaskan sites. Significance was adjusted with a standard Bonferroni correction.

| Mantel Tests | *r* | p value |
|---|---|---|
| $F_{ST}$ + Mean TTX (mg/cm$^2$) | -0.028 | 0.9059 |
| $F_{ST}$ + Proportion Toxic | -0.120 | 0.6039 |
| Mean TTX (mg/cm$^2$) + Geographic Distance | -0.227 | 0.3208 |
| Proportion Toxic + Geographic Distance | -0.397 | 0.0497 |


**Figure 1.** Sampling locations in southeastern Alaska and western British Columbia. The hypothesized geographic range is shown for *Th. sirtalis* (Rossman et al. 1996; Frost et al. 2015) and *Ta. granulosa* (Nussbaum and Brodie 1981; AmphibiaWeb 2016); however, the precise range boundaries of each species are not known.

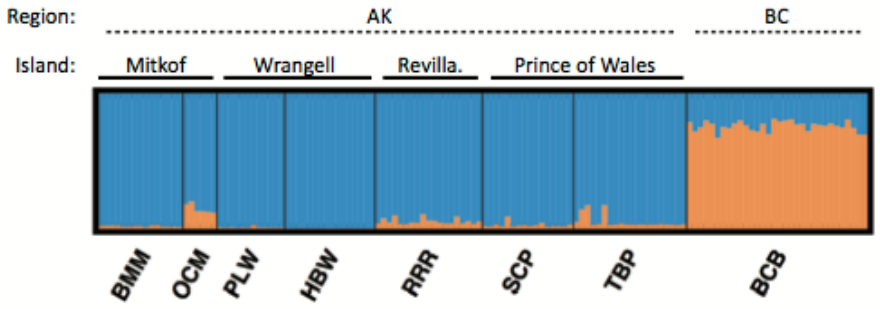


**Figure 2**. Bar plot obtained from STRUCTURE with $K = 2$ for populations from Alaska (AK) and British Columbia (BC). Each vertical bar represents an individual and the height of each colored segment of a bar represents the probability of that individual's assignment to each cluster. Black vertical lines delineate sampling sites, which are labeled with codes from Table 1.

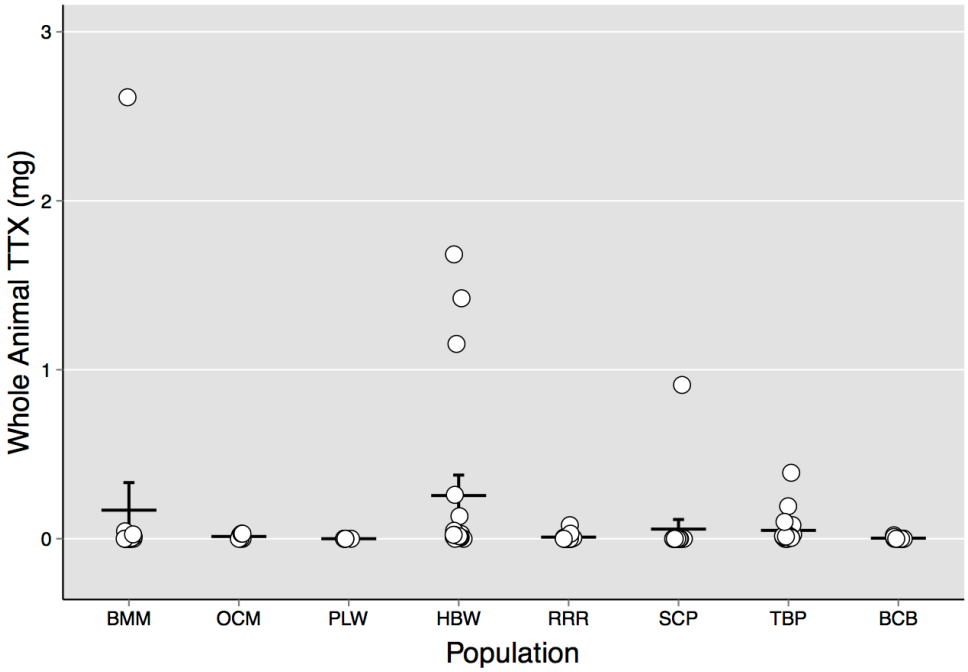


**Figure 3.** Among-site variation in levels of whole animal TTX. Points are horizontally jittered. Black lines indicate site means (horizontal) ± standard error (vertical).

# CHAPTER FOUR:

Signatures of asymmetric adaptation upend evidence for a geographic mosaic of coevolution in classic predator-prey arms race[4]

[4] Formatted as a co-authored manuscript: Michael T.J. Hague, Amber N. Stokes, Chris R. Feldman, Edmund D. Brodie, Jr., Edmund D. Brodie III

**Abstract**

Reciprocal adaptation is the hallmark of arms race coevolution, but this retaliatory process has often gone untested, even in the best-studied battles between natural enemies. We tested whether observed patterns of local co-adaptation deviate from neutral expectations in the classic example of a geographic mosaic of coevolution between toxic newts (*Taricha granulosa*) and resistant garter snakes (*Thamnophis sirtalis*). Contrary to conventional wisdom, we found that variation in newt toxicity is parsimoniously explained by neutral population divergence, not predator resistance. In contrast, garter snake resistance is best predicted by prey toxicity. Neutral divergence among prey populations structures variation in toxicity, which in turn structures selection on predators—calling into question whether reciprocal adaptation is the primary source of geographic variation in this textbook example of a coevolutionary mosaic.

**Main Text**

Coevolutionary relationships are usually inferred when a pair of species share matched abilities in the traits that mediate their interactions (*1*, *2*). Reciprocal selection, generated by each species on the other, drives local co-adaptation at this phenotypic interface of coevolution (*3*, *4*). Because species interactions and their fitness consequences vary spatially, heterogeneity in the form of reciprocal selection is expected to generate a geographic mosaic of coevolution in which phenotypes of both species covary due to adaptation to local conditions (*2*, *5*–*7*).

Landscape patterns of phenotypic matching alone, however, do not confirm the existence of reciprocal co-adaptation (*8*, *9*). A simpler, non-adaptive explanation for matched trait variation could arise from the population genetic structure of each species. Common barriers to dispersal or a shared biogeographic history, for example, could structure phenotypic divergence congruently in co-occurring species (*10*). Only when phenotypic variation deviates from the neutral expectations of population structure in both species can we infer local adaptation in the geographic mosaic of coevolution (*11*). Otherwise, drift, gene flow, and phylogeography can provide a parsimonious explanation for patterns of divergence across the landscape.

We tested whether population divergence at the phenotypic interface of coevolution deviates from neutral expectations in a textbook example of a geographic mosaic of coevolution, the arms race between deadly newt prey and their resistant snake predators. In western North America, rough-skinned newts (*Taricha granulosa*) secrete the deadly neurotoxin tetrodotoxin (TTX), which binds to the outer pore of voltage-gated sodium channels ($Na_V$) and prevents the initiation of action potentials (*12*, *13*). Common

garter snakes (*Thamnophis sirtalis*) exhibit resistance to TTX that is largely due to specific amino acid substitutions in the fourth domain pore-loop (DIV p-loop) of the skeletal muscle sodium channel ($Na_V1.4$) that disrupt toxin-binding (Figure 1) (*14*, *15*). Channel-level TTX resistance conferred by each allele in the DIV p-loop is tightly correlated with muscle and whole-animal levels of phenotypic resistance in *Th. sirtalis* (*14–16*). TTX-resistant alleles occur at high frequency in coevolutionary "hotspots" with highly toxic newts, but are largely absent in surrounding "coldspots" where newts are non-toxic, creating a putative mosaic of local adaptation in which predator and prey have roughly matched abilities at the interface of toxin-binding (*9*, *17*, *18*).

We conducted fine-scale population sampling of newts (n=138) and garter snakes (n=169) along a latitudinal transect of nine locations on the Pacific Coast in Washington and Oregon that spans the geographic mosaic (Figure 1, Table S1), ranging from low levels of newt toxicity and snake resistance (northern Washington) to a hotspot of extreme escalation in both species (central Oregon). At each location, we characterized levels of TTX in newt populations and TTX resistance in garter snakes, including whole-animal phenotypic resistance and $Na_V1.4$ channel genotypes. We then compared these data to neutral patterns of population genomic variation using single nucleotide polymorphisms (SNPs) in each species.

Mosaic patterns of newt toxicity and snake resistance were broadly consistent with previous work suggesting arms race coevolution has led to closely matched phenotypes in each species (*9*). The TTX toxicity ($\mu g/cm^2$) of newts varied by population (ANOVA; $F[8,114]=37.43$, $p<0.001$) and by sex ($F[1,114]=4.37$, $p=0.039$) along the latitudinal transect (Figure 1; Table S1). TTX resistance (50% MAMU dose) of snakes

also varied by population (according to non-overlapping 95% confidence intervals; Figure 1; Table S1) and was closely matched to prey toxicity. The presence of TTX-resistant alleles in the $Na_V1.4$ channel co-varied with phenotypic resistance in garter snakes, such that pairwise $F_{ST}$ divergence at the DIV p-loop was correlated with population divergence in phenotypic resistance (Mantel test, r=0.47, p=0.032).

Population divergence in newt toxicity, however, does not deviate from neutral expectations, calling into question whether selection from a resistant predator structures variation in prey toxicity across the geographic mosaic. We used neutral SNPs to assess population genomic structure and a found clear pattern of isolation-by-distance (IBD) in both species (distance-based redundancy analysis; newts, F=-38.528, p=0.002; snakes, F=22.021, p=0.001). Principal coordinate (PCoA) and STRUCTURE analyses indicated that newts and snakes have distinct spatial patterns of population structure along the transect (Figure 2). We generated distance matrices to test whether phenotypic divergence in one species (e.g., newt toxicity) is best explained by (1) neutral genomic divergence (pairwise $F_{ST}$; Table S3) or (2) phenotypic divergence in the natural enemy (snake resistance) (*19–22*). In simple regressions, population divergence in TTX toxicity of newts was predicted by neutral $F_{ST}$ divergence and TTX resistance of garter snakes (Table 1). $F_{ST}$ divergence remained significant in the multiple regression, indicating that population structure of newts predicts TTX toxicity, even after controlling for TTX resistance of the predator (which was only marginally significant; p=0.056). In contrast, garter snake resistance was strictly predicted by newt toxicity and not neutral $F_{ST}$ divergence. Both phenotypic resistance and $F_{ST}$ divergence at the DIV p-loop (the site of toxin-binding in $Na_V1.4$) were uncorrelated with neutral $F_{ST}$ values in garter snakes

(Table 1). These results imply that neutral genetic divergence structures variation in prey toxicity, which in turn predicts TTX resistance in predator populations. Population genetic structure of the newts appears so important that divergence in both phenotypic resistance and $F_{ST}$ at the DIV p-loop of garter snakes are significantly correlated with neutral $F_{ST}$ divergence of newts (Table 1).

Clinal variation in the TTX toxicity of newts is also highly congruent with neutral genomic variation from the STRUCTURE analysis (Figure 3) (*23–25*). TTX resistance of garter snakes, in contrast, clearly deviates from neutral expectations to track variation in prey toxicity. Cline-fitting analyses show that prey toxicity and predator resistance are tightly matched along the 611 km transect; the geographic center points of each cline are located just 43 km apart and do not differ statistically. The cline center of TTX-resistant alleles in snakes is also located nearby, although it differed significantly from newt toxicity. Despite similar clines in prey and predator, variation in newt toxicity showed an even tighter match to clinal variation in neutral population structure. The center points of the toxicity and neutral clines were located only 36 km apart. Conversely, variation in phenotypic resistance and TTX-resistant alleles in snakes both deviated significantly from the neutral cline. For instance, the center points of the phenotypic resistance and neutral clines were located a distant 238 km apart.

Prey toxicity and predator resistance are tightly matched across the landscape, but we find this pattern does not satisfy basic assumptions of reciprocal adaptation. Mosaic variation in prey toxicity does not appear to be the sole result of arms race coevolution. Although predator resistance is geographically structured by the signature of local adaptation to prey, toxicity of the prey is clearly structured according to neutral

population divergence. These results imply that variation in newt toxicity may not be the result of local adaptation to resistant predators, but instead, can easily be explained by neutral processes, like drift and historical biogeography. For example, latitudinal patterns of newt toxicity and neutral divergence are both consistent with a population history of northward expansion after the Pleistocene glacial period (*26*, *27*).

An asymmetric signature of adaptation in prey and predator may reflect differences in the mechanisms that underlie trait variation in each species. The evolutionary response in newts could be obscured by environmental effects that disproportionally contribute to variance in TTX toxicity compared to resistance. Little is known about the basis of TTX toxicity, but some researchers suggest external factors, like environmentally-derived precursors, may affect the ability of *Taricha* newts to synthesize or sequester TTX (*28–30*). Evidence from a sister species, the California newt (*Ta. torosa*), suggests TTX toxicity could also be a plastic response to sustained stressful conditions, like predation (*31*, *32*). On the other hand, TTX resistance in garter snakes is largely due to a small number of amino acid changes to the DIV p-loop of the $Na_V1.4$ channel (*14–16*, *18*). These large-effect mutations could make TTX resistance more evolutionarily labile than toxicity, permitting rapid adaptation in predator populations (*9*).

The asymmetry we observed could also be due to a selective imbalance that arises from interactions between prey and predator. The species under more intense selection is generally expected to be most locally adapted to antagonistic interactions (*33*). Prey are typically thought to experience stronger selection than their predators (*34*); however, this imbalance may be reversed when prey contain deadly toxins like TTX (*3*). In fact, newt

populations in central Oregon are the most toxic known to occur in the genus *Taricha* (*9*), so non-resistant predators can experience severe fitness consequences.

Given the escalated toxicity and resistance in central Oregon, arms race coevolution may still explain phenotypic matching in some populations. For example, perhaps newt toxicity was under strong selection in the past, but is now subject to neutral processes like drift and gene flow. Or, reciprocal coevolution may be ongoing in hotspots like central Oregon, and toxicity in surrounding regions is spatially structured by outward patterns of gene flow. These homogenizing effects may be less influential in snake populations due to the simple genetic basis of TTX resistance or the strong selection on predators. This overall pattern would support the geographic mosaic theory of coevolution, which suggests gene flow out from hotspots can alter dynamics in surrounding populations (*35–37*). When gene flow is high, the location with the strongest reciprocal effects on fitness is expected to dictate global patterns of trait variation (*33*, *35*, *38*).

Even if reciprocal selection occurs in certain populations, our results emphasize that broader mosaic patterns of phenotypic matching are not the inherent result of coevolution. External factors like abiotic conditions (*39*), evolutionary constraints (*40*), or interactions with other species (*41*) are likely to affect the evolution of each species in unique ways. Here, it appears that neutral processes and population structure disproportionally affect newt toxicity, which in turn, determines mosaic patterns of phenotypic variation in both species across the landscape. The evolutionary response, if any, to selection at the phenotypic interface is almost certain to differ in two interacting species—so much so that coevolution may not be the most parsimonious explanation for

observed patterns of population divergence and trait matching across the mosaic landscape.

**Literature Cited**


1. D. H. Janzen, When is it coevolution? *Evolution* (1980).
2. J. N. Thompson, *The Geographic Mosaic of Coevolution* (University of Chicago Press, Chicago, 2005).
3. E. D. Brodie III, E. D. Brodie, Jr., Predator-prey arms races. *BioScience*. **49**, 557–568 (1999).
4. E. D. Brodie III, B. J. Ridenhour, Reciprocal selection at the phenotypic interface of coevolution. *Integr. Comp. Biol.* **43**, 408–418 (2003).
5. C. W. Benkman, T. L. Parchman, A. Favis, A. M. Siepielski, Reciprocal selection causes a coevolutionary arms race between crossbills and lodgepole pine. *Am. Nat.* **162**, 182–194 (2003).
6. A. R. Zangerl, M. R. Berenbaum, Phenotype matching in wild parsnip and parsnip webworms: causes and consequences. *Evolution*. **57**, 806–815 (2003).
7. H. Toju, S. Ueno, F. Taniguchi, T. Sota, Metapopulation structure of a seed-predator weevil and its host plant in arms race coevolution. *Evolution*. **65**, 1707–1722 (2011).
8. R. Gomulkiewicz *et al.*, Dos and don'ts of testing the geographic mosaic theory of coevolution. *Heredity*. **98**, 249–258 (2007).
9. C. T. Hanifin, E. D. Brodie, Jr., E. D. Brodie III, Phenotypic mismatches reveal escape from arms-race coevolution. *PLoS Biol*. **6**, e60 (2008).
10. N. G. Swenson, D. J. Howard, A. E. M. E. Hellberg, E. J. B. Losos, Clustering of contact zones, hybrid zones, and phylogeographic breaks in North America. *Am. Nat.* **166**, 581–591 (2005).

11. R. B. Langerhans, T. J. DeWitt, Shared and unique features of evolutionary diversification. *Am. Nat.* **164**, 335–349 (2004).

12. H. A. Fozzard, G. M. Lipkind, The tetrodotoxin binding site is within the outer vestibule of the sodium channel. *Mar. Drugs*. **8**, 219–234 (2010).

13. D. B. Tikhonov, B. S. Zhorov, Architecture and pore block of Eukaryotic voltage-gated sodium channels in view of NavAb bacterial sodium channel structure. *Mol. Pharmacol.* **82**, 97–104 (2012).

14. S. Geffeney, E. D. Brodie, Jr., P. C. Ruben, E. D. Brodie III, Mechanisms of adaptation in a predator-prey arms race: TTX-resistant sodium channels. *Science*. **297**, 1336–1339 (2002).

15. S. L. Geffeney, E. Fujimoto, E. D. Brodie III, E. D. Brodie, Jr., P. C. Ruben, Evolutionary diversification of TTX-resistant sodium channels in a predator-prey interaction. *Nature*. **434**, 759–763 (2005).

16. C. R. Feldman, E. D. Brodie, Jr., E. D. Brodie III, M. E. Pfrender, Genetic architecture of a feeding adaptation: garter snake (*Thamnophis*) resistance to tetrodotoxin bearing prey. *Proc. R. Soc. B Biol. Sci.* **277**, 3317–3325 (2010).

17. E. D. Brodie, Jr., B. J. Ridenhour, E. D. Brodie III, The evolutionary response of predators to dangerous prey: hotspots and coldspots in the geographic mosaic of coevolution between garter snakes and newts. *Evolution*. **56**, 2067–2082 (2002).

18. M. T. J. Hague, C. R. Feldman, E. D. Brodie, Jr., E. D. Brodie III, Convergent adaptation to dangerous prey proceeds through the same first-step mutation in the garter snake *Thamnophis sirtalis*. *Evolution*. **71**, 1504–1518 (2017).

19. B. F. J. Manly, Randomization and regression methods for testing for associations with geographical, environmental and biological distances between populations. *Res. Popul. Ecol.* **28**, 201–218 (1986).

20. P. E. Smouse, J. C. Long, R. R. Sokal, Multiple regression and correlation extensions of the mantel test of matrix correspondence. *Syst. Zool.* **35**, 627 (1986).

21. P. Legendre, F.-J. Lapointe, P. Casgrain, Modeling brain evolution from behavior: a permutational regression approach. *Evolution*. **48**, 1487–1499 (1994).

22. J. W. Lichstein, Multiple regression on distance matrices: a multivariate spatial analysis tool. *Plant Ecol.* **188**, 117–131 (2007).

23. J. M. Szymura, N. H. Barton, Genetic analysis of a hybrid zone between the fire-bellied toads, *Bombina bombina* and *B. variegata*, near Cracow in southern Poland. *Evolution*. **40**, 1141–1159 (1986).

24. J. M. Szymura, N. H. Barton, The genetic structure of the hybrid zone between the fire-bellied toads *Bombina bombina* and *B. variegata*: comparisons between transects and between loci. *Evolution*. **45**, 237–261 (1991).

25. E. P. Derryberry, G. E. Derryberry, J. M. Maley, R. T. Brumfield, HZAR: hybrid zone analysis using an R software package. *Mol. Ecol. Resour.* **14**, 652–663 (2014).

26. G. Hewitt, K. Ibrahim, in *Integrating Ecology and Evolution in a Spatial Context* (Blackwell Science, Oxford, 2001).

27. B. J. Ridenhour, E. D. Brodie, Jr., E. D. Brodie III, Patterns of genetic differentiation in *Thamnophis* and *Taricha* from the Pacific Northwest. *J. Biogeogr.* **34**, 724–735 (2007).

28. T. Yasumoto *et al.*, Interspecies distribution and possible origin of tetrodotoxin. *Ann. N. Y. Acad. Sci.* **479**, 44–51 (1986).

29. M. Yotsu, M. Iorizzi, T. Yasumoto, Distribution of tetrodotoxin, 6-epitetrodotoxin, and 11-deoxytetrodotoxin in newts. *Toxicon*. **28**, 238–241 (1990).

30. T. Yasumoto, M. Yotsu-Yamashita, Chemical and etiological studies on tetrodotoxin and its analogs. *Toxin Rev.* **15**, 81–90 (1996).

31. G. M. Bucciarelli, D. B. Green, H. B. Shaffer, L. B. Kats, Individual fluctuations in toxin levels affect breeding site fidelity in a chemically defended amphibian. *Proc. R. Soc. B Biol. Sci.* **283** (2016).

32. G. M. Bucciarelli, H. B. Shaffer, D. B. Green, L. B. Kats, An amphibian chemical defense phenotype is inducible across life history stages. *Sci. Rep.* **7** (2017).

33. S. Gandon, Local adaptation and the geometry of host–parasite coevolution. *Ecol. Lett.* **5**, 246–256 (2002).

34. R. Dawkins, J. R. Krebs, Arms races between and within species. *Proc. R. Soc. Lond. B Biol. Sci.* **205**, 489–511 (1979).

35. R. Gomulkiewicz, J. N. Thompson, R. D. Holt, Nuismer Scott L., M. E. Hochberg, Hot spots, cold spots, and the geographic mosaic theory of coevolution. *Am. Nat.* **156**, 156–174 (2000).

36. S. Gandon, S. L. Nuismer, Interactions between genetic drift, gene flow, and selection mosaics drive parasite local adaptation. *Am. Nat.* **173**, 212–224 (2009).

37. J. N. Thompson, S. L. Nuismer, R. Gomulkiewicz, Coevolution and maladaptation. *Integr. Comp. Biol.* **42**, 381–387 (2002).

38. S. Gandon, Y. Michalakis, Local adaptation, evolutionary potential and host–parasite coevolution: interactions between migration, mutation, population size and generation time. *J. Evol. Biol.* **15**, 451–462 (2002).

39. S. G. Johnson, C. D. Hulsey, F. J. G. León, Spatial mosaic evolution of snail defensive traits. *BMC Evol. Biol.* **7**, 1–11 (2007).

40. M. T. J. Hague *et al.*, Large-effect mutations generate trade-off between predatory and locomotor ability during arms race coevolution with deadly prey. *Evol. Lett.* **2**, 406–416 (2018).

41. C. W. Benkman, W. C. Holimon, J. W. Smith, The influence of a competitor on the geographic mosaic of coevolution between crossbills and lodgepole pine. *Evolution*. **55**, 282–294 (2001).

## Tables and Figures

**Table 1.** Results from multiple regression of distance matrices (MRMs) comparing population divergence in phenotypic and genetic data.

| Response Variable | Explanatory Variable(s) | Coefficient | p-value |
|---|---|---|---|
| **Newts** | | | |
| TTX toxicity | Neutral $F_{ST}$ | 5.998 | 0.003* |
| TTX toxicity | TTX resistance of snakes | 0.415 | 0.014* |
| TTX toxicity | Neutral $F_{ST}$ + TTX resistance | | |
| | Neutral $F_{ST}$ | 4.805 | 0.010* |
| | TTX resistance | 0.254 | 0.056· |
| **Garter snakes** | | | |
| TTX resistance | Neutral $F_{ST}$ | 1.637 | 0.662 |
| TTX resistance | TTX toxicity of newts | 0.671 | 0.029* |
| TTX resistance | Neutral $F_{ST}$ + TTX toxicity | | |
| | Neutral $F_{ST}$ | -5.651 | 0.206 |
| | TTX toxicity | 0.875 | 0.017* |
| TTX resistance | Neutral $F_{ST}$ of newts | 4.689 | 0.041* |
| $F_{ST}$ of DIV p-loop | Neutral $F_{ST}$ | 2.649 | 0.203 |
| $F_{ST}$ of DIV p-loop | Neutral $F_{ST}$ of newts | 3.196 | 0.006* |

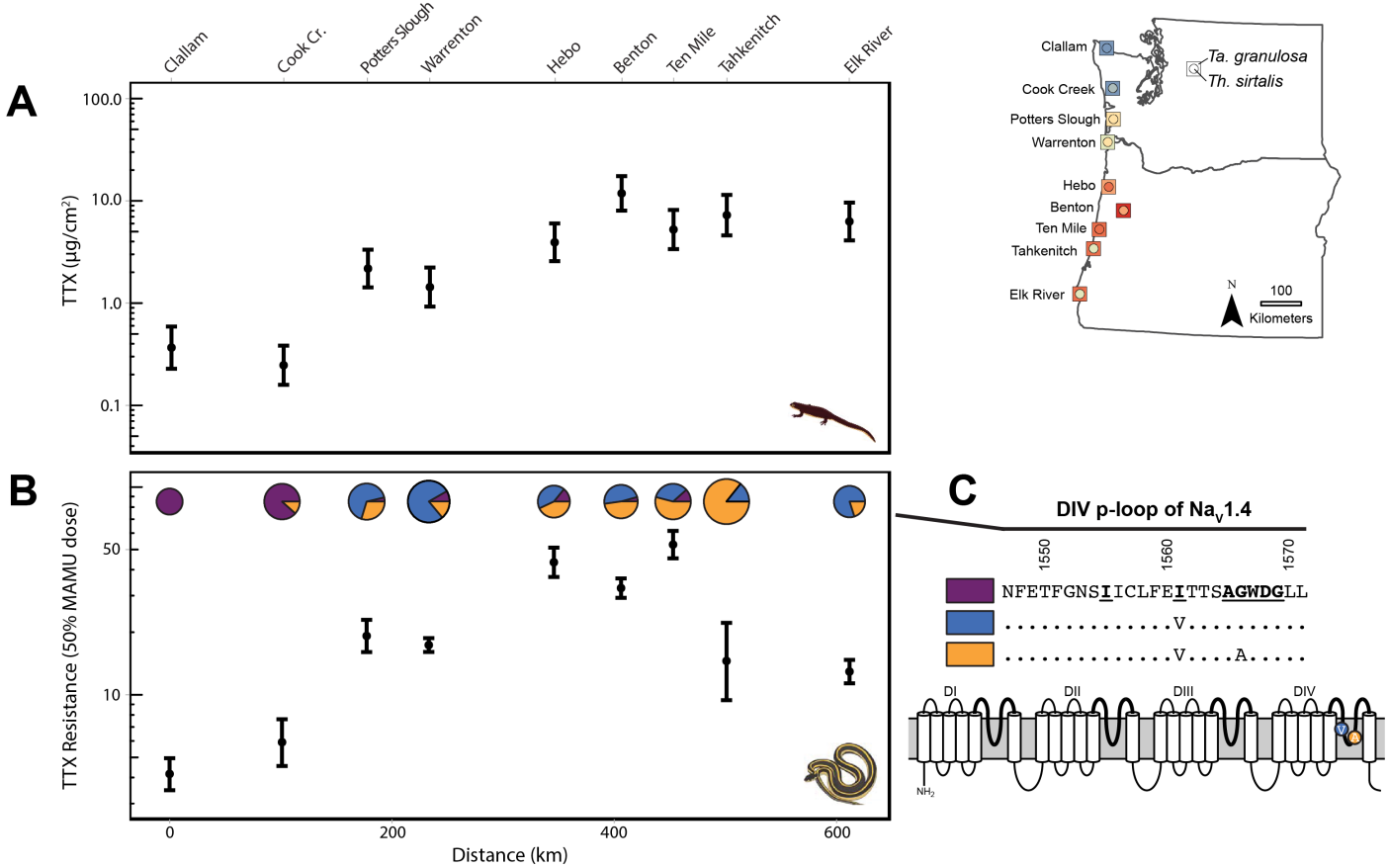


**Figure 1. Matching phenotypes in prey and predator imply arms race coevolution.** (**A**) Population means of TTX toxicity (µg/cm$^2$) in newts and (**B**) phenotypic TTX resistance (50% MAMU dose) in snakes along the latitudinal transect. Error bars indicate 95% confidence intervals (CI). The x-axis represents linear distance (km) from the northernmost sampling site (Clallam; 0 km). (**C**)

For snakes, the frequency of TTX-resistant alleles in the $Na_V1.4$ channel is shown with pie charts proportional to sample size. To the right, the schematic of $Na_V1.4$ shows the four domains of the channel (DI–DIV), with the extracellular pore loops (p-loops) highlighted with bold lines. Specific amino acid changes in the DIV p-loop are shown in their relative positions within the pore. The TTX-sensitive ancestral sequence (purple) is listed, followed by the two derived alleles known to confer increases in channel resistance. Map inset illustrates mosaic patterns of prey toxicity and predator resistance at each location along the transect.

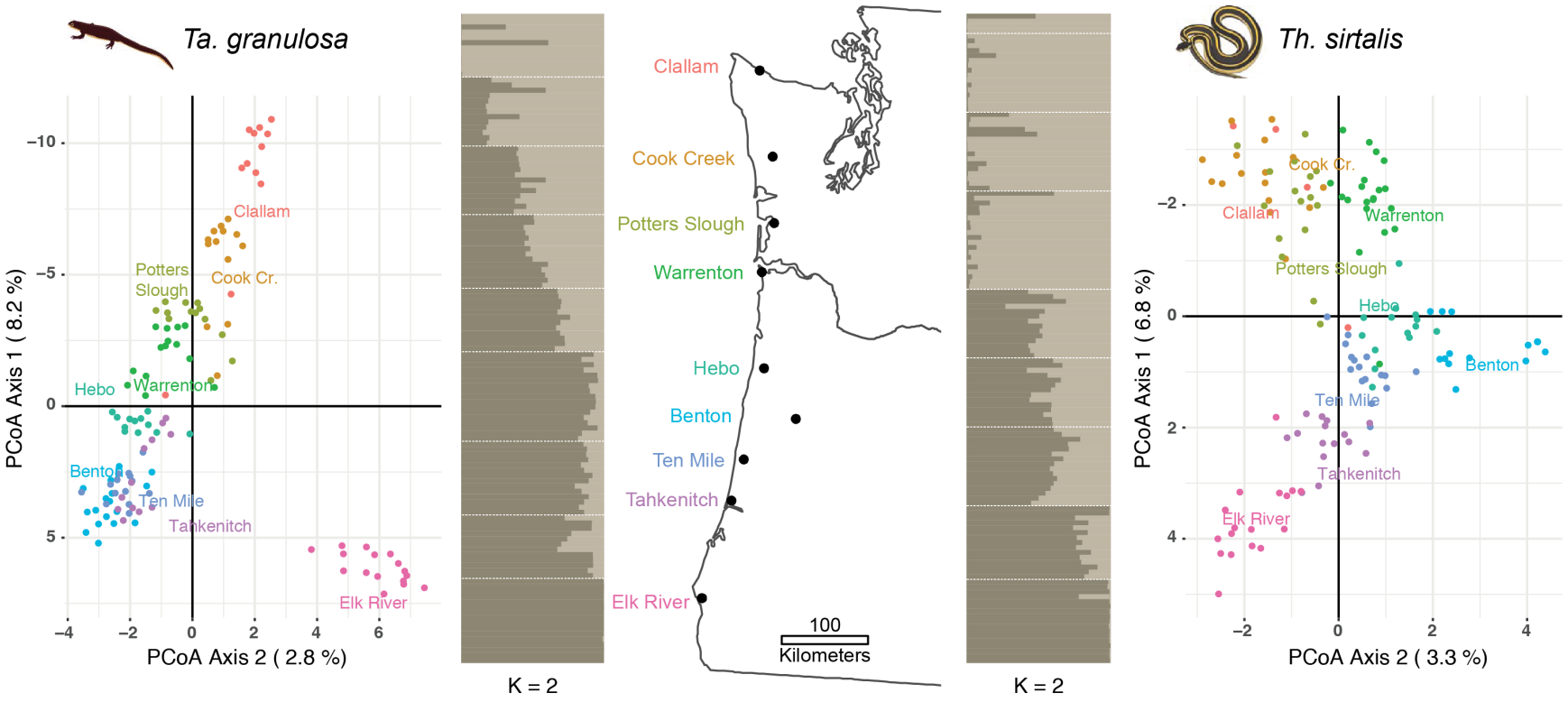


**Figure 2. Populations of prey and predator differ in geographic structure.** Results from the principal coordinate (PCoA) and STRUCTURE analyses of neutral SNPs from newts and snakes. PCoA graphs are rotated 90º to emphasize the major axis of variation corresponding to latitude. STRUCTURE plots are arranged latitudinally by population, in the same order as the map. Each horizontal

bar represents the ancestry assignment of an individual, with populations separated by white dashed lines. Average ancestry assignment values for each population were used as a neutral expectation in the cline-fitting analyses.

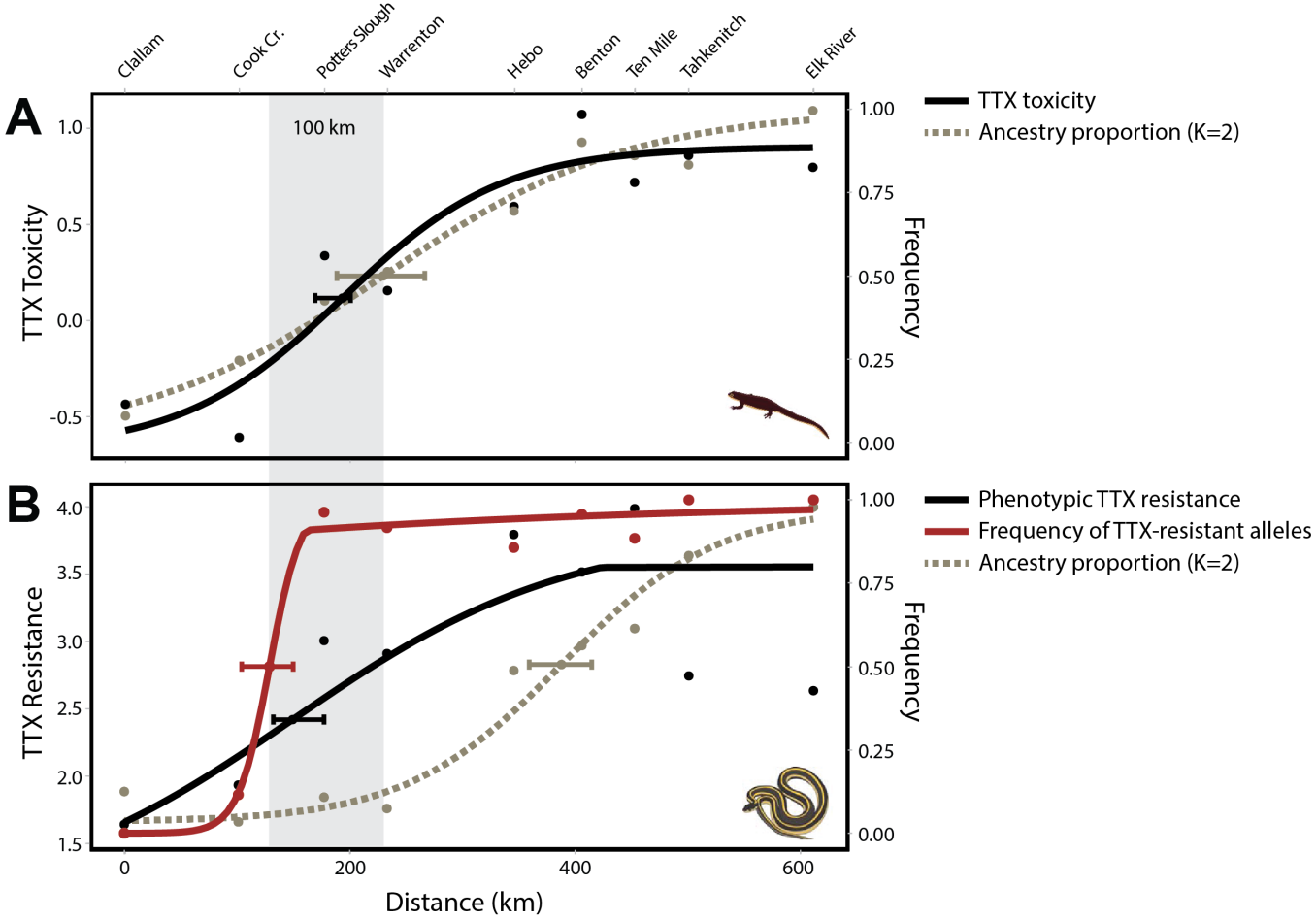


**Figure 3. Prey toxicity is best predicted by neutral population structure, whereas predator resistance is predicted by prey toxicity.** Cline-fitting results for phenotypic and genetic variation are shown, with error bars indicating confidence intervals

surrounding the geographic cline centers. (**A**) Phenotypic clines of TTX toxicity (log[TTX μg/cm$^2$ + 0.1]) and (**B**) TTX resistance (ln[MAMU + 1]) are shown in black. For snakes, the frequency of TTX-resistant alleles in the $Na_V1.4$ channel was also modeled (in red). Gray dashed lines represent the neutral expectation for trait variation based on population genomic structure for STRUCTURE. The cline center points of newt neutral structure, toxicity, phenotypic resistance, and TTX-resistant alleles are all located within in 100 km of each other along the 611 km transect.

**Supplemental Information**

**Materials and Methods**

We sampled phenotypic and genomic data from *Ta. granulosa* (n=138) and *Th. sirtalis* (n=169) at nine locations along a latitudinal transect in the states of Washington and Oregon (Figure 1; Table S1) and compared mosaic patterns of escalation in the arms race to neutral population genomic structure across the landscape.

*TTX toxicity of* Ta. granulosa

We estimated levels of TTX in *Ta. granulosa* using a Competitive Inhibition Enzymatic Immunoassay (CIEIA) and TTX-specific antibodies (Gall et al. 2011; Stokes et al. 2012). We quantified the amount of TTX in a 5mm circle skin punch from the dorsum of each newt using a human skin-biopsy punch (Acu-Punche, Acuderm Inc.) (Hanifin et al. 2002, 2004; Hague et al. 2016). These data were used to estimate the dorsal skin concentration of TTX ($\mu g/cm^2$) in each individual. TTX is uniformly distributed throughout the dorsum and levels of TTX in the dorsal skin are tightly correlated with toxicity in other regions (Hanifin et al. 2004). We conducted a two-way ANOVA to test whether TTX differed by population and by sex, because past work suggests toxicity may vary by sex (Hanifin et al. 2002). Distribution and leverage analyses indicated that a $\log(x + 0.1)$ transformation of TTX was needed. Transformed mean and variance values were used in the cline-fitting analysis of TTX toxicity along the transect.

Although a considerable body of work has described the genetic basis of TTX resistance in *Th. sirtalis* (see below), similar information regarding toxicity of *Ta.*

*granulosa* is unavailable. Although we were unable to characterize genetic variation underlying prey toxicity, we assume that TTX production probably has a polygenic basis. For example, biosynthesis of saxitoxin (STX), a similar neurotoxin found in puffer fish, involves gene expression in a cluster of up to 26 genes (Moczydlowski 2013).

*TTX resistance of* Th. sirtalis

We measured phenotypic TTX resistance using a well-established bioassay of whole animal performance from previous studies (Brodie and Brodie 1990; Brodie et al. 2002; Ridenhour et al. 2004; Hague et al. 2017). Briefly, each individual was assayed on a 4 m racetrack to characterize its "baseline" crawl speed, then injected intraperitoneally with a known dose of TTX and assayed for "post-injection" speed. Population estimates of phenotypic TTX resistance are reported on a scale of mass-adjusted mouse units (MAMUs) to control for differences in body size (Brodie et al. 2002). Resistance was estimated as the relative performance after injection: the 50% MAMU dose of TTX that reduces performance by 50% of baseline speed. We incorporated racetrack data from previously published estimates of resistance from the same sampling locations to generate precise population estimates of phenotypic resistance in this study (see Table S1; Brodie et al. 2002; Ridenhour 2004).

The 50% MAMU dose was estimated separately for each population from a dose-response curve using curvilinear regression and the general transform $y' = \ln(1/y - 1)$ (Brodie et al. 2002). Individuals from each population received a series of TTX doses, with an average of 2.6 different doses per individual. At $y = 0.5$ (i.e., 50%), $y' = 0$ and the 50% dose is estimable $\hat{x} = -\alpha/\beta$ (where $\alpha$ is the intercept and $\beta$ the slope from the

curvilinear regression). Because $\hat{x}$ takes the form of a ratio, the standard error for the estimated 50% dose is calculated using standard methods for the variance of a ratio (Lynch et al. 1998 p. 818; Brodie et al. 2002). Confidence intervals of 95% were calculated as ±1.96 SE. Regression was performed in R with the "lmer" function implemented in the lme4 package (Bates et al. 2015). The individual ID of each snake was included as a random effect to account for the fact that each snake received multiple injections. Distribution and leverage analysis indicated that a transformation of the $x$ variable (MAMU of TTX) was needed, so we transformed the data using $x' = \ln(x + 1)$ (as in Brodie et al. 2002). Differences among populations in phenotypic TTX resistance were deemed significant if 95% confidence intervals did not overlap by more than half of a one-sided error bar (Cumming and Finch 2005).

We genotyped snakes for their amino acid sequence in the DIV p-loop of the $Na_V1.4$ channel. Methods for Sanger sequencing are described in Hague et al. (2017). For each individual, we sequenced a 666 bp fragment that includes the DIV p-loop region of $Na_V1.4$. The $Na_V1.4$ protein is encoded by the *SCN4A* gene located on the Z sex chromosome of *Th. sirtalis* (Hague et al., *unpublished*). Colubrid snakes, including garter snakes, have heteromorphic sex chromosomes (ZZ males, ZW females) that are non-recombining (Vicoso et al. 2013; Augstenová et al. 2018), and females appear to be hemizygous for the Z-linked *SCN4A* gene. In males, heterozygous positions on chromatograms were identified by eye and confirmed in both directions with sequencing. The haplotype phase of the DIV p-loop sequence for each male was inferred computational with the program PHASE (Stephens et al. 2001).

We translated the aligned DIV p-loop coding sequences into the amino acids and tested for departures from Hardy-Weinberg Equilibrium (HWE) using a joint test for HWE and equality of allele frequencies (EAF) using the *HWTriExact* function in the HardyWeinberg package in R (Graffelman and Morales-Camarena 2008; Graffelman and Weir 2018a,b). Standard tests for HWE rely on the assumption of EAF in males and females. The joint exact test for HWE and EAF accounts for the hemizygous sex and tests for joint departures of HWE and EAF (Graffelman and Weir 2016, 2018a,b). We also calculated pairwise $F_{ST}$ divergence at the DIV p-loop in the program Arlequin (Excoffier and Lischer 2010) and used a Mantel test to test for a relationship between pairwise $F_{ST}$ divergence at the DIV p-loop and phenotypic divergence in whole-animal TTX resistance. Significance was tested with 1000 permutations.

*ddRADseq library preparation*

We prepared ddRADseq libraries separately for *Ta. granulosa* and *Th. sirtalis* using the protocol described in Peterson et al. (2012). Genomic DNA was extracted using the DNeasy Blood & Tissue kit (Qiagen Inc., Valencia, CA.). We digested 600 ng of genomic DNA for each sample using the restriction enzymes *EcoRI* and *SbfI* for *Ta. granulosa* and *MfeI* and *SbfI* for *Th. sirtalis*. Unique combinations of individual P1 and P2 barcoded adapters were annealed to the digested genomic DNA of each sample. Each barcode was six base pairs long and differed by at least two nucleotides. After barcoding, *Ta. granulosa* and *Th. sirtalis* samples were pooled separately, purified with AmpureXP beads (Beckman Coulter, Inc., Brea, CA, USA), and size selected for 500 to 600 bp fragments using a Pippin Prep (Sage Science, Inc., Beverly, MA, USA). We enriched the

adapter-ligated fragments in the size-selected libraries using 16 PCR cycles and then purified the product with AmpureXP beads. The *Ta. granulosa* and *Th. sirtalis* libraries were each run on two lanes of the Illumina HiSeq 2500 platform (Illumina, Inc., San Diego, CA, USA) to generate 125 bp paired-end reads.

*Data processing of Illumina sequencing*

Read quality of the raw sequence data was assessed using FastQC 0.11.5 (Andrew 2016). We used *process_radtags* in Stacks 1.46 (Catchen et al. 2013) on both the *Ta. granulosa* and *Th. sirtalis* datasets to demultiplex reads and removed sequences with low-quality scores or uncalled bases. For the *Ta. granulosa* dataset, we used the *denovo_map.pl* pipeline in Stacks, because a reference genome is not currently available. We used a minimum depth of three (-*m*), a distance of three between stacks (-*M*), and a distance of three between catalog loci (-*n*). The *Th. sirtalis* reads were aligned to the *Th. sirtalis* genome using Bowtie2 2.2.9 (Langmead and Salzberg 2012). We discarded reads that did not align or had more than one match to the genome. We used *ref_map.pl* in Stacks to assemble the reference-aligned sequences into loci, with a minimum depth of three (-*m*). For both species, we used *populations* in Stacks to select loci with a minimum depth of 10x coverage. To avoid linkage among sites within the same locus, we only retained one single nucleotide polymorphism (SNP) per locus.

We used the dartR package in R (Gruber et al. 2017; R Core Team 2018) to remove loci and individuals with >30% missing data. We also removed loci with a minor allele frequency (MAF) <5%, including those that were invariant. Finally, we removed putative loci under selection. The program BayeScan 2.1 was used to search for loci with

$F_{ST}$ coefficients that were significantly different than those expected under neutrality (Foll and Gaggiotti 2008). The Bayesian analysis used 20 pilot runs with 5,000 iterations followed by an additional burn-in of 50,000 and 50,000 output iterations. An outlier analysis with FDR-corrected p-values (q-values) <0.05 was used to identify and remove outlier loci putatively under selection.

*Analysis of neutral population structure*

The filtered SNPs for each species were used to calculate observed heterozygosity ($H_O$) and gene diversity ($H_S$) for each population (Nei 1987) using the hierfstat package in R (Goudet and Jombart 2015). To estimate neutral population genomic structure, we calculated global and pairwise $F_{ST}$ values (Weir and Cockerham 1984). Confidence intervals were estimated by running 1000 bootstraps over loci using the hierfstat and stAMPP packages in R (Pembleton et al. 2013). We tested for a pattern of isolation-by-distance (IBD) along each transect by performing Mantel tests on matrices of linearized $F_{ST}$ and geographic distance (Rousset 1997). We also conducted distance-based redundancy analyses (dbRDA), which are thought to be more reliable than Mantel tests at detecting spatial patterns like IBD (Legendre and Fortin 2010; Meirmans 2015). We conducted dbRDA analyses in the vegan package in R (Oksanen et al. 2018) to test for a relationship between pairwise $F_{ST}$ values and the geographic coordinates (latitude and longitude) of sampling locations. We assessed significance of IBD tests with 1000 permutations.

We visualized population structure of each species using a principal coordinate analysis (PCoA) in the dartR package in R. We also used a Bayesian assignment

approach implemented in the program STRUCTURE (Pritchard et al. 2000; Falush et al. 2003). We estimated the optimal number of genetic clusters (K) ranging for one to nine, without populations included as priors. The model assumed population admixture and correlated allele frequencies (Falush et al. 2003). The analysis first ran for 100,000 iterations as burn-in and then we collected data from the following 1,000,000 interactions in 10 different independent runs. STRUCTURE HARVESTER (Earl and vonHoldt 2012) was used to detect the most probable K using the Evanno's method (Evanno et al. 2005). Ancestry proportion (Q) values of the 10 runs for each value of the most probable K we averaged using CLUMPP (Jakobsson and Rosenberg 2007) and visualized using the pophelper package in R (Francis 2017). We calculated the average Q value for each population, which represent the fraction of membership to each genetic cluster (K). These Q estimates were used in cline-fitting analyses (see below).

*Multiple regression of distance matrices (MRMs)*

MRMs are an extension of Mantel tests that involve multiple regression of a response distance matrix on explanatory matrices (Manly 1986; Smouse et al. 1986; Legendre et al. 1994; Lichstein 2007). Partial regression coefficients can be used to understand the relationship between two matrices while controlling for the effects of a third matrix (e.g. Rosenblum 2005; Toju et al. 2011). For each species, we generated two distance matrices: (1) pairwise phenotypic divergence in the coevolutionary trait (e.g., log-transformed TTX of *Taricha*) and (2) pairwise genomic divergence ($F_{ST}$) from neutral SNPs. We then tested whether population patterns of phenotypic escalation in a focal species (e.g., TTX of *Ta. granulosa*) are best explained by neutral genomic

divergence (pairwise $F_{ST}$) or escalation in the natural enemy (TTX resistance of *Th. sirtalis*). MRM analyses can be confounded when explanatory variables are spatially autocorrelated, so we compared results when the two explanatory variables were analyzed separately and together (Raufaste and Rousset 2001; Rousset and Waller 2002; Rosenblum 2005).

*Cline analyses*

We performed ML cline-fitting analyses on the phenotypic and genetic data from each species (Szymura and Barton 1986, 1991). For *Ta. granulosa*, we fit a cline to TTX toxicity using the mean and variance of the log-transformed TTX data (μg/cm$^2$). For *Th. sirtalis*, we fit (1) a cline to phenotypic TTX resistance using the 50% MAMU dose and variance from the ln-transformed MAMU data and (2) a genetic cline to the frequency of TTX-resistant alleles in each population. Due to the presence of two different TTX-resistant DIV alleles in the Pacific Northwest, we fit separate clines for each derived allele ($Na_V1.4^V$ and $Na_V1.4^{VA}$) and a third cline that combined the frequency of the two alleles. Only the combined analysis showed a clear pattern of clinal variation. For each species, we compared clinal variation in coevolutionary traits to variation at the neutral SNPs. We fit clines to the STRUCTURE ancestry proportions (Q) from the most likely value of K for each species (K=2). We reran cline-fitting analyses with the Elk River population removed from the *Ta. granulosa* dataset, because the PCoA (Figure 2) and STRUCTURE plot of K=3 (Figure S1) both suggest the population is genetically distinct from all others; however, this produced the same qualitative result as when the population was included.

We fit clines using the HZAR package in R (Derryberry et al. 2014). We calculated distances along the cline as kilometers (km) from the northernmost sampling site (Clallam). We ran 15 separate models that varied in the number of cline shape parameters estimated. All models estimated the cline center (distance from sampling location 1, *c*) and width (1/maximum slope, *w*), but could additionally estimate combinations of exponential decay curve (tail) parameters (neither tail, right tail only, left tail only, mirrored tails, or both tails separately), which represent the distance from the cline center to the tail (δ) and the slope of the tail (τ). The genetic models varied as to whether they estimated allele frequencies at the cline ends ($p_{min}$ and $p_{max}$) or fixed them at 0 and 1. All models were then compared using AIC corrected for small sample sizes (AICc) and maximum likelihood parameters were extracted for the best-fitting model. We considered cline centers with non-overlapping two log-likelihood unit support limits (confidence intervals; CIs) to occur in significantly different geographic locations (e.g., Baldassarre et al. 2014; Scordato et al. 2017).

## Supplementary Text

### Extended Description of Results

*ddRADseq results*

Illumina HiSeq sequencing yielded an average of 1,093,529 raw reads per sample of *Ta. granulosa* (n=137). After initial quality control in *process_radtags*, the *denovo_map* pipeline in Stacks identified an average of 32,469 loci per individual, with a mean of 19x coverage. After further filtering steps in *populations*, dartR, and Bayescan, we retained 3,634 unlinked neutral SNPs in 123 individuals. For *Th. sirtalis*, sequencing

yielded an average of 2,451,623 raw reads per sample (n=143). The *ref_map* pipeline identified an average of 13,501 loci per individual, with a mean of 80x coverage. After additional filtering, we retained 1,027 unlinked neutral SNPs in 132 individuals. Estimates of population genetic diversity from the final SNP dataset of each species are reported in Table S2. Global $F_{ST}$ values for *Ta. granulosa* ($F_{ST}$=0.068, 95% CI [0.065, 0.069]) and *Th. sirtalis* ($F_{ST}$=0.070, 95% CI [0.067, 0.075]) were very similar; however, estimates of pairwise $F_{ST}$ revealed different spatial patterns of divergence in each species (Table S3). Pairwise $F_{ST}$ values were used in the IBD and MRM analyses.

**Supplementary Tables and Figures**

**Table S1.** Datasets for each sampling location along the latitudinal transect. The total number of animals sampled in this study are shown first, followed by the number of individuals (n) included in each analysis. For estimates of phenotypic resistance in *Th. sirtalis*, we combined individuals from this study with previously published racetrack data from the same sampling locations (Brodie et al. 2002; Ridenhour 2004). In the DIV p-loop, the number (n) of alleles sampled accounts for females, the hemizygous sex with only one genetic copy of $Na_V1.4$. Results are shown for the joint test of Hardy-Weinberg Equilibrium (HWE) and Equality of Allele Frequencies (EAF).

| | | Total animals sampled in this study | | *Ta. granulosa* | | | | *Th. sirtalis* | | | | | |
|---|---|---|---|---|---|---|---|---|---|---|---|---|---|
| | | | | TTX | | | ddRADseq | Phenotypic TTX resistance | | | DIV p-loop | | ddRADseq |
| Location | County | *Ta. granulosa* | *Th. sirtalis* | n | mean (ug/cm$^2$) | SE | n | n | 50% MAMU | SE | n alleles | HWE & EAF test p-value | n |
| Clallam | Clallam, WA | 12 | 11 | 12 | 0.731 | 0.307 | 12 | 53 | 4.163 | 0.076 | 14 | NA | 4 |
| Cook Creek | Grays Harbor, WA | 14 | 17 | 14 | 0.236 | 0.112 | 13 | 14 | 5.915 | 0.119 | 26 | 1.000 | 16 |
| Potter's Slough | Pacific, WA | 15 | 20 | 15 | 2.75 | 0.686 | 13 | 42 | 19.203 | 0.090 | 27 | 1.000 | 16 |
| Warrenton | Clatsop, OR | 15 | 24 | 14 | 1.63 | 0.241 | 14 | 323 | 17.357 | 0.038 | 36 | 0.257 | 20 |
| Hebo | Tillamook, OR | 15 | 15 | 15 | 4.65 | 0.822 | 12 | 2 | 43.413 | 0.085 | 21 | 0.708 | 14 |
| Benton | Benton., OR | 18 | 20 | 18 | 16.9 | 3.1 | 17 | 345 | 32.626 | 0.055 | 23 | 0.347 | 14 |
| Ten Mile | Lane, OR | 15 | 16 | 14 | 7.43 | 1.85 | 14 | 93 | 52.817 | 0.079 | 26 | 0.451 | 16 |
| Lake Tahkenitch | Douglas, OR | 14 | 29 | 13 | 10.7 | 2.56 | 12 | 17 | 14.552 | 0.227 | 42 | 0.182 | 15 |
| Elk River | Curry, OR | 20 | 17 | 15 | 6.52 | 0.612 | 16 | 43 | 12.935 | 0.063 | 20 | 0.324 | 17 |
| | **Total** | 138 | 169 | 130 | | | 123 | 932 | | | 235 | | 132 |

**Table S2.** Population genetic diversity statistics from neutral SNPs in each species. Sample size (n), average observed heterozygosity ($H_O$), and gene diversity ($H_S$) are shown, along with standard deviations (SD).

| | *Ta. granulosa* | | | | | *Th. sirtalis* | | | | |
|---|---|---|---|---|---|---|---|---|---|---|
| **Population** | **n** | **$H_O$** | **$H_O$ SD** | **$H_S$** | **$H_S$ SD** | **n** | **$H_O$** | **$H_O$ SD** | **$H_S$** | **$H_S$ SD** |
| Clallam | 12 | 0.278 | 0.248 | 0.253 | 0.196 | 4 | 0.328 | 0.297 | 0.294 | 0.218 |
| Cook Creek | 13 | 0.324 | 0.237 | 0.294 | 0.178 | 16 | 0.311 | 0.231 | 0.288 | 0.177 |
| Potters Slough | 13 | 0.352 | 0.225 | 0.320 | 0.163 | 16 | 0.319 | 0.230 | 0.293 | 0.169 |
| Warrenton | 14 | 0.321 | 0.200 | 0.323 | 0.156 | 20 | 0.297 | 0.218 | 0.292 | 0.170 |
| Hebo | 12 | 0.330 | 0.205 | 0.332 | 0.159 | 14 | 0.292 | 0.218 | 0.302 | 0.168 |
| Benton | 17 | 0.335 | 0.198 | 0.330 | 0.154 | 14 | 0.337 | 0.270 | 0.288 | 0.184 |
| Ten Mile | 14 | 0.325 | 0.201 | 0.332 | 0.157 | 16 | 0.363 | 0.246 | 0.303 | 0.163 |
| Tahkenitch | 12 | 0.376 | 0.244 | 0.332 | 0.169 | 15 | 0.303 | 0.220 | 0.296 | 0.169 |
| Elk River | 16 | 0.300 | 0.204 | 0.318 | 0.174 | 17 | 0.306 | 0.232 | 0.285 | 0.180 |
| Total | 123 | 0.327 | 0.218 | 0.315 | 0.168 | 132 | 0.317 | 0.240 | 0.293 | 0.178 |

**Table S3.** Pairwise $F_{ST}$ statistics for the neutral SNP datasets of each species. For *Th. sirtalis*, $F_{ST}$ divergence at the DIV p-loop of the $Na_V1.4$ channel is also shown. $F_{ST}$ values are shaded red to illustrate the extent of divergence among different populations (white=0.00, red=1.00).

***Ta. granulosa* pairwise $F_{ST}$ of neutral SNPs**

| | Clallam | Cook Creek | Potters Slough | Warrenton | Hebo | Benton | Ten Mile | Tahkenitch |
|---|---|---|---|---|---|---|---|---|
| **Cook Creek** | 0.040 | | | | | | | |
| **Potters Slough** | 0.066 | 0.011 | | | | | | |
| **Warrenton** | 0.077 | 0.024 | 0.004 | | | | | |
| **Hebo** | 0.111 | 0.058 | 0.031 | 0.019 | | | | |
| **Benton** | 0.158 | 0.096 | 0.057 | 0.039 | 0.020 | | | |
| **Ten Mile** | 0.147 | 0.088 | 0.053 | 0.034 | 0.013 | 0.007 | | |
| **Tahkenitch** | 0.144 | 0.088 | 0.055 | 0.040 | 0.022 | 0.016 | 0.009 | |
| **Elk River** | 0.218 | 0.154 | 0.116 | 0.101 | 0.081 | 0.066 | 0.065 | 0.067 |

***Th. sirtalis* pairwise $F_{ST}$ of neutral SNPs**

| | Clallam | Cook Creek | Potters Slough | Warrenton | Hebo | Benton | Ten Mile | Tahkenitch |
|---|---|---|---|---|---|---|---|---|
| **Cook Creek** | 0.044 | | | | | | | |
| **Potters Slough** | 0.058 | 0.025 | | | | | | |
| **Warrenton** | 0.069 | 0.054 | 0.044 | | | | | |
| **Hebo** | 0.067 | 0.063 | 0.051 | 0.052 | | | | |
| **Benton** | 0.120 | 0.104 | 0.084 | 0.082 | 0.045 | | | |
| **Ten Mile** | 0.066 | 0.070 | 0.058 | 0.062 | 0.024 | 0.056 | | |
| **Tahkenitch** | 0.097 | 0.087 | 0.075 | 0.086 | 0.031 | 0.065 | 0.029 | |
| **Elk River** | 0.150 | 0.129 | 0.114 | 0.127 | 0.083 | 0.110 | 0.064 | 0.031 |

***Th. sirtalis* pairwise $F_{ST}$ of DIV p-loop**

| | Clallam | Cook Creek | Potters Slough | Warrenton | Hebo | Benton | Ten Mile | Tahkenitch |
|---|---|---|---|---|---|---|---|---|
| **Cook Creek** | 0.039 | | | | | | | |
| **Potters Slough** | 0.688 | 0.625 | | | | | | |
| **Warrenton** | 0.722 | 0.665 | 0.014 | | | | | |
| **Hebo** | 0.575 | 0.497 | 0.034 | 0.154 | | | | |
| **Benton** | 0.652 | 0.579 | 0.025 | 0.162 | -0.034 | | | |
| **Ten Mile** | 0.593 | 0.514 | 0.105 | 0.251 | -0.028 | -0.019 | | |
| **Tahkenitch** | 0.820 | 0.739 | 0.455 | 0.595 | 0.254 | 0.245 | 0.147 | |
| **Elk River** | 0.805 | 0.725 | -0.010 | -0.024 | 0.141 | 0.132 | 0.230 | 0.603 |

**Table S4.** Results from cline-fitting analyses. The mean value and its geographic center point along the cline are shown for each dataset, in addition to cline width. Confidence intervals (CI) are also listed.

| | | Mean | Center (km) | Lower CI | Upper CI | Width (km) | Lower CI | Upper CI |
|---|---|---|---|---|---|---|---|---|
| ***Ta. granulosa*** | **TTX** | 0.118 | 193.184 | 168.778 | 200.283 | 284.949 | 207.732 | 363.750 |
| | **STRUCTURE (K=2)** | 0.500 | 229.646 | 188.078 | 265.566 | 440.284 | 348.296 | 574.741 |
| ***Th. sirtalis*** | **50% MAMU dose** | 2.420 | 149.352 | 132.245 | 177.267 | 487.621 | 308.045 | 496.891 |
| | **Freq. of TTX resistant alleles** | 0.500 | 128.843 | 104.118 | 149.925 | 55.589 | 5.569 | 101.699 |
| | **STRUCTURE (K=2)** | 0.506 | 387.698 | 359.552 | 415.000 | 276.425 | 206.047 | 368.235 |

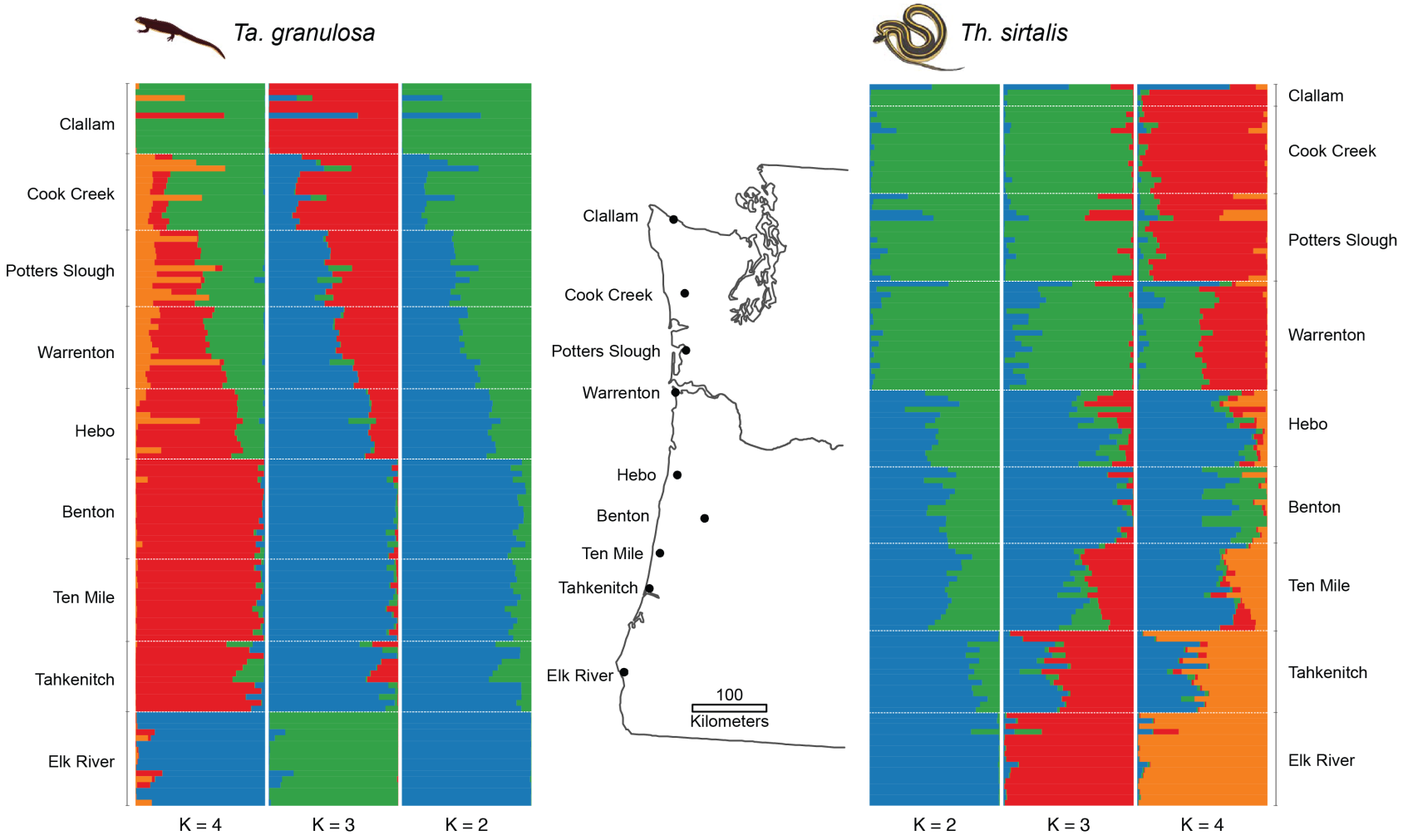


**Figure S1.** STRUCTURE results for K=2-4. The most likely number of genetic cluster was K=2 for both species (Figure 2).

# APPENDIX 1:

Analysis of coevolution and population structure in the California lineages of *Thamnophis sirtalis* and *Taricha* species

## Introduction

Using the methodology described in Chapter 4, I estimated phenotypic and genomic divergence in prey and predator populations along a second latitudinal transect in California. Populations of *Thamnophis sirtalis* in the Pacific Northwest and California represent two distinct evolutionary lineages that each independently evolved TTX-resistant mutations to the $Na_V1.4$ channel (Janzen et al. 2002; Hague et al. 2017). The results from California do not contradict those from the Pacific Northwest described in Chapter 4. A number of sampling issues restricted the scope of this analysis, so the results are presented separately herein.

I conducted fine-scale population sampling of rough-skinned newts (*Taricha granulosa*; n=91), California newts (*Ta. torosa*; n=76), and common garter snakes (*Th. sirtalis*; n=138) along a transect of 10 locations that span the phenotypic extremes of the geographic mosaic (Figure 1; Table S1), ranging from low levels of newt toxicity and snake resistance (northern California) to a hotspot of phenotypic escalation (the Bay Area). I attempted to characterize levels of TTX in both newt species at all the locations where they co-occur; however, in most cases, I was unable to obtain an adequate sample of both *Taricha* species for each site. I estimated TTX resistance of garter snakes at each location, including whole-animal phenotypic resistance and $Na_V1.4$ channel genotypes. I then compared these data to neutral patterns of population genomic variation using single nucleotide polymorphisms (SNPs) in each species. Issues arose with the genomic analysis due to the poor quality of double digest restriction-site associated DNA sequencing (ddRADseq) in some of the garter snake samples. Challenges associated with the analysis are summarized in the Discussion.

**Results**

I found that TTX toxicity ($\mu g/cm^2$) of *Taricha* newts varied among location (ANOVA; $F[9,146]=35.13$, $p<0.001$), species ($F[1,146]=56.80$, $p<0.001$), and sex ($F[1,146]=5.17$, $p=0.025$) along the latitudinal transect (Figure 1, Table 1). TTX resistance (50% MAMU dose) of snakes also varied among populations (according to non-overlapping 95% confidence intervals; Figure 1, Table 1). Populations of *Th. sirtalis* in central California (Hopland, Knoxville, and Russian River) are extremely resistant, such that the 50% dose far exceeds 250 MAMUs. Due to limited availability of TTX, a maximum dose of 250 MAMUs was used in assays of resistance, so I was unable to estimate the true 50% dose in these highly resistant snakes. In the $Na_V1.4$ channel, observed allele frequencies of the DIV p-loop were in Hardy-Weinberg Equilibrium (HWE) for all populations except Russian River and Ledson Marsh, according to a joint HWE and equality of allele frequencies (EAF) test (Figure 1, Table 1).

I used neutral SNPs to assess population genetic structure in *Taricha* spp. and *Th. sirtalis*. Illumina HiSeq sequencing yielded an average of 1,001,285 raw reads per sample of *Taricha* (n=165). After initial quality control in *process_radtags*, the *denovo_map* pipeline identified an average of 30,976 loci per individual at a mean of 18x coverage. Further filtering in *populations*, dartR, and MrBayes resulted in 3,352 unlinked neutral SNPs in 74 individuals for *Ta. granulosa*, and 3,162 SNPs in 57 individuals for *Ta. torosa*. Because *Ta. torosa* were only sampled at four localities, I present only the results from the *Ta. granulosa* SNP dataset. For *Th. sirtalis*, sequencing yielded an average of 1,529,289 reads per sample (n=138). The *ref_map* pipeline identified an average of 8,923

loci per individual at a mean of 79x coverage. After additional filtering, I retained 441 unlinked neutral SNPs in 103 individuals.

Estimates of heterozygosity are presented in Table 2. Global $F_{ST}$ values for *Ta. granulosa* were high ($F_{ST}$=0.255, 95% CI [0.249, 0.261]), whereas *Th. sirtalis* had low-to-moderate levels of population divergence ($F_{ST}$=0.088, 95% CI [0.081, 0.095]). Pairwise $F_{ST}$ values for each population are listed in Table 3. Distance-based redundancy analyses (dbRDA) did not detect significant evidence of isolation-by-distance (IBD) in either species. Principal coordinate (PCoA; Figure 2) and STRUCTURE (Figure 3) analyses revealed different spatial patterns of geographic population structure in prey and predator. Interestingly, the two populations of *Th. sirtalis* that deviated significantly from HWE, Russian River and Ledson Marsh, showed evidence of admixture between the two genetic clusters identified in STRUCTURE (Figure 3). Finally, I used multiple regression of distance matrices (MRMs) to test whether phenotypic divergence in one species (e.g., toxicity of *Ta. granulosa*) is predicted by (1) neutral genomic divergence (pairwise $F_{ST}$) or (2) phenotypic divergence in the natural enemy (TTX resistance of *Th. sirtalis*); however, I detected no significant relationships.

**Discussion**

I found an overall pattern of phenotypic matching in prey and predator populations, similar to that found in the Pacific Northwest (Chapter 4). Among-site differences in newt toxicity appear to be primarily driven by species-differences in TTX toxicity. *Taricha torosa* newts have escalated toxicity in populations north of the Bay Area (e.g., Hopland), whereas *Ta. granulosa* have escalated toxicity south of the Bay

(e.g., Gilroy). However, I was unable to confirm this pattern, because both *Taricha* species were not sampled at each location. For example, *Ta. granulosa* may also have escalated toxicity at Hopland.

The MRM analyses revealed no significant relationships among matrices of divergence in prey toxicity, predator resistance, or neutral genetic divergence. The absence of any significant relationship may reflect limited power due to the small number of sampling sites. Only six localities, all from the northern end of the transect, had all requisite phenotypic and genetic data (for both *Ta. granulosa* and *Th. sirtalis*) to be included in the MRM analyses: Dry Lagoon, Angelo, Willits, Knoxville, Russian River, and Ledson Marsh.

In the Pacific Northwest (Chapter 4), I found that phenotypic divergence in TTX toxicity was tightly correlated with the population genetic structure of *Ta. granulosa*, whereas TTX resistance in *Th. sirtalis* deviated from neutral expectations to track prey toxicity. This relationship is less clear in California, which may be partly due to the presence of multiple toxic newt species, both of which were poorly sampled in this dataset. Highly toxic *Ta. torosa* seem to occur north of the Bay Area, where I only sampled three populations (Figure 1). In contrast, toxic *Ta. granulosa* appear to occur south of the Bay, where I only sampled one population. Future studies should focus fine-scale sampling around these hotspots of toxicity to test whether mosaic patterns of phenotypic divergence are correlated with population genetic structure in either newt species.

In *Th. sirtalis*, population variation in TTX resistance appears to track the toxicity of the most toxic newt species of each location, while also deviating from expectations of

neutral genetic structure. For example, TTX resistance is low at Angelo and Willits where newts are non-toxic, but then sharply increases to the south at Hopland and Knoxville where *Ta. torosa* have high toxicity. This sharp cline in resistance occurs across a set of snake populations that otherwise lack neutral genetic divergence (Figure 3), implying that phenotypic divergence in resistance is the result of selection imposed by toxic prey, and not geographic population structure.

**Tables and Figures**

**Table 1.** Datasets for each sampling location along the latitudinal transect. The total number of animals sampled in this study are shown first, followed by the number of individuals (n) included in each analysis. Mean estimates of TTX toxicity at each location include samples from both newt species, *Ta. granulosa* and *Ta. torosa*. For estimates of phenotypic resistance in *Th. sirtalis*, we combined individuals from this study with previously published racetrack data from the same sampling locations (Brodie et al. 2002; Ridenhour 2004). In the DIV p-loop, the number (n) of alleles sampled accounts for females, the hemizygous sex with only one genetic copy of $Na_V1.4$. Results are shown for the joint test of Hardy-Weinberg Equilibrium (HWE) and Equality of Allele Frequencies (EAF).

| | | Total animals sampled in this study | | | *Taricha* species | | | | | *Th. sirtalis* | | | | | |
|---|---|---|---|---|---|---|---|---|---|---|---|---|---|---|---|
| | | | | | TTX | | | ddRADseq | | Phenotypic TTX resistance | | | DIV p-loop | | ddRAD seq |
| **Location** | **County** | ***Ta. granulosa*** | ***Ta. torosa*** | ***Th. sirtalis*** | **n** | **mean (ug/cm$^2$)** | **SE** | ***Ta. granulosa* n** | ***Ta. torosa* n** | **n** | **50% MAMU** | **SE** | **n alleles** | **HWE & EAF p-value** | **n** |
| Dry Lagoon | Humboldt, CA | 6 | NA | 20 | 6 | 0.043 | 0.020 | 5 | NA | 312 | 4.322 | 0.048 | 23 | NA | 20 |
| Angelo | Mendocino, CA | 17 | NA | 18 | 17 | 0.496 | 0.129 | 16 | NA | 9 | 11.383 | 0.591 | 31 | NA | 16 |
| Willits | Mendocino, CA | 9 | 6 | 12 | 15 | 1.670 | 0.367 | 6 | 4 | 78 | 7.873 | 0.063 | 16 | 0.1 | 11 |
| Hopland | Mendocino, CA | 0 | 15 | 17 | 15 | 7.990 | 1.130 | 0 | 11 | 9 | >250 | NA | 30 | NA | 16 |
| Knoxville | Napa, CA | 11 | 27 | 19 | 37 | 8.300 | 1.170 | 8 | 18 | 12 | >250 | NA | 27 | 0.655 | 18 |
| Russian River | Sonoma, CA | 14 | 0 | 19 | 14 | 0.844 | 0.224 | 9 | 0 | 83 | >250 | NA | 13 | 0.002 | 8 |
| Ledson Marsh | Sonoma, CA | 6 | 8 | 14 | 14 | 4.320 | 1.130 | 6 | 8 | 81 | 12.600 | 0.115 | 19 | 0.033 | 14 |
| Sonoma Mountain Ranch | Sonoma, CA | 20 | 0 | 0 | 20 | 0.874 | 0.167 | 20 | 0 | 0 | NA | NA | 0 | NA | 0 |
| Gilroy | Santa Cruz, CA | 8 | 0 | 11 | 8 | 7.950 | 2.010 | 4 | 0 | 141 | 86.179 | 0.290 | 8 | 1.286 | 0 |
| Santa Lucia | Monterey, CA | 0 | 20 | 8 | 20 | 1.150 | 1.050 | 0 | 16 | 190 | 33.116 | 0.147 | 0 | NA | 0 |
| | **Total** | **91** | **76** | **138** | **166** | | | **74** | **57** | **915** | | | **167** | | **103** |

**Table 2.** Population genetic diversity statistics from neutral SNPs in each species. Sample size (N), average observed heterozygosity ($H_O$), and gene diversity ($H_S$) are shown, along with standard deviations (SD).

| | *Ta. granulosa* | | | | | *Th. sirtalis* | | | | |
|---|---|---|---|---|---|---|---|---|---|---|
| **Population** | **N** | **$H_O$** | **$H_O$ SD** | **$H_S$** | **$H_S$ SD** | **N** | **$H_O$** | **$H_O$ SD** | **$H_S$** | **$H_S$ SD** |
| Dry Lagoon | 5 | 0.374 | 0.316 | 0.339 | 0.226 | 20 | 0.377 | 0.254 | 0.325 | 0.17 |
| Angelo | 16 | 0.235 | 0.219 | 0.232 | 0.193 | 16 | 0.355 | 0.24 | 0.314 | 0.169 |
| Willits | 6 | 0.322 | 0.257 | 0.29 | 0.19 | 11 | 0.314 | 0.246 | 0.309 | 0.175 |
| Hopland | NA | NA | NA | NA | NA | 16 | 0.308 | 0.236 | 0.311 | 0.181 |
| Knoxville | 8 | 0.234 | 0.223 | 0.208 | 0.176 | 18 | 0.325 | 0.218 | 0.313 | 0.161 |
| Russian River | 9 | 0.262 | 0.227 | 0.261 | 0.191 | 8 | 0.373 | 0.276 | 0.33 | 0.18 |
| Ledson Marsh | 6 | 0.209 | 0.249 | 0.22 | 0.223 | 14 | 0.364 | 0.253 | 0.316 | 0.167 |
| Sonoma Mtn. Ranch | 20 | 0.201 | 0.215 | 0.205 | 0.199 | NA | NA | NA | NA | NA |
| Gilroy | 4 | 0.153 | 0.249 | 0.163 | 0.228 | NA | NA | NA | NA | NA |
| **Total** | 74 | 0.249 | 0.244 | 0.24 | 0.203 | 103 | 0.345 | 0.246 | 0.317 | 0.172 |

**Table 3.** Pairwise $F_{ST}$ statistics for the neutral SNP datasets of each species. For *Th. sirtalis*, $F_{ST}$ divergence at the DIV p-loop of the $Na_V1.4$ channel is also shown. $F_{ST}$ values are shaded red to illustrate the extent of divergence among different populations (white=0.00, red=1.00).

***Ta. granulosa* pairwise $F_{ST}$ of neutral SNPs**

| | Dry Lagoon | Angelo | Willits | Knoxville | Russian River | Ledson Marsh | Sonoma Mtn. Ranch |
|---|---|---|---|---|---|---|---|
| **Angelo** | 0.228 | | | | | | |
| **Willits** | 0.131 | 0.041 | | | | | |
| **Knoxville** | 0.324 | 0.309 | 0.263 | | | | |
| **Russian River** | 0.216 | 0.103 | 0.080 | 0.267 | | | |
| **Ledson Marsh** | 0.320 | 0.216 | 0.203 | 0.304 | 0.145 | | |
| **Sonoma Mtn. Ranch** | 0.390 | 0.271 | 0.274 | 0.357 | 0.214 | 0.097 | |
| **Gilroy** | 0.365 | 0.332 | 0.307 | 0.470 | 0.278 | 0.383 | 0.407 |

***Th. sirtalis* pairwise $F_{ST}$ of neutral SNPs**

| | Dry Lagoon | Angelo | Willits | Hopland | Knoxville | Russian River |
|---|---|---|---|---|---|---|
| **Angelo** | 0.086 | | | | | |
| **Willits** | 0.109 | 0.040 | | | | |
| **Hopland** | 0.139 | 0.081 | 0.082 | | | |
| **Knoxville** | 0.092 | 0.079 | 0.063 | 0.082 | | |
| **Russian River** | 0.078 | 0.086 | 0.075 | 0.094 | 0.061 | |
| **Ledson Marsh** | 0.107 | 0.087 | 0.083 | 0.111 | 0.069 | 0.070 |

***Th. sirtalis* pairwise $F_{ST}$ of DIV p-loop**

| | Dry Lagoon | Angelo | Willits | Hopland | Knoxville | Russian River |
|---|---|---|---|---|---|---|
| **Angelo** | 0.000 | | | | | |
| **Willits** | 0.101 | 0.133 | | | | |
| **Hopland** | 1.000 | 1.000 | 0.905 | | | |
| **Knoxville** | 0.835 | 0.856 | 0.672 | 0.124 | | |
| **Russian River** | 0.594 | 0.647 | 0.282 | 0.565 | 0.183 | |
| **Ledson Marsh** | 0.547 | 0.594 | 0.356 | 0.719 | 0.512 | 0.25543 |

**Table 4.** Results from multiple regression of distance matrices (MRMs) comparing population divergence in phenotypic and genetic data.

| Response Variable | Explanatory Variable(s) | Coefficient | p-value |
|---|---|---|---|
| ***Ta. granulosa*** | | | |
| TTX toxicity | Neutral $F_{ST}$ | 0.538 | 0.626 |
| TTX toxicity | TTX Resistance of *Th. sirtalis* | -0.033 | 0.445 |
| TTX toxicity | Neutral $F_{ST}$ + TTX Resistance | | |
| | Neutral $F_{ST}$ | 1.904 | 0.227 |
| | TTX Resistance | -0.064 | 0.120 |
| ***Th. sirtalis*** | | | |
| TTX Resistance | Neutral $F_{ST}$ | 10.292 | 0.370 |
| TTX Resistance | TTX toxicity of *Taricha* species | 1.026 | 0.119 |
| TTX Resistance | Neutral $F_{ST}$ + TTX toxicity | | |
| | Neutral $F_{ST}$ | -2.183 | 0.902 |
| | TTX toxicity | 1.084 | 0.201 |

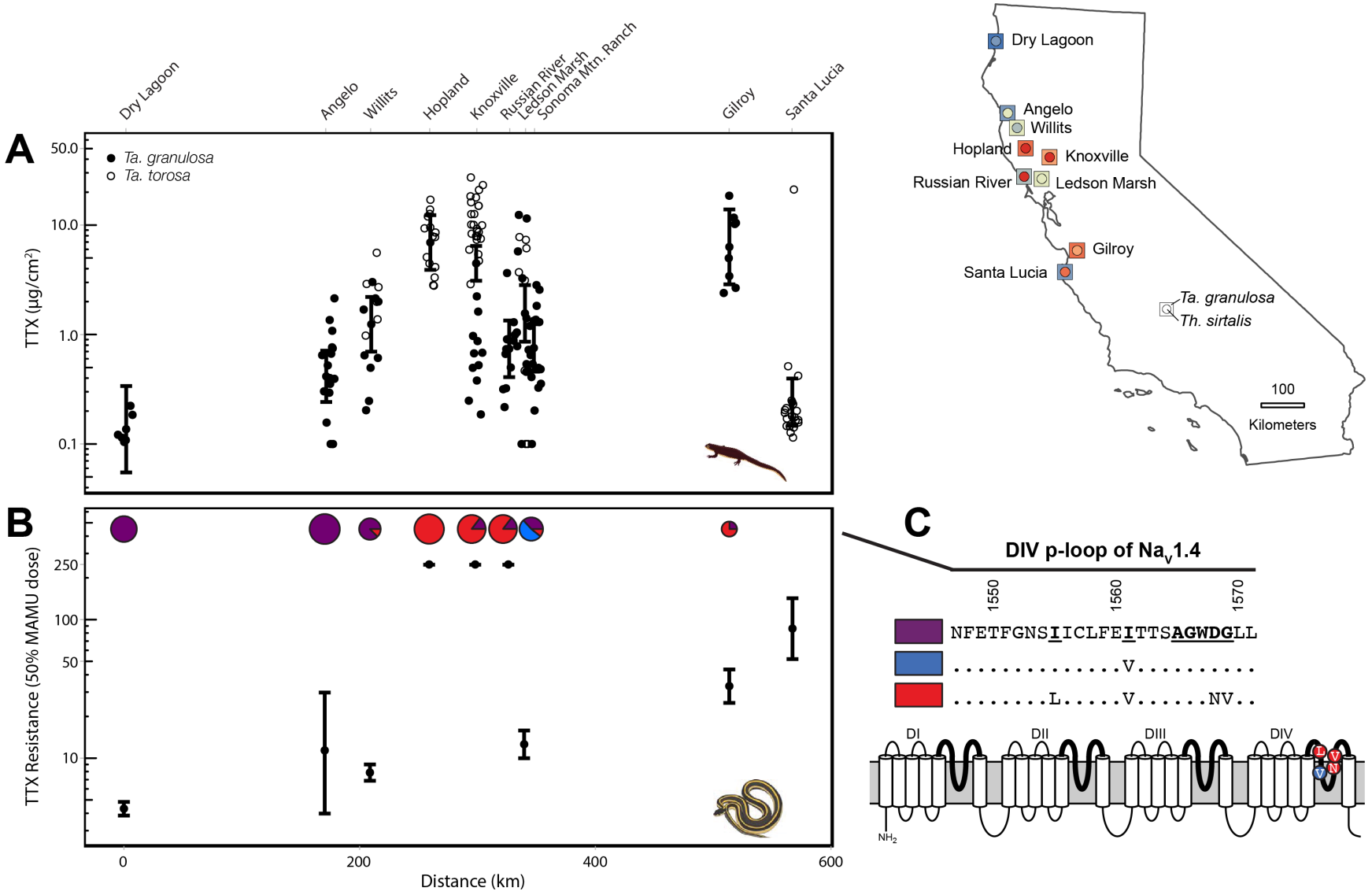
A
Ta. granulosa
Ta. torosa
TTX (µg/cm²)
50.0
10.0
1.0
0.1
Dry Lagoon
Angelo
Willits
Hopland
Knoxville
Russian River
Ledson Marsh
Sonoma Mtn. Ranch
Gilroy
Santa Lucia
B
TTX Resistance (50% MAMU dose)
250
100
50
10
0
200
400
600
Distance (km)
Dry Lagoon
Angelo
Willits
Hopland
Knoxville
Russian River
Ledson Marsh
Gilroy
Santa Lucia
Ta. granulosa
Th. sirtalis
100
Kilometers
C
DIV p-loop of Na$_V$1.4
1550
1560
1570
NFETFGNSIICLFEITTSAGWDGLL
.....V.....
.....L.....V.....NV..
DI
DII
DIII
DIV
NH$_2$

**Figure 1.** (**A**) Population means of newt TTX toxicity (μg/cm$^2$) for each sampling location, which include samples from both *Taricha* species. Error bars indicate 95% confidence intervals (CI). The x-axis represents linear distance (km) from the northernmost sampling site (Dry Lagoon; 0 km). (**B**) Phenotypic TTX resistance (50% MAMU dose) in *Th. sirtalis* along the latitudinal transect. We were unable to assess the 50% MAMU dose of snakes at Hopland, Knoxville, and Russian River due to their extreme resistance. (**C**) For *Th. sirtalis*, the frequency of TTX-resistant alleles in the $Na_V1.4$ channel is shown with pie charts proportional to sample size. To the right, the schematic of $Na_V1.4$ shows the four domains of the channel (DI–DIV), with the extracellular pore loops (p-loops) highlighted with bold lines. Specific amino acid changes in the DIV p-loop are shown in their relative positions within the pore. The TTX-sensitive ancestral sequence (purple) is listed, followed by the two derived alleles known to confer increases in channel resistance. Map inset illustrates mosaic patterns of prey toxicity and predator resistance at each location along the transect. Sonoma Mtn. Ranch is not shown on the map due to its close southern proximity (8 km) to Ledson Marsh.

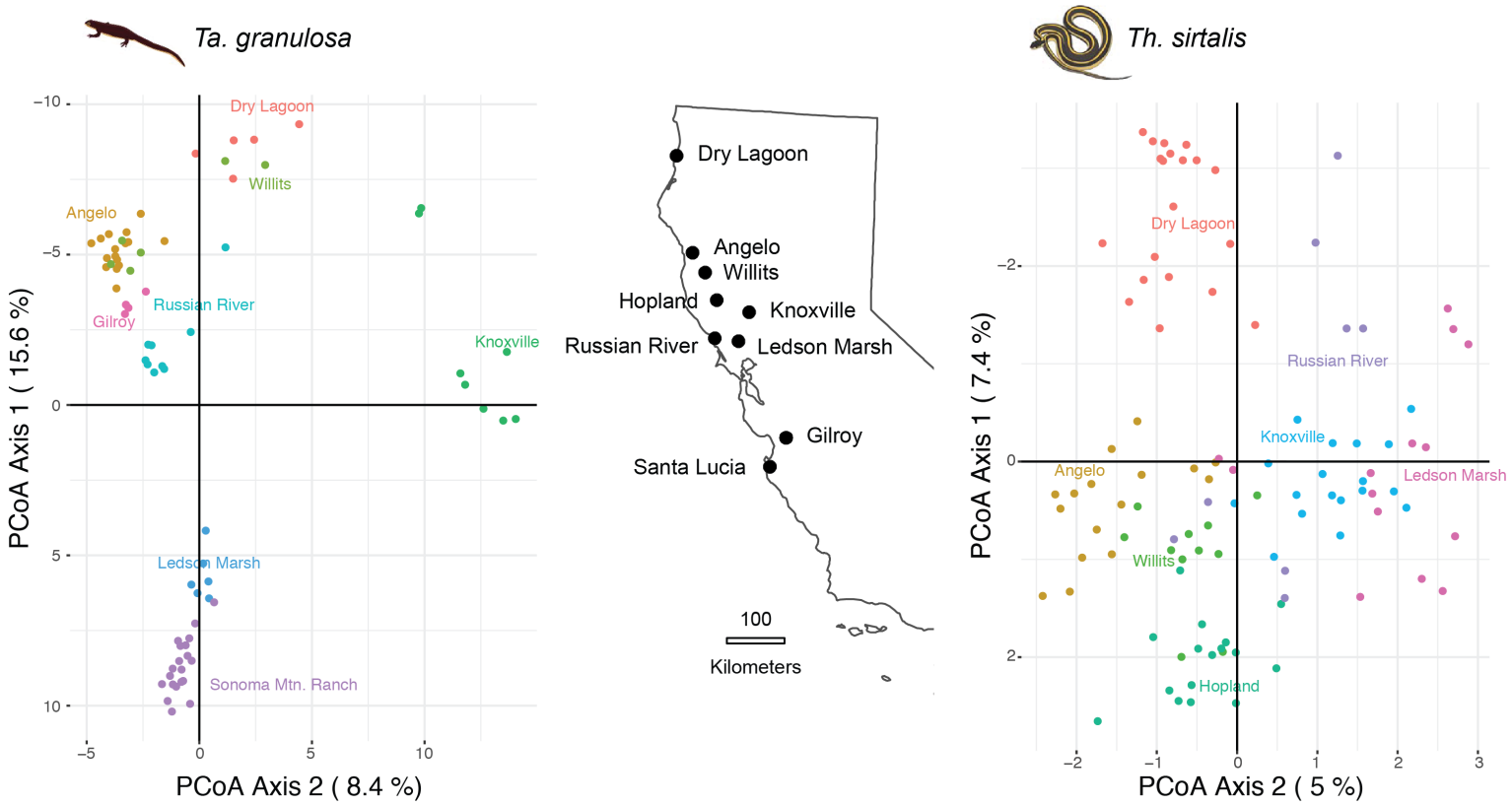


**Figure 2.** Results from the principal coordinate (PCoA) analysis of neutral SNPs from *Ta. granulosa* and *Th. sirtalis*. PCoA graphs are rotated 90º to emphasize the major axis of variation corresponding to latitude.

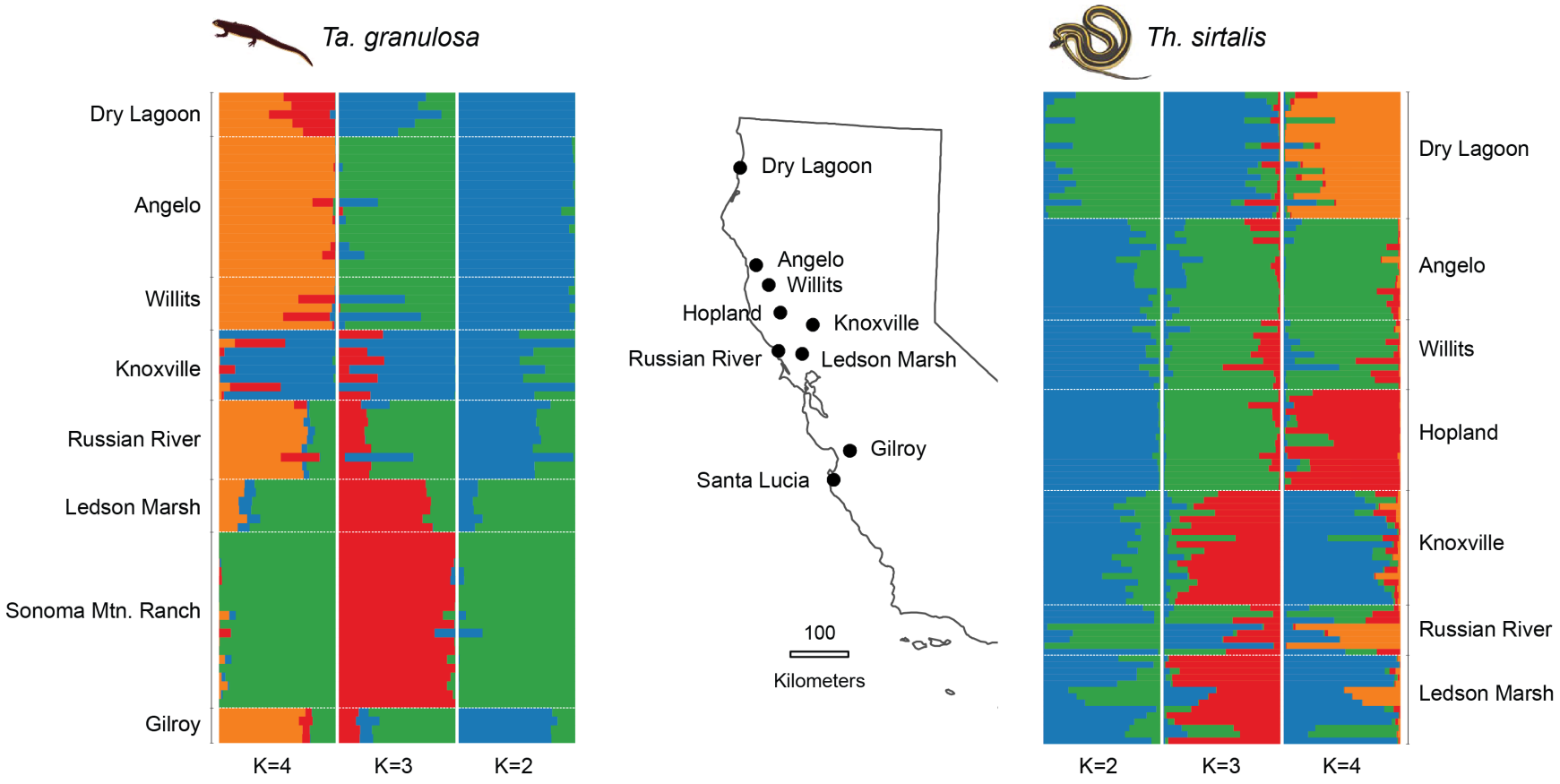


**Figure 3.** Results from the STRUCTURE analysis of neutral SNPs from *Ta. granulosa* and *Th. sirtalis*. Plots are ordered latitudinally by population. The Evanno's method indicated K=2 is the most likely number of genetic cluster for both species.